USGS
science for a changing world

Prepared in cooperation with the California Department of Water Resources and U.S. Bureau of Reclamation

Hydrology and Hydrodynamics on the Sacramento River Near the Fremont Weir, California—Implications for Juvenile Salmon Entrainment Estimates

Scientific Investigations Report 2018–5115

U.S. Department of the Interior
U.S. Geological Survey

Cover photographs:

Front: Aerial photo looking downstream (east) on the Sacramento River. The Fremont Weir, a concrete structure, lies to the right of the river (south) in the photograph. The river bend where the field study was conducted is on the right side of the image. Photograph courtesy of Patrick Huber, University of California, Davis, taken July 26, 2013.

Top rear: Looking downstream along the Sacramento River near the apex of the river bend at the western end of the Fremont Weir. Taken October 2013, at a river stage of about 15 feet, referenced to the North American Vertical Datum of 1988. Photograph courtesy of Chris Austin, Maven's Notebook.

Bottom rear: Looking downstream along the Sacramento River near the apex of the river bend at the western end of the Fremont Weir. Taken December 2014, at a river stage of about 32 feet, referenced to the North American Vertical Datum of 1988. Boat, acoustic Doppler current profiler, and global positioning system mount used for velocity mapping. Photograph courtesy of Chris Valle, U.S. Geological Survey.

Hydrology and Hydrodynamics on the Sacramento River Near the Fremont Weir, California—Implications for Juvenile Salmon Entrainment Estimates

By Paul R. Stumpner, Aaron R. Blake, and Jon R. Burau

Prepared in cooperation with the California Department of Water Resources and U.S. Bureau of Reclamation

Scientific Investigations Report 2018–5115

U.S. Department of the Interior
U.S. Geological Survey

U.S. Department of the Interior
RYAN K. ZINKE, Secretary

U.S. Geological Survey
James F. Reilly II, Director

U.S. Geological Survey, Reston, Virginia: 2018

For more information on the USGS—the Federal source for science about the Earth, its natural and living resources, natural hazards, and the environment—visit https://www.usgs.gov or call 1–888–ASK–USGS.

For an overview of USGS information products, including maps, imagery, and publications, visit https://store.usgs.gov.

Suggested citation:
Stumpner, P.R., Blake, A.R., and Burau, J.R., 2018, Hydrology and hydrodynamics on the Sacramento River near the Fremont Weir, California—Implications for juvenile salmon entrainment estimates: U.S. Geological Survey Scientific Investigations Report 2018–5115, 50 p., https://doi.org/10.3133/sir20185115.

ISSN 2328-0328 (online)

Acknowledgments

The authors would like to thank the State and Federal water contractors and the California Department of Water Resources for their support in funding the 2016 experiment, the analysis of the data, and the writing of this report. Appreciation is extended to Curt Schmutte (California Department of Water Resources, retired) and managers at the Metropolitan Water District for recognizing the critical need and generating contractor's funding support for this effort. To the California Department of Water Resources program manager, Brett Harvey, and the California Department of Water Resources contracting manager, Jacob McQuirk, thank you for dealing with all of the contracting and purchasing issues associated with doing things on short notice and helping to guide the experiment and facilitating interagency coordination and communication. Ted Sommer, at the California Department of Water Resources, provided insightful comments on the initial draft proposal for this work and, along with Brett Harvey, helped guide the adaptive management of the study.

These experiments involved many dedicated and talented people who worked in the field under challenging conditions—bad weather and high water, in this case. None of the results from this study would be possible without the heroic efforts of the fish-tagging and release teams, led by Marty Liedtke, and the instrument programming, deployment, and recovery teams, led by Chris Vallee; all are gratefully acknowledged.

Finally, thanks to the following for their reviews of the draft report: Chris Campbell, CBEC Engineering; Brett Harvey, California Department of Water Resources; Josh Israel, Bureau of Reclamation; and Maureen Downing-Kunz and Paul Work, U.S. Geological Survey. Their feedback improved this report immensely.

Contents

Figures

Figures—Continued

Tables

Conversion Factors

U.S. customary units to International System of Units

Multiply	By	To obtain
	Length	
foot (ft)	0.3048	meter (m)
mile (mi)	1.609	kilometer (km)
	Area	
square foot (ft^2)	0.092903	square meter (m^2)
	Flow rate	
foot per second (ft/s)	0.3048	meter per second (m/s)
cubic foot per second (ft^3/s)	0.02832	cubic meter per second (m^3/s)

Datums

Horizontal coordinate information is referenced to the North American Datum of 1983 (NAD 83).

Vertical coordinate information is referenced to the North American Vertical Datum of 1988 (NAVD 88) and the National Geodetic Vertical Datum of 1929 (NGVD 29).

Elevation of land surface, as used in this report, refers to distance above the vertical datum.

Abbreviations

BRW	Bear River at Wheatland
BSL	Butte Slough at Meridian
CDF	cumulative distribution function
CLW	Sacramento River at Colusa Weir
DL-ADCP	downward-looking acoustic Doppler current profiler
DWR	California Department of Water Resources
FBL	Feather River at Boyd's Landing
FRE	Sacramento River near the Fremont Weir
FRE.temp	Sacramento River above Fremont Weir near Knights Landing
IQR	interquartile range
NCC	Natomas cross canal
Reclamation	Bureau of Reclamation
RPA	reasonable and prudent alternative
TIS	Tisdale Weir
UL-ADCP	upward-looking acoustic Doppler current profiler
USGS	U.S. Geological Survey
VMT	Velocity Mapping Toolbox
VON	Sacramento River at Verona
WLK	Sacramento River below Wilkins Slough
YBUS	Yolo Bypass Utilization Study

Hydrology and Hydrodynamics on the Sacramento River Near the Fremont Weir, California—Implications for Juvenile Salmon Entrainment Estimates

By Paul R. Stumpner, Aaron R. Blake, and Jon R. Burau

Abstract

Estimates of fish entrainment on the Sacramento River near the Fremont Weir are a critical component in determining the feasibility and design of a proposed notch in the weir to increase access to the Yolo Bypass, a seasonal floodplain of the Sacramento River. Detailed hydrodynamic and velocity measurements were made at a river bend near the Fremont Weir in the winter and spring of 2016 to examine backwater conditions and estimate the hydraulic entrainment zone, a zone where fish would be predicted to be entrained into the notch. Secondary circulation near the river bend was shown to shift the velocity and discharge distributions toward the outside of the bend. Variability in the stage-discharge relation was shown to be the biggest source of uncertainty in determining the location of the hydraulic entrainment zone. Outflow from the Sutter Bypass and high flow on the Feather River resulted in backwater conditions near the Fremont Weir about 25 percent of the time over the 27-year period from April 1990–April 2017. Velocity measurements used to estimate the critical streakline position (the outer edge of the hydraulic entrainment zone) were not made over a sufficient range of conditions to explicitly quantify the variability in the location of the critical streakline. The variability in the critical streakline position was therefore represented stochastically with a random effects model. The estimated position of the critical streakline and the random effects model are input parameters used in a simulation designed to estimate fish entrainment over a 15-year period. The estimates of the critical streakline and likely fish entrainment could be much improved with velocity measurements over a broader range of stage and discharge conditions.

Introduction

The Sacramento River watershed supplies water for human use (drinking and agricultural) for approximately 30 million people in the State of California. A massive infrastructure has been built to effectively manage water routing and delivery, but this infrastructure and routing of water have placed a great deal of stress on the ecosystem in the Sacramento–San Joaquin Delta and the San Francisco Bay estuary. As a result, there has been a major decline in pelagic organism populations, partly due to decades-long water management by State and Federal agencies. For instance, winter and spring runs of Chinook salmon (*Oncorhynchus tshawytscha*) are listed as threatened and endangered, respectively, under the Federal Endangered Species Act (National Marine Fisheries Service, 1989, 1999). In 2009, the National Marine Fisheries Service issued a Biological and Conference Opinion that stated State and Federal water management was likely to jeopardize federally listed species including salmon, and established reasonable and prudent alternatives (RPAs) that would allow water export operations to continue. The RPA Action I.6.1 states that Restoration of Floodplain Rearing Habitat, through the increase of seasonal inundation in the lower Sacramento River Basin, is needed to allow water export operations to continue (National Marine Fisheries Service, 2009). In response to this RPA, the California Department of Water Resources (DWR) and the Bureau of Reclamation (Reclamation) developed the Yolo Bypass Salmonid Habitat Restoration and Fish Passage Plan (Bureau of Reclamation and California Department of Water Resources, 2012). This project is designed to increase access for out-migrating juvenile salmon and inundate the Yolo Bypass, a floodplain that receives excess water from the Sacramento River, more frequently during the months of December–March.

The Yolo Bypass is typically inundated when the Fremont Weir overtops, at an elevation of approximately 32.5 feet (ft). The Fremont Weir, approximately 20 miles (mi) north of Sacramento, Calif. (fig. 1), was designed primarily to provide flood control for the city. Historically, the frequency of inundation is low, about 12 percent of the time from December to March, based on the frequency of occurrence from stage data at the Fremont Weir (fig. 2); therefore, access to the Yolo Bypass for out-migrating juvenile salmon is also low. A notch in the Fremont Weir is proposed that will be activated for stages below the elevation of the weir crest, at an elevation ranging from approximately 19 to 32.5 ft, and operational from December to mid-March. The operational window was chosen to minimize impact to stakeholders who use the Yolo Bypass for agriculture during the spring through fall months. The operational design is intended to increase the frequency at which water flows into the Yolo Bypass via the Fremont Weir. On the basis of historical stage data, the frequency will increase from about 12 to 45 percent of the time during December to mid-March, and this will also increase access for juvenile salmon out-migrants to the Yolo Bypass. Six locations are being considered for the proposed notch (fig. 3). Alternatives 1 and 2 are near the eastern end of the Fremont Weir, alternative 5 is near the central part of the weir, and alternatives 3, 4, and 6 are near the western end of the weir.

To facilitate informed decision making about the amount of water required to entrain fish, the U.S. Geological Survey (USGS), in collaboration with DWR and Reclamation, conducted an acoustic telemetry and hydrodynamic field study, the Yolo Bypass Utilization Study (YBUS), in the winter and spring of 2016 to assess a range of river conditions and associated fish movements through the river bend near the western end of the Fremont Weir. The data collection and analysis for this study included a two-dimensional acoustic telemetry array to track movements of fish and estimate spatial distributions, an acoustic receiver network to determine survival probabilities through the Sacramento River versus the Yolo Bypass (Pope and others, 2018), hydrodynamics measurements at the river bend, which is covered in this report, and combining fish spatial distributions and hydrodynamic data to estimate entrainment into the proposed notch (Blake and others, 2017).

Purpose and Scope

Initially, this project was aimed at making fish entrainment estimates at the western notch alternatives (3, 4, and 6), based solely on data collected in the 2016 YBUS study. Because the field study was near the western end of the Fremont Weir, the hydrodynamics at alternatives 1, 2, and 5 are beyond the scope of this report. Analysis of the 2016 and historical data indicated substantial variability in the stage-discharge relation on the Sacramento River near the Fremont Weir. River stage controls the notch flow, and the ratio of notch flow to the Sacramento River flow determines the fraction of Sacramento River discharge entrained into the Yolo Bypass, which in turn affects the juvenile salmon entrainment rate. Determining the correct discharge on the Sacramento River is critical for making accurate predictions of juvenile salmon entrainment into the Bypass, therefore, an additional component of this analysis quantified and accounted for this large variability in the stage-discharge relation. One of the major challenges with a project of this magnitude is that water withdrawn from the Sacramento River at this location results in water that is not available for downstream use. Downstream effects on the ecosystem and human consumption should be considered but are beyond the scope of this report.

This report has several objectives. The first objective was to document and explain the variability in the stage-discharge relation due to backwater effects using data collected in 2016, historical data, and discharge on the Sacramento River near the Fremont Weir estimated with a statistical model. The second objective was to describe the hydrodynamic processes that can influence the distribution of fish in a river bend, and how these processes apply to the river bend near the western end of the Fremont Weir using data collected in the 2016 YBUS study. The third objective was to present the methodology used to estimate the hydraulic entrainment zone, with application to this river bend. The hydraulic entrainment zone includes regions in the river where fish entrainment would be expected to occur. The hydraulic entrainment zone will inform estimates of actual fish entrainment. The conceptual models of using river hydraulics to maximize entrainment and the method used to estimate the hydraulic entrainment zone are discussed in the following section.

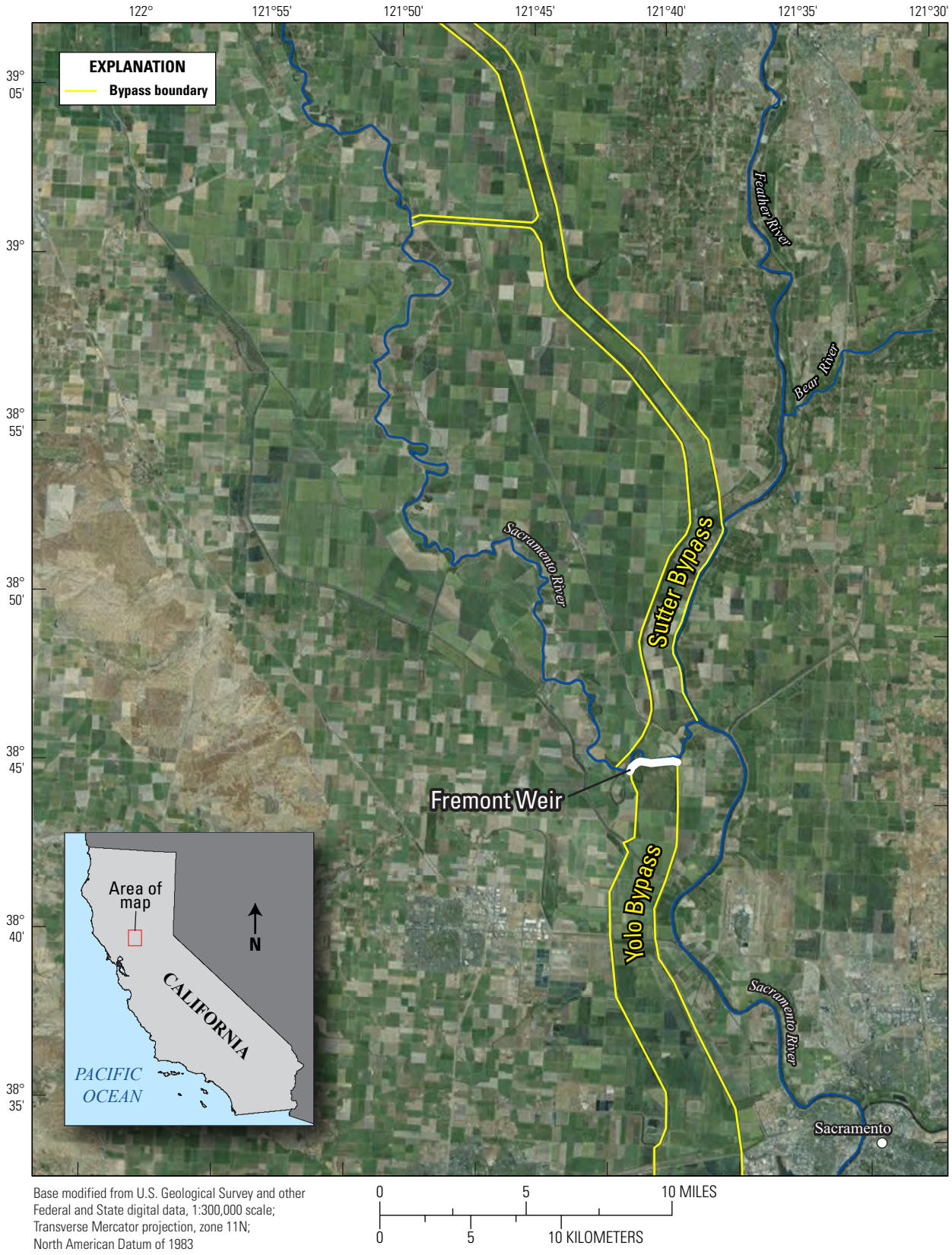

Figure 1. Location of the study area along the Sacramento River near the Fremont Weir, California.

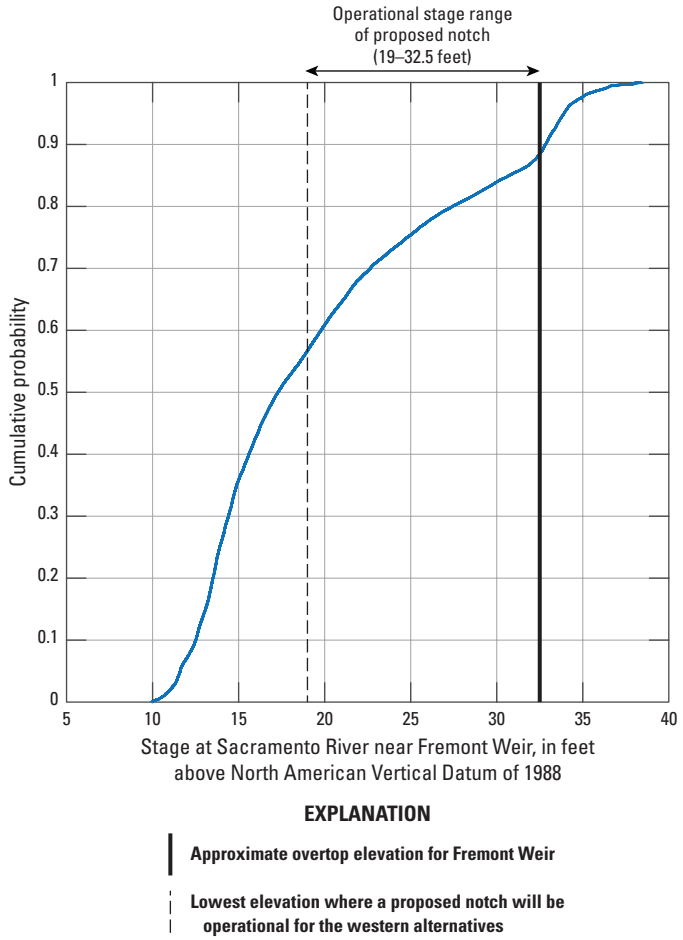

Figure 2. Empirical cumulative probability distribution of stage measured at the Fremont Weir along the Sacramento River, California, from 1984 to 2017. Only the months of December to mid-March are included because that is the proposed time frame of notch operation. The vertical black line indicates the approximate elevation at which the Fremont Weir overtops. The vertical dashed line indicates the lowest elevation where a proposed notch will be operational for the western alternatives.

Conceptual Models Used in Analyses

The first conceptual model central to an analysis of fish entrainment at a river bend, is that secondary circulation (lateral flow structures perpendicular to primary flow direction) will accumulate fish along the outside of the bend, such that a notch location can be optimized to maximize fish entrainment rates (fig. 4). As water is transported through a river bend, along-stream momentum is transferred to cross-stream momentum, which creates cross-stream flow structures perpendicular to the primary flow direction, termed secondary circulation. Secondary circulation is characterized by surface currents that move toward the outside of a river bend, which creates a down-welling region near the outside of the bend and return flow near the streambed toward the inside of the bend. The magnitude of the secondary currents peaks near the apex of the bend where the secondary currents also skew the velocity and discharge distribution toward the outside of the bend (Blanckaert, 2010). The interaction among secondary circulation, fish movement and behavioral responses, and the ways in which this interaction varies with stage and discharge is not only crucial to an understanding of how fish are distributed in the river, but also is critical for determining notch location and design to maximize entrainment of fish into the notch.

In order for the outside of a river bend to function as a hydraulic entrainment zone that could transport fish into another channel, fish must accumulate in the near-surface zone. Because secondary circulation induces down-welling at the outside of a bend, fish must exhibit behavior that keeps them surface-oriented for the notch to function as intended. There are a few consistent features in a number of data sets that allow inferences about fish behavior to be made and demonstrate that the resultant fish mass distributions are not equal to water mass distribution. First, there is typically a deficit of fish mass near riverbanks and a sharp gradient in distribution that are generally coincident with bathymetric gradient-induced cross-channel velocity gradients (California Department of Water Resources, 2015, 2016). This implies that fish may be avoiding zones of increased velocity shear, down-welling, or other turbulent features near the river bank. Second, if fish are surface-oriented and can overcome or avoid down-welling zones, then the fraction of fish mass may become disproportionately higher than the fraction of flow toward the outside of the bend because they will not get caught in the bottom layer return flow.

Figure 3. Alternative locations (green circles) that are being considered for a notch in the Fremont Weir along the Sacramento River, California. Alternative 5 is a multi-gate option with three locations. Alternatives 1 and 2, and Alternatives 4 and 6 are at the same location, and are represented by a single circle.

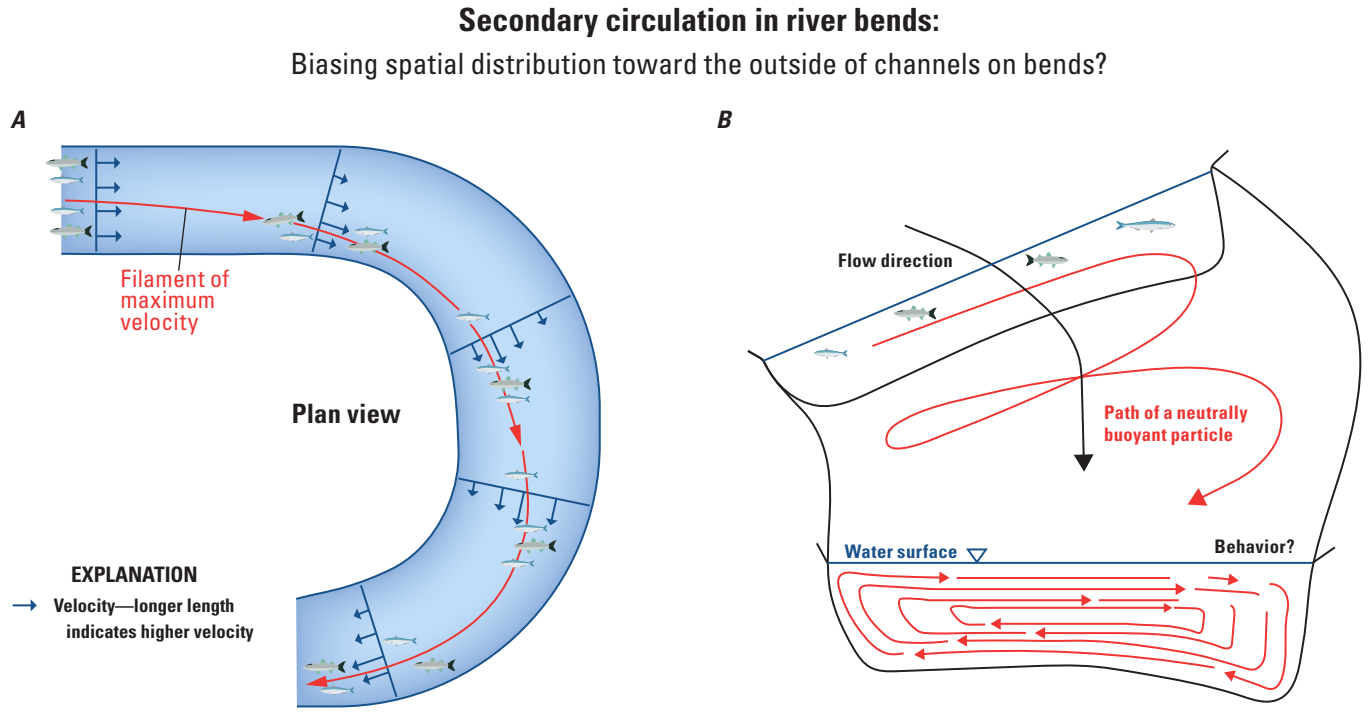

Figure 4. How river hydraulics at a river bend can bias the spatial distribution of fish toward the outside of the bend: *A*, plan view map shows the velocity distribution in the primary flow direction; and *B*, cross-section view shows how fish will accumulate near the outside of the bend in greater proportion than that of neutrally buoyant particles, if surface orientation is maintained.

Last, the majority of fish tracks from other studies (California Department of Water Resources, 2012, 2015, 2016) show cross-stream fish velocities on the order of 0.60 foot per second (ft/s) in riverine environments with very low mean cross-stream water velocities, indicating that the observed cross-stream velocity in the fish track was the result of swimming behavior. If fish swim at an equal cross-stream velocity to river right and river left, then in sections of river without strong secondary currents, one would expect fish to be distributed equally on both sides of the river center. However, in river bends with stronger cross-stream currents toward the outside of the bend, a population of fish with equal left and right swimming speeds will have a net cross-stream velocity that is higher toward the outside of the bend. After the cross-stream currents decrease downstream from the bend, fish that have been transported near the outside riverbank will initiate a cross-stream movement away from the bank, possibly to avoid elevated velocity shear or turbulence, in a direction toward the inside bank. In this case, the fish mass distribution toward the bank will decrease faster than water mass distribution given a sufficiently high cross-stream swimming speed.

The second conceptual model used in the analysis is that the entrainment of water and fish can be predicted upstream from a river junction using an approach called the critical streakline (fig. 5; see California Department of Water Resources, 2016, for details on the theory behind this method). In this analysis, the critical streakline represents the outer boundary of the hydraulic entrainment zone, which is the zone where water is entrained into a proposed notch. The critical streakline has been shown to be a primary predictor of entrainment of acoustically tagged juvenile salmon at tidal river junctions in the Sacramento–San Joaquin Delta, such that fish on the distributary channel side of the critical streakline will have a higher probability of entrainment down that distributary channel (Perry and others, 2014; Perry and others, 2016; Romine and others, 2017). Because the proposed modifications to the Fremont Weir will create an engineered distributary river junction, an estimate of fish distribution superimposed on the location of the critical streakline can be used to provide estimates of fish entrainment for proposed modifications to the weir given a set of hydraulic conditions. The critical streakline can be accurately estimated given detailed velocity and bathymetry information.

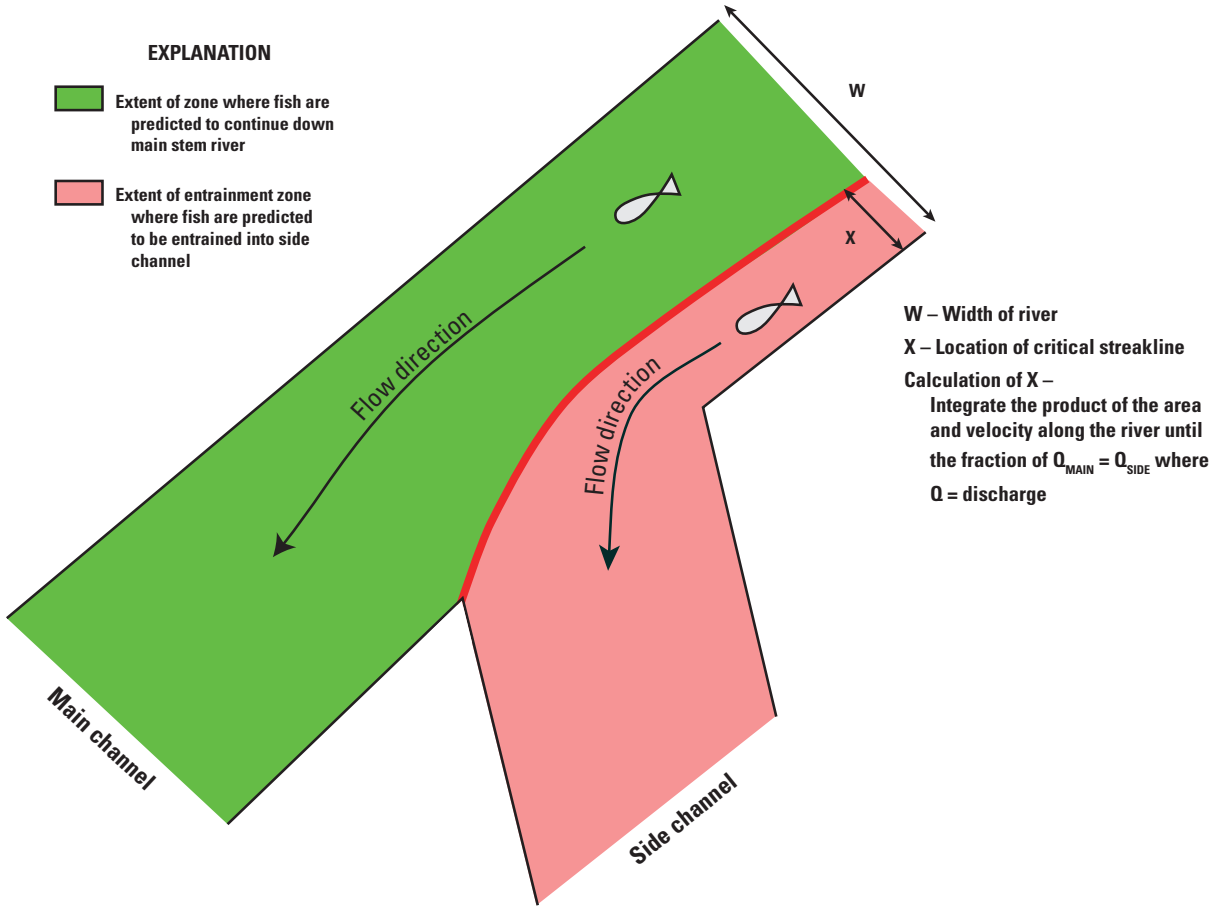

Figure 5. Hydraulic entrainment zone based on the critical streakline approach.

Methods

The first component of the 2016 YBUS study was to examine backwater effects near the western end of the Fremont Weir using discharge data from the 2016 YBUS study and historical data. For the 2016 YBUS study, a temporary gage (FRE.temp) was installed 1.24 mi upstream from the western end of the Fremont Weir (fig. 6) to estimate discharge from January 22 to April 22, 2016. This location was chosen because there are no discharge data available, and a more accurate estimate of discharge at this location was needed to make entrainment estimates. The second component of the 2016 YBUS study was to document the evolution of secondary circulation and estimate the hydraulic entrainment zone for various notch configurations using velocity transects at river cross sections through the study domain for a range of river stage and discharge conditions.

River Stage and Velocity Data

River stage at FRE.temp (fig. 6) was measured using a Campbell Scientific CS456 vented pressure sensor (accuracy = 0.05 percent of full scale). The stability (drift or fouling) of the sensor was not verified until after February 9, 2016, but there were no obvious shifts in the data during the data-collection period, and typically this sensor does not significantly drift over months of deployment, based on the authors' experience.

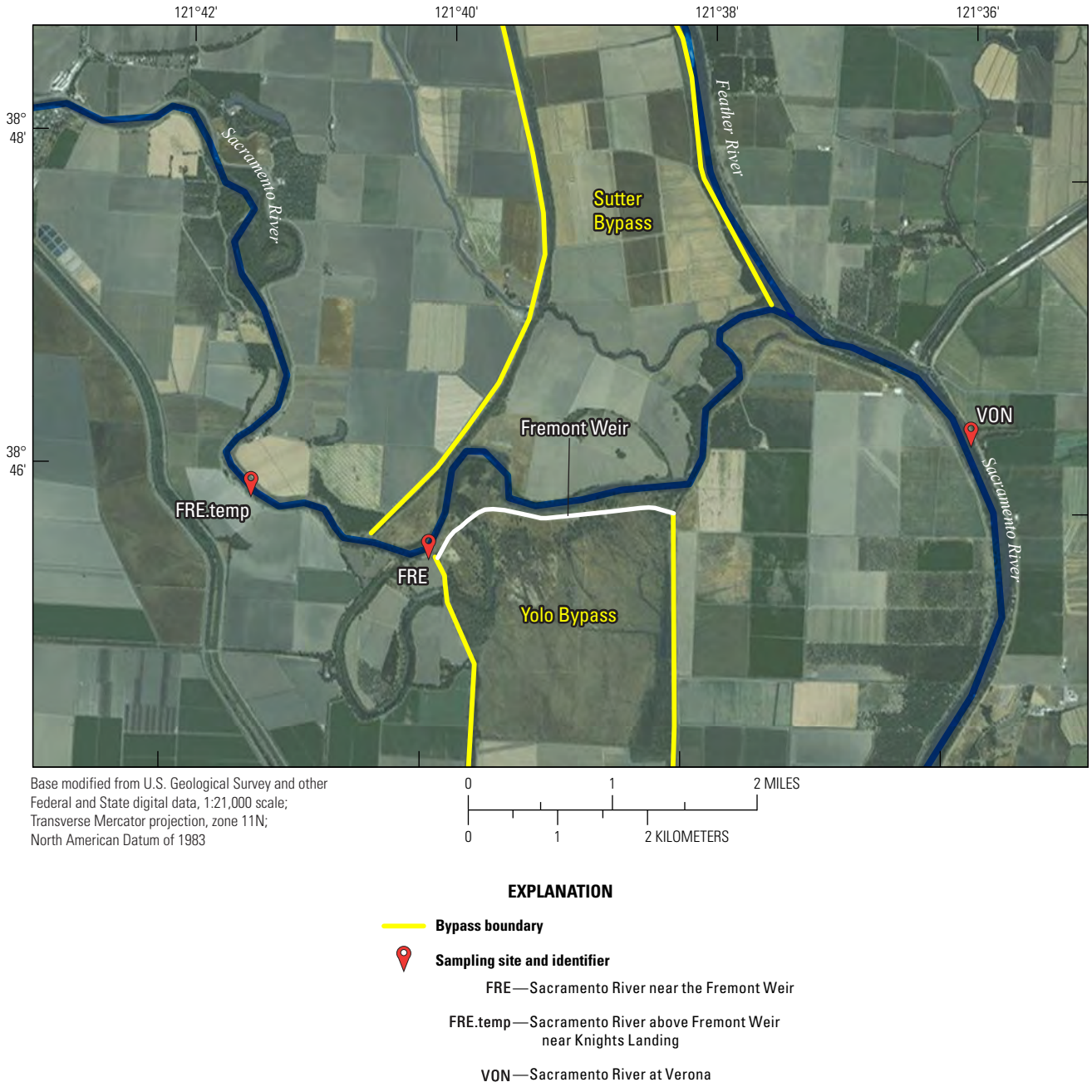

Figure 6. Locations of the temporary Fremont Weir gage (FRE.temp) and two longer-term monitoring locations (FRE and VON) on the Sacramento River, California. The Yolo Bypass Utilization Study was done at the western end of the Fremont Weir near the FRE.temp station.

The datum of the stage gage at FRE.temp was initially set to the same value as the FRE gage (fig. 6). It was not possible to survey the FRE.temp gage datum to an absolute elevation because there were no control points near this location, but setting the datum to the same value as FRE allowed for easy comparison. On February 9, 2016, a survey using a Real-Time Kinematic–Global Positioning System was done by the USGS near the FRE gage, because there were control points at that location. The precision and accuracy of the survey were acceptable, as demonstrated by the close agreement between the control points (between 0.01 and 0.03 ft in the vertical direction). The datum of the stage measurement was then set to the water-surface elevation (North American Vertical Datum of 1988 [NAVD 88]) as surveyed at the location of FRE. The USGS survey also showed that the water-surface elevation reported at FRE was 0.5-foot higher than the surveyed water-surface elevation. The USGS survey also included measurements of the elevation of the crest of the Fremont Weir, which were 32.23 ft and 32.34 ft at different concrete sections of the weir. These values are in close agreement with the weir elevation that is used in the Hydrologic Engineering Center's River Analysis System model (Rajat Saha, California Department of Water Resources, written commun., March 28, 2017). Based on these lines of evidence the 2016 USGS survey was chosen as the correct elevation (NAVD 88) at the FRE gage, with the assumption that the relative elevation measurements at FRE are sufficiently accurate and need only be corrected by the offset determined during the USGS survey. In this document and any USGS analyses that use elevation data from the FRE gage, an offset of –0.5 ft was applied to correct the elevation data to the NAVD 88 datum.

Stage data were also compiled from upstream at the Sacramento River below Wilkins Slough (WLK) gage and downstream at the Sacramento River at Verona (VON) gage (fig. 7 and table 1). These two gaging stations are operated by the USGS and the elevation at both stations is based on the National Geodetic Vertical Datum of 1929 (NGVD 29) with a +3.0-foot offset. To convert these stages to the datum at FRE (NAVD 88), a –0.615-foot conversion factor was used for WLK stage data and a –0.572-foot conversion factor was used for the VON stage data. The conversions were done using the North American Vertical Datum Conversion software available online (National Geodetic Survey, 2017). These data were used as input data for the statistical model used to predict discharge at the Fremont Weir from historical records (see "Statistical Model to Predict Discharge on the Sacramento River Near the Fremont Weir" section).

River velocity at FRE.temp was measured by using a Workhorse Monitor 1,200-kilohertz upward-looking acoustic Doppler current profiler (UL-ADCP) deployed on the riverbed to measure a three-dimensional velocity profile with up to 27 depth bins at 1.64-foot increments through the water column. The UL-ADCPs have a stated accuracy of 0.3 percent of water velocity, plus or minus 0.001 foot per second (ft/s). The UL-ADCP was programmed to measure velocity in an east-north-up coordinate system, and the east and north velocity components were rotated (in post processing) into along-channel and cross-channel velocity components. The along-channel velocity profile was averaged over all depth bins to produce a single velocity measurement that was used as the index velocity for developing a regression to estimate discharge. The water depth varied by approximately 20 ft (from 10 to 30 ft) during the course of the deployment; therefore, the number of depth bins averaged to produce the index velocity was variable for the length of the record. The stage and velocity data were averaged over a 15-minute time span and recorded continuously for the duration of the study.

Discharge Estimates

The methods used to estimate discharge with field measurements on the Sacramento River near the Fremont Weir, an estimate of Sutter Bypass outflow using mass balance, and the notch-stage discharge ratings developed by DWR are discussed in this section.

Sacramento River Near Fremont Weir

For the 2016 YBUS study, discharge at FRE.temp was estimated using two techniques: the stage-discharge (Buchanan and Somers, 1969) and index velocity (Ruhl and Simpson, 2005; Levesque and Oberg, 2012) methods. The stage-discharge method is widely used for estimating discharge in riverine environments that are not influenced by tides or backwater conditions. When tides or backwater conditions are present, the relation between stage and discharge becomes either nonlinear or poorly correlated, and the index-velocity method is often used. Empirical evidence of backwater conditions on the Sacramento River at the western end of the Fremont Weir associated with higher magnitude flows in the Sutter Bypass and the Feather River suggests that discharge estimated from the index-velocity method rather than the stage-discharge method would be more accurate.

The velocity and stage data were used to develop regressions with discrete discharge measurements and estimate a continuous time series of discharge for the study period (table 1). Discharge measurements (table 2) were made using a moving boat with a mounted downward-looking acoustic Doppler current profiler (DL-ADCP), on 7 separate days to cover an adequate range of conditions observed for the study period and processed in accordance with USGS standards (Mueller and others, 2009). A linear regression between the stage data and discharge measurements was developed for the stage-discharge relation. For the index-velocity method, two regressions are needed: (1) a linear regression between the measured (index) velocity from the UL-ADCP and the mean cross-sectional velocity from the moving boat measurements, and (2) a quadratic fit regression between the river stage and the cross-sectional area obtained from the moving boat measurements.

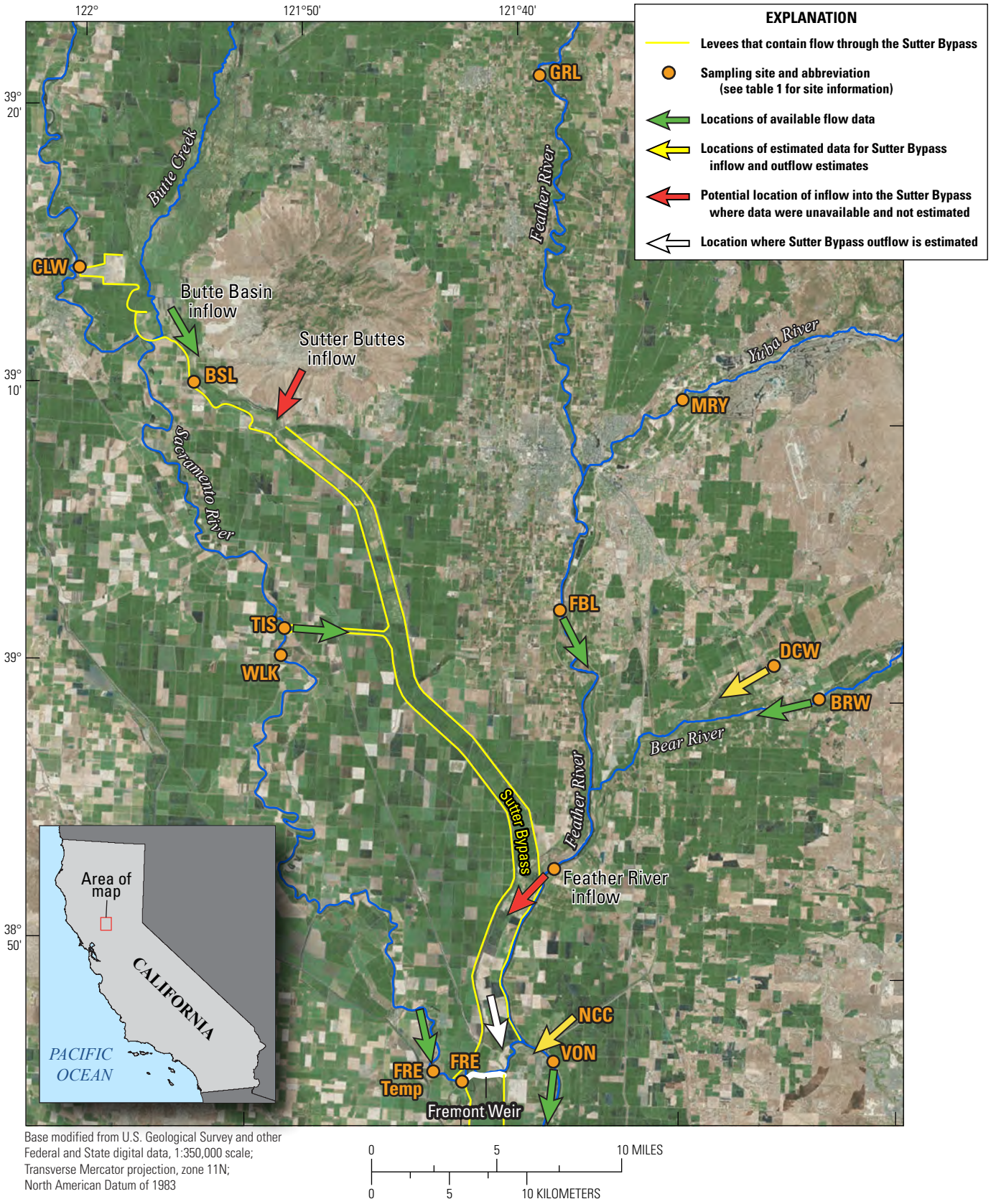

Figure 7. Locations of gaging stations (orange circles) along the Sacramento, Feather, Yuba, and Bear Rivers, California, that were used to analyze discharge conditions for this study.

Table 1. Summary of data accessed for this report from gaging stations along the Sacramento River and its tributaries, California.

[All stations are located in California. **Abbreviations**: CDEC, California Data Exchange Center, http://cdec.water.ca.gov/; NWIS, National Water Information System, https://waterdata.usgs.gov/nwis; N/A, not applicable; USGS, U.S. Geological Survey]

Station name	CDEC identifier or abbreviation	USGS station number	Type of data accessed	Location where data were accessed
Bear River near Wheatland	BRW	11424000	Discharge	NWIS
Butte Slough near Meridian	BSL	N/A	Discharge	CDEC
Sacramento River at Colusa Weir	CLW	N/A	Discharge	CDEC
Dry Creek near Wheatland	DCW	11390500	Discharge	NWIS
Feather River near Gridley	GRL	N/A	Discharge	CDEC
Feather River at Boyd's Landing	FBL	N/A	Discharge	CDEC
Sacramento River near the Fremont Weir	FRE	N/A	Stage	CDEC
Sacramento River above Fremont Weir near Knights Landing	FRE.temp[1]	384553121412301	Discharge, stage, velocity	Collected for this report and available on NWIS
Yuba River near Marysville	MRY	11421000	Discharge	NWIS
Natomas cross canal	NCC[1]	N/A	N/A	N/A
Sacramento River at Tisdale Weir	TIS	N/A	Discharge	CDEC
Sacramento River at Verona	VON	11425500	Discharge, stage	NWIS
Sacramento River below Wilkins Slough	WLK	11390500	Discharge, stage	NWIS

[1]Not a CDEC identifier; abbreviation used for this report.

Table 2. Summary of discharge measurements on the Sacramento River above Fremont Weir near Knights Landing, California, used for regressions to estimate a discharge time series, and comparison of estimates to measured discharge.

[ft, foot; ft/s; foot per second; ft^2, square foot; ft^3/s, cubic foot per second; hh:mm, hour:minute; mm/dd/yyyy, month/day/year; NAVD 88, North American Vertical Datum of 1988; PST, Pacific Standard Time]

Measurement date (mm/dd/yyyy)	Time, PST (hh:mm)	Stage, NAVD 88 (ft)	Velocity (ft/s)	Area (ft^2)	Measured discharge (ft^3/s)	Stage-discharge estimated discharge (ft^3/s)	Percent difference from measured	Index-velocity estimated discharge (ft^3/s)	Percent difference from measured
01/22/2016	13:40	30.46	3.31	7,940	26,800	24,300	9.3	25,800	3.7
01/22/2016	13:42	30.46	3.28	7,940	26,600	24,300	8.6	25,700	3.4
01/22/2016	13:45	30.46	3.27	7,940	26,200	24,300	7.3	25,600	2.3
01/22/2016	13:47	30.46	3.28	7,940	26,400	24,300	8.0	25,600	3.0
01/22/2016	13:53	30.46	3.29	7,940	25,800	24,300	5.8	25,700	0.4
01/22/2016	13:55	30.46	3.30	7,940	25,700	24,300	5.4	25,700	0.0
01/22/2016	13:58	30.46	3.30	7,940	26,400	24,300	8.0	25,800	2.3
01/22/2016	14:02	30.45	3.30	7,940	24,900	24,300	2.4	25,700	–3.2
01/22/2016	14:04	30.45	3.29	7,940	25,600	24,300	5.1	25,700	–0.4
01/22/2016	14:06	30.45	3.29	7,940	25,700	24,300	5.4	25,700	0.0
01/22/2016	14:08	30.45	3.28	7,940	26,200	24,300	7.3	25,600	2.3
01/22/2016	14:10	30.45	3.27	7,940	25,200	24,300	3.6	25,600	–1.6

Table 2. Summary of discharge measurements on the Sacramento River above Fremont Weir near Knights Landing, California, used for regressions to estimate a discharge time series, and comparison of estimates to measured discharge.—Continued

[ft, foot; ft/s; foot per second; ft^2, square foot; ft^3/s, cubic foot per second; hh:mm, hour:minute; mm/dd/yyyy, month/day/year; NAVD 88, North American Vertical Datum of 1988; PST, Pacific standard time]

Measurement date (mm/dd/yyyy)	Time, PST (hh:mm)	Stage, NAVD 88 (ft)	Velocity (ft/s)	Area (ft^2)	Measured discharge (ft^3/s)	Stage-discharge estimated discharge (ft^3/s)	Percent difference from measured	Index-velocity estimated discharge (ft^3/s)	Percent difference from measured
01/22/2016	14:12	30.45	3.27	7,940	25,900	24,300	6.2	25,600	1.2
01/22/2016	14:14	30.45	3.26	7,940	25,500	24,300	4.7	25,600	–0.4
02/04/2016	09:45	22.45	2.78	5,500	16,300	16,200	0.6	16,100	1.2
02/04/2016	09:50	22.45	2.74	5,500	17,400	16,200	6.9	16,000	8.0
02/04/2016	09:55	22.45	2.71	5,500	16,000	16,200	–1.3	15,900	0.6
02/04/2016	09:58	22.45	2.68	5,500	16,900	16,200	4.1	15,800	6.5
02/04/2016	10:03	22.45	2.69	5,500	16,200	16,200	0.0	15,900	1.9
02/04/2016	10:07	22.45	2.72	5,500	17,300	16,200	6.4	16,000	7.5
02/09/2016	16:07	16.98	2.26	3,950	10,700	10,700	0.0	10,400	2.8
02/09/2016	16:10	16.97	2.28	3,950	10,900	10,700	1.8	10,400	4.6
02/09/2016	16:14	16.97	2.29	3,950	10,600	10,700	–0.9	10,500	0.9
02/09/2016	16:17	16.97	2.29	3,950	10,900	10,700	1.8	10,500	3.7
02/18/2016	14:38	15.05	1.98	3,430	8,200	8,700	–6.1	8,500	–3.7
02/18/2016	14:41	15.05	1.98	3,430	8,200	8,700	–6.1	8,400	–2.4
02/18/2016	14:44	15.05	1.97	3,430	8,100	8,700	–7.4	8,400	–3.7
02/18/2016	14:48	15.05	1.98	3,430	8,300	8,700	–4.8	8,500	–2.4
03/09/2016	14:01	30.23	3.14	7,870	25,400	24,100	5.1	24,800	2.4
03/09/2016	14:03	30.23	3.17	7,870	24,700	24,100	2.4	24,900	–0.8
03/09/2016	14:07	30.23	3.21	7,870	24,000	24,100	–0.4	25,100	–4.6
03/09/2016	14:10	30.23	3.23	7,870	24,800	24,100	2.8	25,200	–1.6
03/09/2016	14:12	30.23	3.26	7,870	23,300	24,100	–3.4	25,300	–8.6
03/16/2016	12:49	33.84	2.83	9,030	24,900	27,800	–11.6	26,800	–7.6
03/16/2016	12:55	33.84	2.80	9,030	27,400	27,800	–1.5	26,600	2.9
03/16/2016	13:02	33.84	2.77	9,030	25,300	27,800	–9.9	26,500	–4.7
03/16/2016	13:09	33.85	2.77	9,040	26,300	27,800	–5.7	26,500	–0.8
03/16/2016	13:16	33.85	2.77	9,040	24,900	27,800	–11.6	26,500	–6.4
03/16/2016	13:22	33.84	2.81	9,030	25,700	27,800	–8.2	26,700	–3.9
03/16/2016	13:28	33.84	2.84	9,030	23,900	27,800	–16.3	26,800	–12.1
03/16/2016	13:30	33.84	2.84	9,030	27,000	27,800	–3.0	26,900	0.4
03/30/2016	15:15	23.95	2.29	5,940	15,500	17,700	–14.2	15,700	–1.3
03/30/2016	15:18	23.95	2.29	5,940	15,900	17,700	–11.3	15,700	1.3
03/30/2016	15:21	23.94	2.29	5,940	15,600	17,700	–13.5	15,700	–0.6
03/30/2016	15:24	23.94	2.29	5,940	16,000	17,700	–10.6	15,700	1.9

Sutter Bypass Outflow

Backwater effects near the western end of the Fremont Weir were investigated using discharge records from all the channels upstream from the Sacramento and Feather River junction (fig. 7). The outflow from the Sutter Bypass into the Sacramento River had to be estimated for this analysis. Because the Sutter Bypass enters the Sacramento River upstream from the Fremont Weir, there was no way a measurement could be made. The most significant inflows into the Sutter Bypass are runoff from Butte Basin, and the Colusa (CLW) and Tisdale (TIS) Weirs that release water from the Sacramento River (fig. 7). Additional uncontrolled flows from the Sutter Buttes, along with storage and travel time within the Sutter Bypass, make it difficult to estimate outflow from the Sutter Bypass from the sum of the inflows. However, flow from channels downstream from inputs can be used to estimate outflow from the Sutter Bypass using a mass-balance approach and correcting for travel times based on the following equation:

$$\text{Sutter Bypass outflow} = \text{VON} - \text{FBL} - \text{BRW} - \text{DCW} - \text{FRE.temp} - \text{NCC} \quad (1)$$

VON = Discharge on the Sacramento River at Verona,
FBL = Discharge on the Feather River at Boyd's Landing 22 miles upstream with a 5-hour travel time to VON,
BRW = Discharge on the Bear River near Wheatland 27 miles upstream with a 5-hour travel time to VON,
DCW = Discharge on Dry Creek near Wheatland 27 miles upstream, estimated as a fraction of BRW from 0 to 0.35,
FRE.temp = Discharge on the Sacramento River above Fremont Weir near Knights Landing 7 miles upstream with a 2-hour travel time to VON, and
NCC = Discharge on the Natomas cross canal 0.5 mile upstream from VON, estimated as a fraction of VON from 0 to 0.1.

This calculation was only valid when the Fremont Weir did not overtop because a portion of the Sacramento River upstream from the weir and some unknown portion of the Sutter Bypass outflow enter the Yolo Bypass. Because of the distances of each channel from VON, each was lag corrected to account for travel time of water to VON.

A range of flow conditions were estimated for the NCC and additional flow from the Feather River watershed at Dry Creek (DCW). Discharge data from NCC were not available and were estimated based on a range of flow ratios relative to VON from 0 to 0.1. Estimates of channel capacity at NCC and VON were 22,000 and 107,000 cubic feet per second (ft^3/s), respectively (California Department of Water Resources, 2003), or a capacity ratio of 0.2. Because the channel capacity ratio is low, the potential for backwater is high, so the ratio was adjusted by half to account for this.

The Bear River has one significant tributary downstream from BRW, which has historical daily flow data, but no data were available for the period of analysis. A 20-year period (1946–67) of overlapping peak flows were examined for BRW and DCW, and the average peak flow ratio was 0.35 (range of 0.1–0.7). A range of flow ratios from 0 to 0.35 was applied to estimate the flow from BRW for the analysis period.

Data from FBL were checked because previous investigations indicated this gage might not be accurate. On the basis of measurements in June 2012, it was found that the FBL gage may underestimate discharge on the Feather River by 1,000–1,500 ft^3/s and that a combination of upstream gages Feather River at Gridley and Yuba River at Marysville provided a better estimate of discharge (CBEC, 2012). Discharge records for these gages were examined for the period analyzed and the results were mixed; for some periods the combination of upstream gages was either higher, lower, or in close agreement. Because it could not be determined what the source of error was for all three of these gages for the period analyzed, a decision was made to use the discharge record from the FBL gage.

Notch Stage-Discharge Ratings

As was stated in the "Introduction" section, the analysis described in this report applies to the three notch alternatives that were at the western end of the Fremont Weir (alternatives 3, 4, and 6). The first step for critical streakline estimates was to calculate the notch discharge based on the notch stage-discharge rating for a given stage, which is explained in greater detail in the "Hydraulic Entrainment Zone Estimate" section. The DWR provided the notch stage-discharge ratings for these alternatives, which were calculated by the engineering team working on notch design (Rajat Saha, California Department of Water Resources, written commun., March 28, 2017). These stage-discharge ratings are shown in table 3.

Table 3. Stage-discharge ratings for 2016 discharge on the Sacramento River near the western end of the Fremont Weir and for notch alternatives 3, 4, and 6 in the Fremont Weir along the Sacramento River, California.

[ft, foot; ft^3/s, cubic foot per second; NAVD 88, North American Vertical Datum of 1988]

Stage, NAVD 88 (ft)	2016 Stage-discharge rating for discharge (ft^3/s)	Alternative 3, notch flow (ft^3/s)	Alternative 4, notch flow (ft^3/s)	Alternative 6, notch flow (ft^3/s)
18	0	0	0	0
19	12,733	218	218	0
20	13,746	349	349	679
21	14,759	551	551	1,195
22	15,722	804	804	1,831
23	16,785	1,142	1,142	2,661
24	17,798	1,547	1,547	3,664
25	18,811	2,013	2,013	4,787
26	19,825	2,555	2,555	6,067
27	20,838	3,166	3,166	7,502
28	21,851	3,845	3,166	9,041
29	22,864	4,624	3,166	10,675
30	23,877	5,365	3,166	12,253
31	24,890	6,105	3,166	12,253
32	25,903	6,105	3,166	12,253
33	26,916	6,105	3,166	12,253
34	27,930	6,105	3,166	12,253
35	28,943	6,105	3,166	12,253

Velocity Transect Measurements and Processing

To investigate the evolution of secondary circulation and estimate the hydraulic entrainment zone for various notch configurations, velocity transects at eight cross-section locations were made over a 0.4-mile stretch of river that extended upstream from the river bend near the western end of the Fremont Weir, to just upstream from the river bend near the central notch alternative (fig. 8). The river stages and corresponding discharge at which these measurements were made are shown in table 4. Five measurement sets were made during the 2016 YBUS study, but initial analysis of these data indicated that additional measurements were needed to document variability in the stage-discharge relation; therefore, three additional measurement sets were made in May 2017.

Four repeated transects were made at each cross section to average out instrumental bias and small-scale turbulence to better define the large-scale coherent features (Dinehart and Burau, 2005). The velocity transects were made with a 1,200-kilohertz DL-ADCP that was mounted on a moving boat using methodologies similar to those used in making standard discharge measurements (Mueller and others, 2009). The velocity transect processing and averaging was done using the USGS Velocity Mapping Toolbox (VMT; Parsons and others, 2013). The four repeated transects were combined into a single transect line using least squares regression. The single transect line has a horizontal and vertical spacing of 3.28 and 0.82 ft, respectively. The velocity transects were smoothed using windows of three and two cells (or 9.84 ft and 1.64 ft) in the horizontal and vertical direction, respectively. These smoothing windows are applied to improve the visualization of large coherent secondary circulation structures (Parsons and others, 2013; Bever and MacWilliams, 2016). Results for a single transect, the average of four transects, and the four-transect average with smoothing applied are illustrated on figure 9. These plots demonstrate the need for averaging and smoothing by comparing the cross-stream velocities measured from a single transect to the average of four smoothed transects; the large-scale secondary-circulation cell in the center of the channel is not obvious from a single transect.

The VMT processing software has two rotation schemes that can be chosen to define along-stream and cross-steam velocity vectors: (1) zero-net discharge, and (2) Rozovskiĭ. In the zero-net discharge method the cross-stream velocity vectors are rotated in the horizontal, so that the discharge in the cross-stream plane equals zero. In the Rozovskiĭ method the cross-stream velocity vectors at each ensemble are rotated to obtain a zero-net discharge for that ensemble (Rozovskiĭ, 1957; Lane and others, 2000; Parsons and others, 2013). Bever and MacWilliams (2016) tested these rotation schemes and reported that results from the Rozovskiĭ method were insensitive to the angle of the boat transect (up to about 20 degrees) relative to the predominant direction of flow for a given cross section. This is important to note, particularly because the angle of flow can be variable along the cross section with strong secondary currents; therefore, the Rozovskiĭ rotation method was used. The data processed through VMT are available in a Science Base data release (Stumpner, 2018).

The DL-ADCP was used to measure most of the river cross section, but there were some areas on the edge of the cross section that could not be measured due to a combination of blanking distance (about 3.3 ft below the surface), side lobe interference (3.3–6.6 ft above the riverbed) and boat operational constraints (a range of 3.3–49.5 ft from the riverbanks). The distance from the end of the boat transect to the riverbanks was estimated by field crews using a laser range finder. Bathymetric data were collected multiple times during higher river stages to refine estimates of bank locations and to define the shape of the riverbed. In areas near the riverbanks where the bathymetric survey is incomplete, the location of the banks was determined by duplicating the slope of the banks from observed locations, which introduced some uncertainty in these estimates.

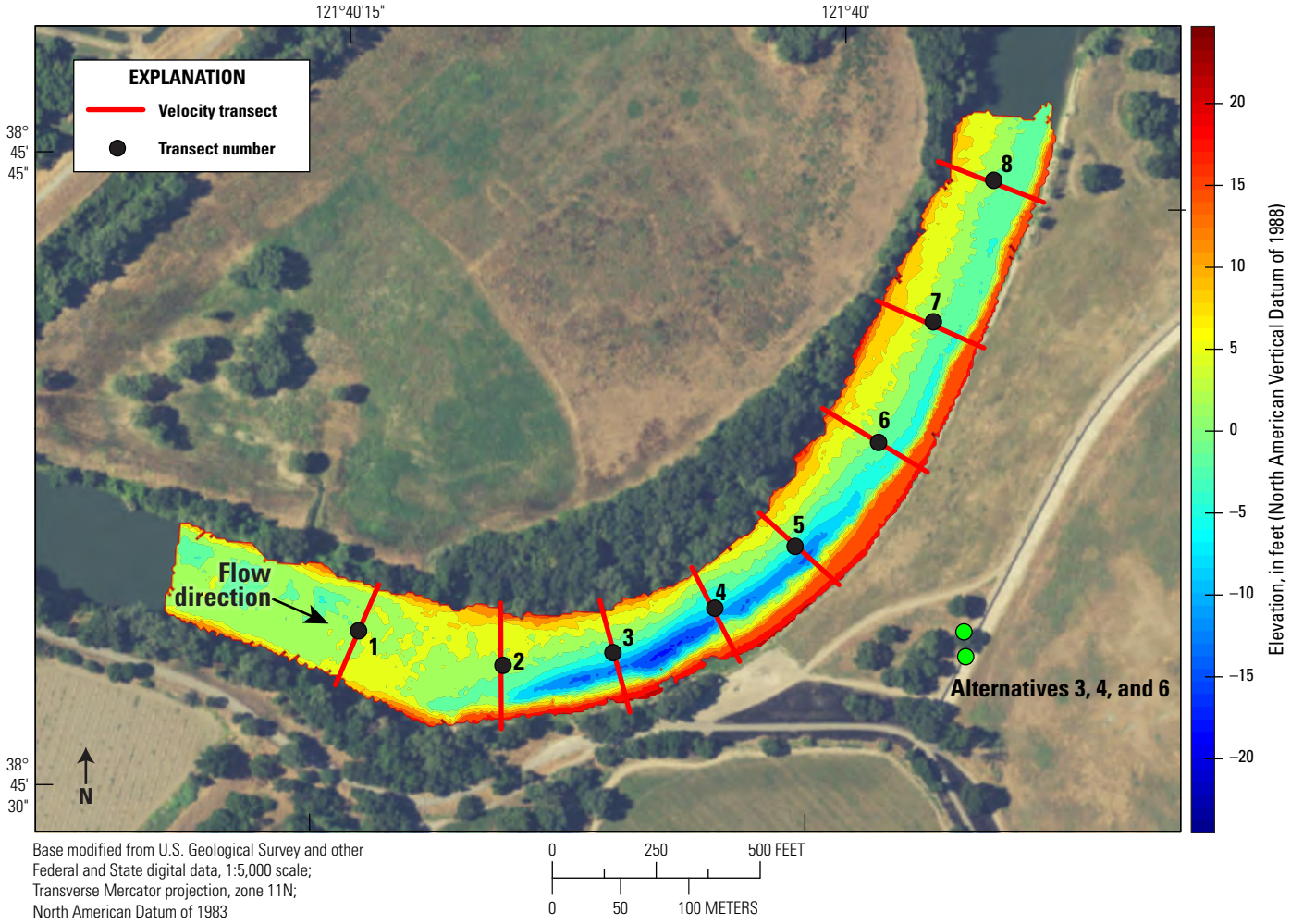

Figure 8. Locations of velocity transects, overlain on bathymetry, for the 2016 Yolo Bypass Utilization Study, and the locations of notch alternatives 3, 4, and 6 along the Fremont Weir, California.

Table 4. Summary of velocity profile measurements and discharge statistics for transects along the Sacramento River near the Fremont Weir, California.

[See figure 8 for locations of transects along the Sacramento River near the Fremont Weir. **Abbreviations**: FRE, Sacramento River near the Fremont Weir; ft, foot; ft^3/s, cubic foot per second; mm/dd/yyyy, month/day/year; NAVD88, North American Vertical Datum of 1988; N/A, not applicable; VON, Verona; WLK, Wilkins]

Measurement date (mm/dd/yyyy)	Stage[1], NAVD88 (ft)	Discharge[2] (ft^3/s)	Percent difference from index-velocity discharge	Percent unmeasured discharge[2, 3]	Percent discharge extrapolated to riverbanks[2]	Ratio of WLK to VON discharge[4]
02/18/2016	15.1	8,800 (350)	3.7	36.7 (4.9)	4.4 (2.4)	0.60
02/09/2016	16.7	11,200 (490)	6.5	35.3 (2.2)	4.8 (2.7)	0.63
02/04/2016	21.8	16,400 (490)	4.1	29.8 (2.0)	3.6 (2.2)	0.58
03/30/2016	24.2	15,900 (360)	–3.4	28.7 (1.5)	2.2 (1.7)	0.47
05/11/2017	24.6	12,300 (330)	N/A	30.9 (2.0)	6.4 (1.5)	0.39
05/16/2017	28.2	12,000 (430)	N/A	26.5 (2.8)	6.1 (4.2)	0.29
03/09/2016	30.2	23,600 (600)	–4.6	23.4 (2.2)	3.7 (3.1)	0.52
05/03/2017	31.2	18,000 (730)	N/A	25.4 (2.6)	6.3 (3.0)	0.35

[1]Stage measured at a temporary gage in 2016 (FRE.temp in fig. 6). For data collected in 2017, a –0.5-foot offset from the FRE gage was applied.

[2]Values are mean for all eight cross sections. Numbers in parentheses are standard deviations for the cross sections.

[3]Percentage of unmeasured discharge that was extrapolated to riverbanks, water surface, and riverbed.

[4]Refer to figure 7 for location of these gages.

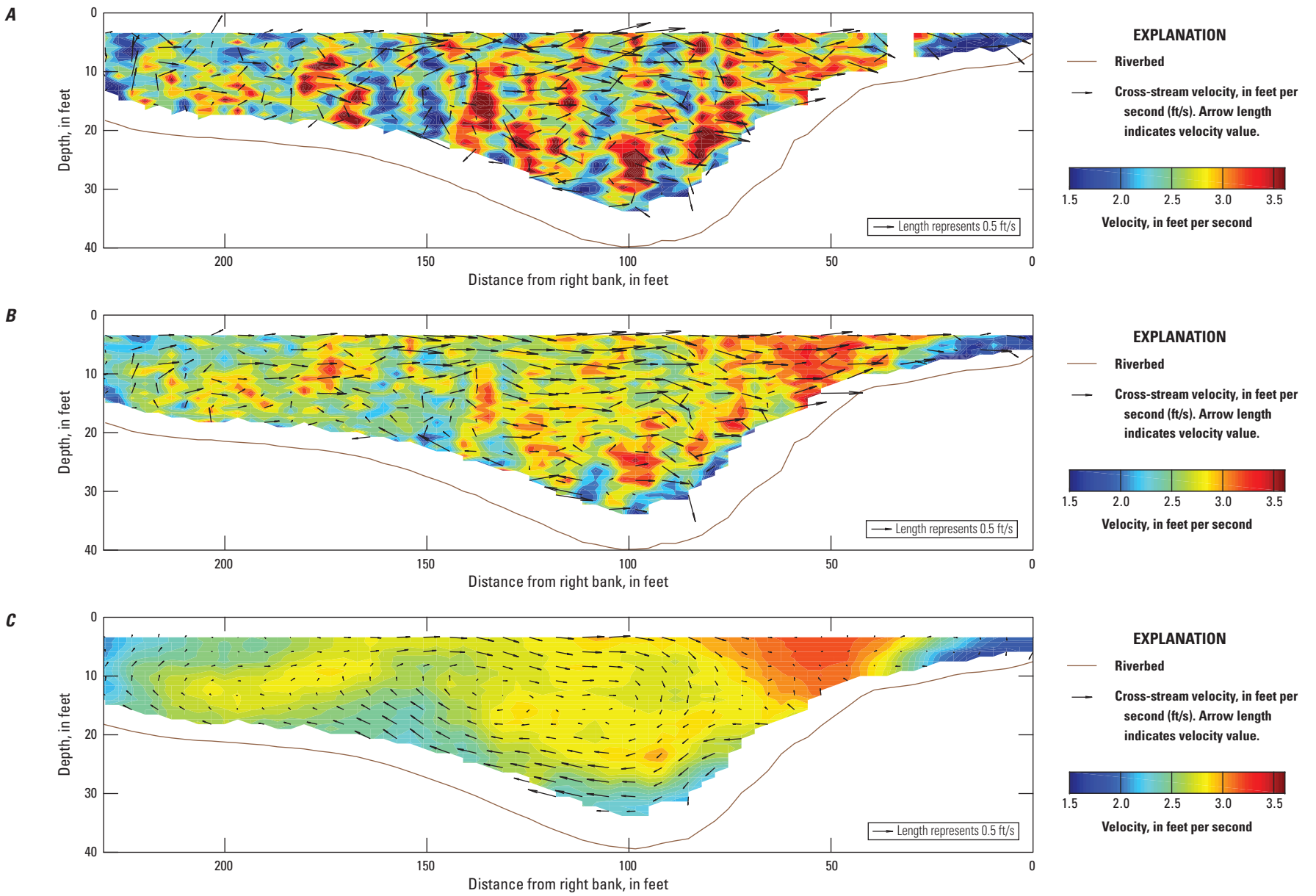

Figure 9. Cross-sectional velocity profiles for transect 5 along a bend in the Sacramento River near the Fremont Weir, California, March 30, 2016. Colored contours are along-stream velocities and arrows indicate a cross-stream velocity of 0.5 foot per second for *A*, 1 transect; *B*, 4-transect average—no smoothing; and *C*, 4-transect average with horizontal and vertical smoothing windows of 3 and 2 bins, respectively. Data are shown for a stage of 24.2 feet and discharge of 15,900 cubic feet per second.

The velocity transects were processed to extrapolate velocity vertically (to the riverbed and water surface) and horizontally to the riverbanks. A widely accepted technique uses either a power law or log law to extrapolate velocity in the vertical direction. The one-sixth power law was used for this application for several reasons: (1) it is insensitive to noisy data (Simpson, 2001); (2) it is the most widely accepted method that describes a wide range of flows (Chen, 1991); and (3) it has been adopted as a default processing protocol for USGS measurements unless the data warrant other power fits (Mueller, 2013).

There are several techniques that are used to extrapolate velocity near the banks. A standard technique is to use the ratio method, where the ratio of the water velocity to the square root of the depth is assumed to be constant for the unmeasured portion near the banks (Simpson, 2001). The ratio method is a form of the Froude number that assumes the ratio of kinetic to potential energy remains constant through the cross section (Le Coz and others, 2008). Although this method might be adequate for applications to estimate one-dimensional river discharge, it was not chosen for several reasons. First, the assumption of constant ratio was not valid at these cross sections based on analysis of measured regions, and secondly, tests of this method have qualitatively shown that the velocity estimates could be substantially biased at some cross sections using this approach. More sophisticated methods exist that use a modified momentum equation that requires a turbulence closure model (Nihei and Kimizu, 2008), or bed roughness length that requires knowledge of grain size and composition of the riverbed (Hoitink and others, 2009; Sassi and others, 2011). Given that the data were not available to correctly parameterize these methods and the percentage of discharge near the riverbanks was on the order of 5 percent or less compared to the total discharge, more sophisticated methods were unwarranted for this analysis.

The one-sixth power law was used to extrapolate velocity near the banks in the horizontal direction, and this method produced qualitatively good results for all cross sections, but there was not a way to validate this method. Several cross sections near the river bend were visually analyzed where the velocity deficit extended well into the cross section, but this is likely due to flow separation and recirculation zones created by the river bend and not an extrapolation error. Additionally, some of the cross sections did not have typical vertical distributions of velocity, where the highest velocity was near the surface and gradually decreased in the water column before rapidly decreasing near the bed. In some cases, particularly near the river bend, the highest velocities were near mid-depth or deeper. Typical practice in velocity extrapolation is to fit the whole profile to a power curve and extrapolate the top, bottom, and near-bank velocities. Because the hydrodynamics were complex enough in this study area, these values were extrapolated on the basis of the last measured values for the top, bottom, and near-bank velocities. An example of the measured and extrapolated along-stream velocities in relation to the riverbed is shown on figure 10. Once a full three-dimensional velocity profile and bathymetry were properly defined, the discharge at each cross section was computed by numerical integration.

Because the Rozovskiĭ method was used in the velocity transect processing, the lateral discharge at a cross section is not zero, but is small enough (typically less than 1 percent of total river discharge) that only the velocity in the along-stream direction was used to compute discharge. Table 4 shows the statistics for the discharge estimate for each velocity transect. For the set of eight cross sections, the average discharge was in close agreement with the index-velocity calculated discharge (under 7-percent difference for all conditions measured), and for each transect the discharge was within 4 percent of the average for that set of transects. A set of transect measurements were therefore, internally consistent for a given condition, and the mean along-river discharge was accurate compared to the discharge estimate using the index-velocity method. The range in the percentage of unmeasured discharge was roughly between 25–35 percent, and the unmeasured percentage generally decreased as the river stage increased. Most of the unmeasured discharge was in the vertical extrapolation because the unmeasured discharge near the riverbanks was 6 percent or less for all cross sections. Errors that arose from the vertical extrapolation likely did not bias the entrainment estimates because these errors were likely similar throughout the cross section. Entrainment prediction errors that propagated from errors in riverbank estimates and velocity extrapolation are discussed in more detail in the "Effect Due to Uncertainty in Bank Estimates" section.

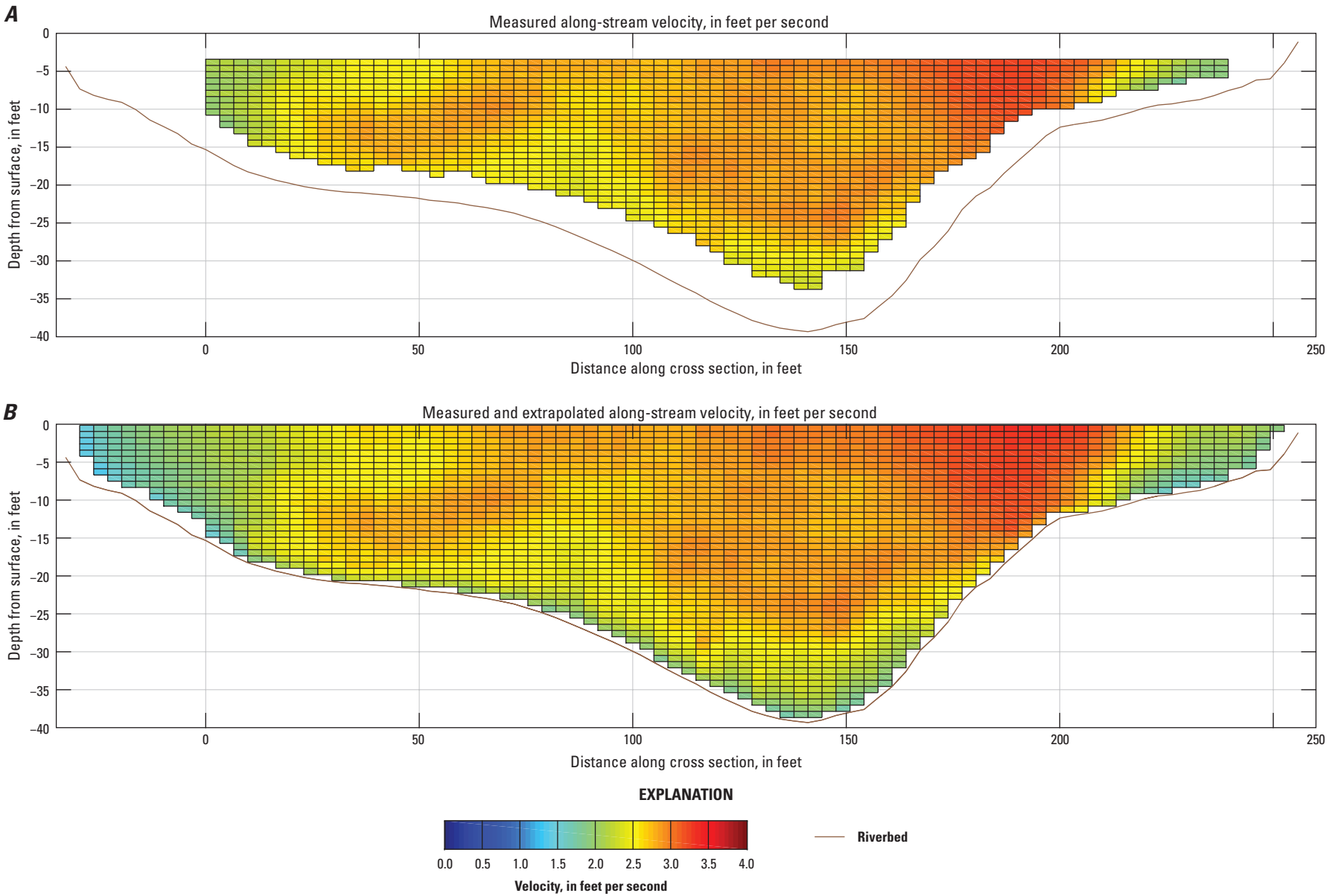

Figure 10. Measured and extrapolated along-stream velocity on the numerical grid used to integrate the discharge at cross-section 5 at a stage of 24.2 feet and discharge of 15,900 cubic feet per second: *A*, measured, averaged, and smoothed velocity in the along-stream direction; and *B*, same as "*A*," with velocities extrapolated to the surface, streambed, and near the riverbanks.

Analysis of Hydrologic Conditions on the Sacramento River Near the Fremont Weir

Hydrologic conditions near the western end of the Fremont Weir were assessed using discharge data collected in the 2016 YBUS study combined with historical discharge records from a number of sites upstream and downstream from the study site. First, the hydrologic results from the 2016 study are presented, and the observations of backwater at the study site are discussed. Outflow from the Sutter Bypass was estimated using equation 1 because this boundary condition is not gaged. Next, a statistical model to predict discharge of the Sacramento River near the Fremont Weir was developed to examine the variability in the stage-discharge relation for a 27-year period. It was important to understand and quantify the variability in the stage-discharge relation at this location because it had a significant effect on entrainment predictions.

Discharge Estimates From 2016 Measurements

Results of discharge estimates from field measurements on the Sacramento River near the Fremont Weir, and an estimate of the Sutter Bypass outflow using a mass-balance approach, are presented in this section.

Sacramento River Discharge Estimate Near the Fremont Weir

Discharge of the Sacramento River was estimated 1.24 miles upstream from the western end of the Fremont Weir (FRE.temp; Sacramento River above Fremont Weir near Knights Landing) using the stage-discharge and index-velocity methods. The stage-discharge and index-velocity regressions are shown on figure 11, and a summary of discharge measurements and discharge estimates from the two techniques are shown in table 2. Compared to the moving boat discharge measurements used to develop the regressions, neither method shows bias in predicting discharge, but on average, the index-velocity method produces a lower average absolute error of 3.0 percent compared to 5.9 percent for the stage-discharge method.

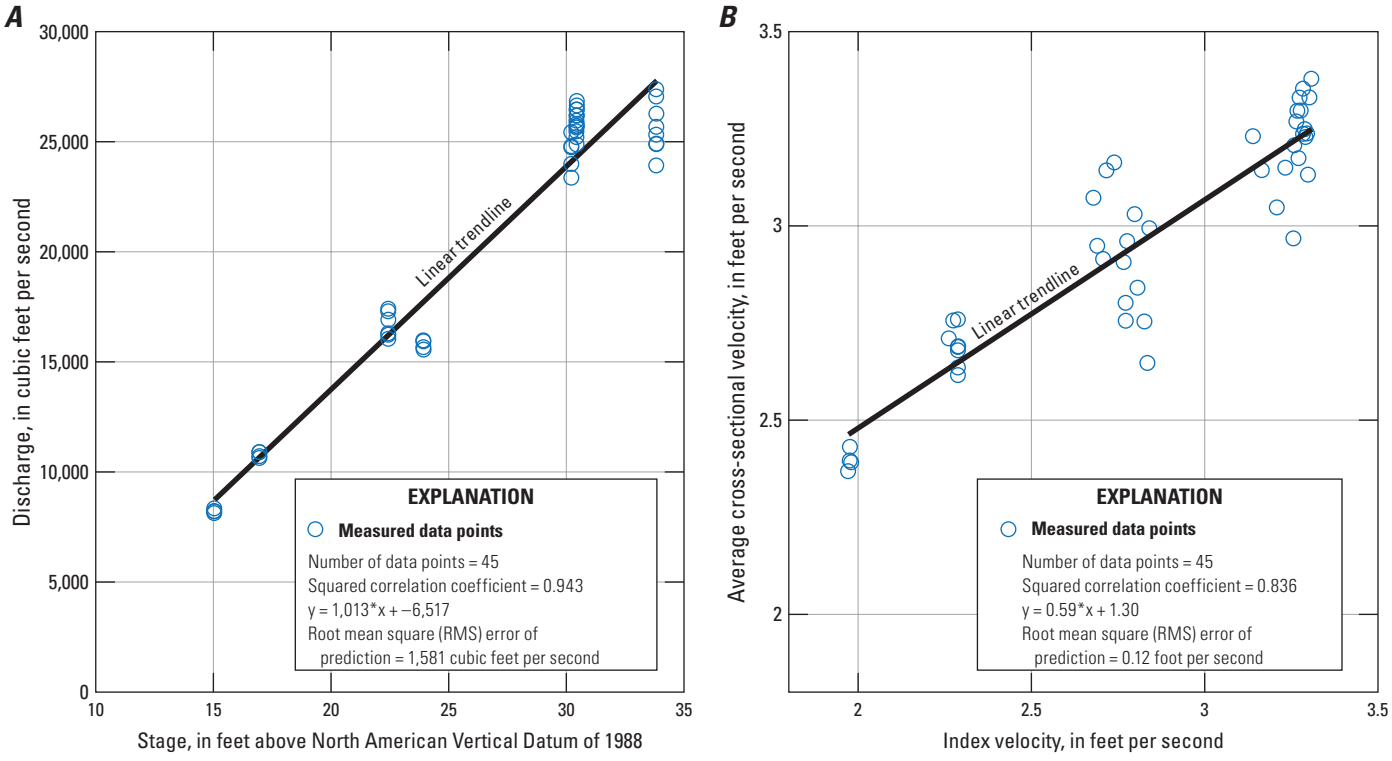

Figure 11. Discharge and velocity estimates during the 2016 data-collection period (January 22–April 22, 2016) at the temporary gage (FRE.temp) Sacramento River above Fremont Weir near Knights Landing, California: *A*, discharge measured with a moving boat versus measured stage; and *B*, average cross-sectional velocity computed from moving boat measurements versus measured index velocity.

There are several well-known sources of instrument, measurement, and computational errors in discharge estimates using both techniques (Simpson, 2001). Generally, a plus or minus 10-percent error between discharge estimates (based on the regression methods) compared to the measured discharge is considered reasonable. The index-velocity method has a lower incidence of measurements outside of the 10-percent error band—2 percent compared to 16 percent of the measurements obtained from the stage-discharge relation. It was concluded that for the period of study, the index-velocity method produced a better estimate of discharge on the Sacramento River near the Fremont Weir.

The difference between the stage-discharge and index-velocity methods is greatest during the rising limb of the hydrograph, a time when juvenile salmon outmigration typically peaks. While the bulk of the discharge data estimated by both methods are in reasonable agreement, a notable discrepancy occurred after March 6, 2016, during the rising limb of the hydrograph when the stage-discharge rating overpredicted discharge by as much as 4,000 ft^3/s or about 40 percent (fig. 12). Initially, when the stage increased at the western end of the Fremont Weir, there was a corresponding decrease in the index velocity. Non-linearity in the relation between water velocity and stage on this date was evidence of backwater effects due to increased flow from the Sutter Bypass and (or) Feather River.

Sutter Bypass Outflow Estimate

The Sutter Bypass outflow estimate and discharge hydrographs used to compute the estimate are shown on figure 13. The magnitude of the Sutter Bypass outflow is shown as a range due to the estimated range in discharge for the Bear River and NCC. During baseline conditions (most of February and April), flow in the Sutter Bypass outflow is generally lower than in the Feather River system. When flows are higher, the magnitude of the Sutter Bypass outflow is equal to or greater than the Feather River system, except for two periods when there was a significant increase in the Feather River, and the Sutter Bypass outflow estimate went close to, or below zero. This is an unrealistic estimate, as it is likely that either (1) some portion of the Feather River flow enters the Sutter Bypass, or (2) that the peak flow from the Feather River is attenuated and has a longer tail close to its junction with the Sacramento River, due to backwater effects from the Sacramento River and Sutter Bypass outflow.

As a first-order check on the accuracy of the SUT outflow estimate, the estimates for inflows and outflows for the Sutter Bypass from mid-January to the beginning of February were examined (fig. 14). The main inputs for the Sutter Bypass are the Butte Basin inflow, the Colusa Weir (CLW), and the Tisdale Weir (TIS; fig. 7). Discharge of the Feather River increased on January 18 and 30, which could account for a portion of the Sutter Bypass outflow; otherwise, the bulk of the outflow from the Sutter Bypass was assumed to be due to inflow from the Butte Basin and upstream weirs on the Sacramento River. Integrating the estimated inflow and outflow for this period showed that the cumulative outflow was overestimated by a factor of three compared to the inflow estimate, so there were either inputs unaccounted for into the Sutter Bypass (some portion of the Feather River or uncontrolled runoff from Butte Basin) or inputs unaccounted for in the mass-balance equation (eq. 1) used to estimate the Sutter Bypass outflow. The Sutter Bypass outflow estimate was likely more accurate when the magnitude of flow in the Feather River was lower and there were not rapid increases in the hydrograph. It was assumed that during these conditions all of the inflows were accounted for; therefore, the mass-balance equation was more accurate. The peaks in the Sutter Bypass outflow were of lower magnitude and lagged behind the peaks in the Sutter Bypass inflow, which was expected from storage and increased travel time in the Sutter Bypass.

Causes of Backwater Conditions Near the Fremont Weir

The combined effects of increased discharge on the Feather River and Sutter Bypass outflow can cause backwater conditions on the Sacramento River near the Fremont Weir. The Feather River discharge increased from 4,000 to 25,000 ft^3/s, 16 hours before a corresponding increase on the Sacramento River on March 7, 2016 (fig. 13). The Sutter Bypass outflow increased, but the estimated magnitude was likely incorrect for this period, as discussed previously. Additionally, the river level on the Sacramento River was not high enough to engage the upstream Sutter Bypass weirs, so the contribution of the Sacramento River to the Sutter Bypass outflow was likely minimal during this period. Therefore, for this event, it was concluded that the Feather River was likely solely responsible for the backwater effects observed on the Sacramento River near the Fremont Weir.

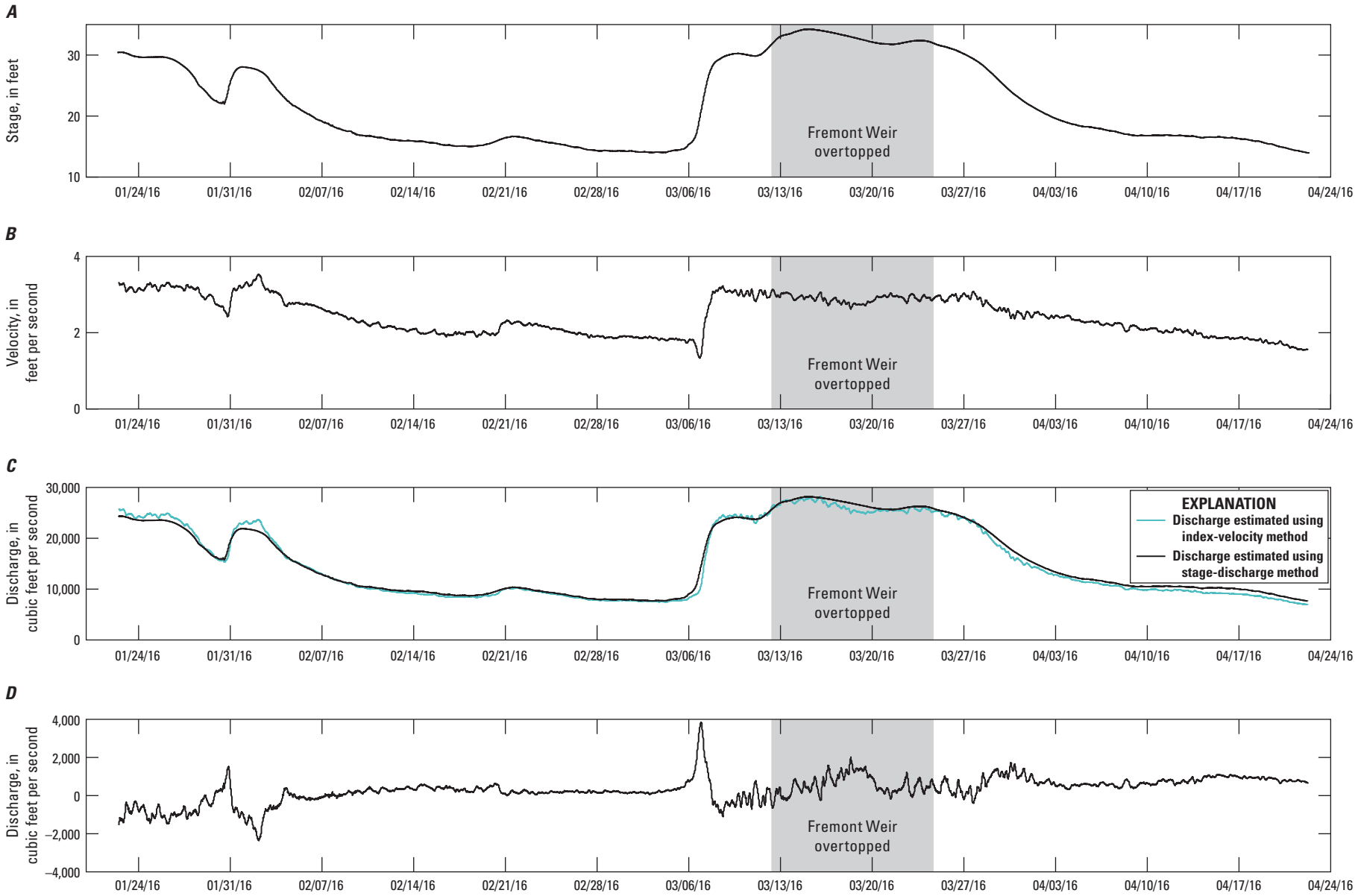

Figure 12. Time series of hydrodynamic measurements at the temporary gage (FRE.temp) along the Sacramento River near the Fremont Weir, California: *A*, river stage; *B*, measured water velocity; *C*, discharge estimated using the stage-discharge and index-velocity methods; and *D*, difference in discharge using the index-velocity and stage-discharge methods.

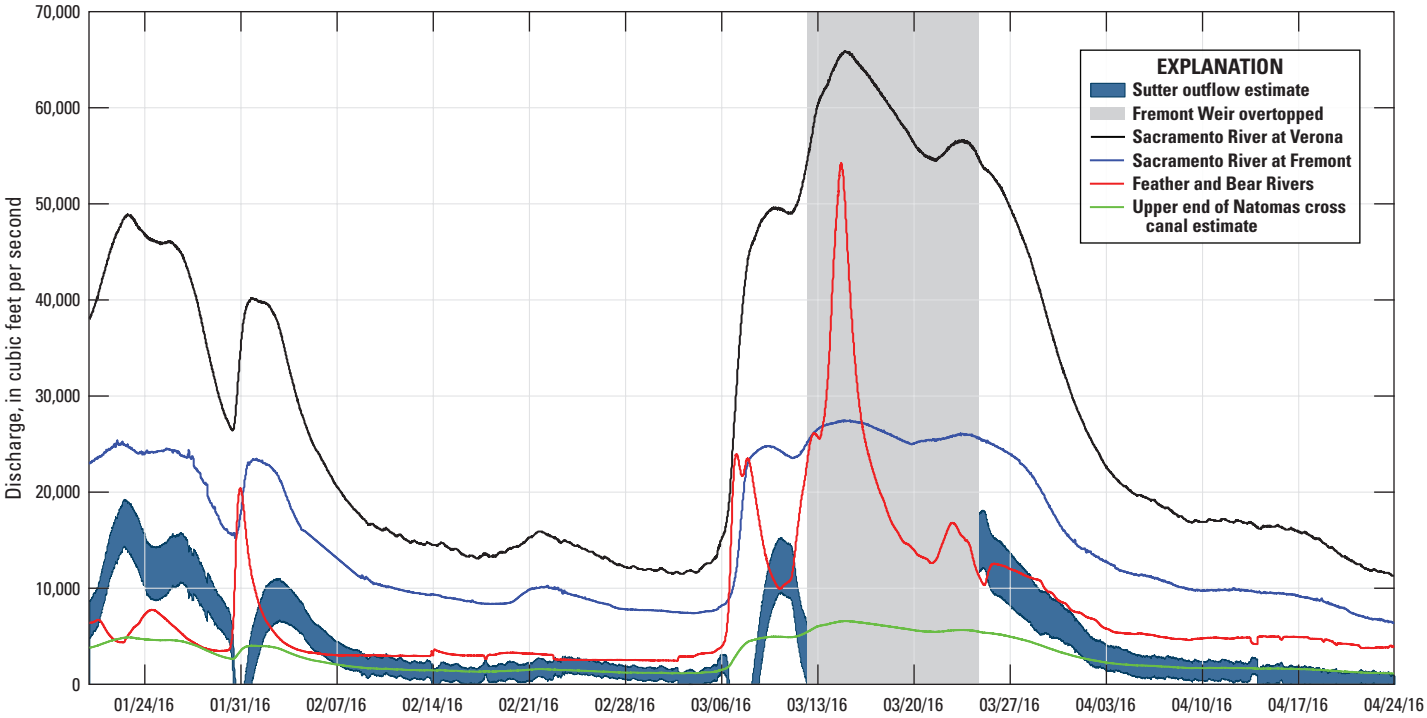

Figure 13. Time series of hydrographs at gaging stations used to estimate Sutter Bypass outflow, flow in the Sacramento River at Fremont Weir and at Verona, the Feather and Bear Rivers, and flow in the Natomas cross canal, California.

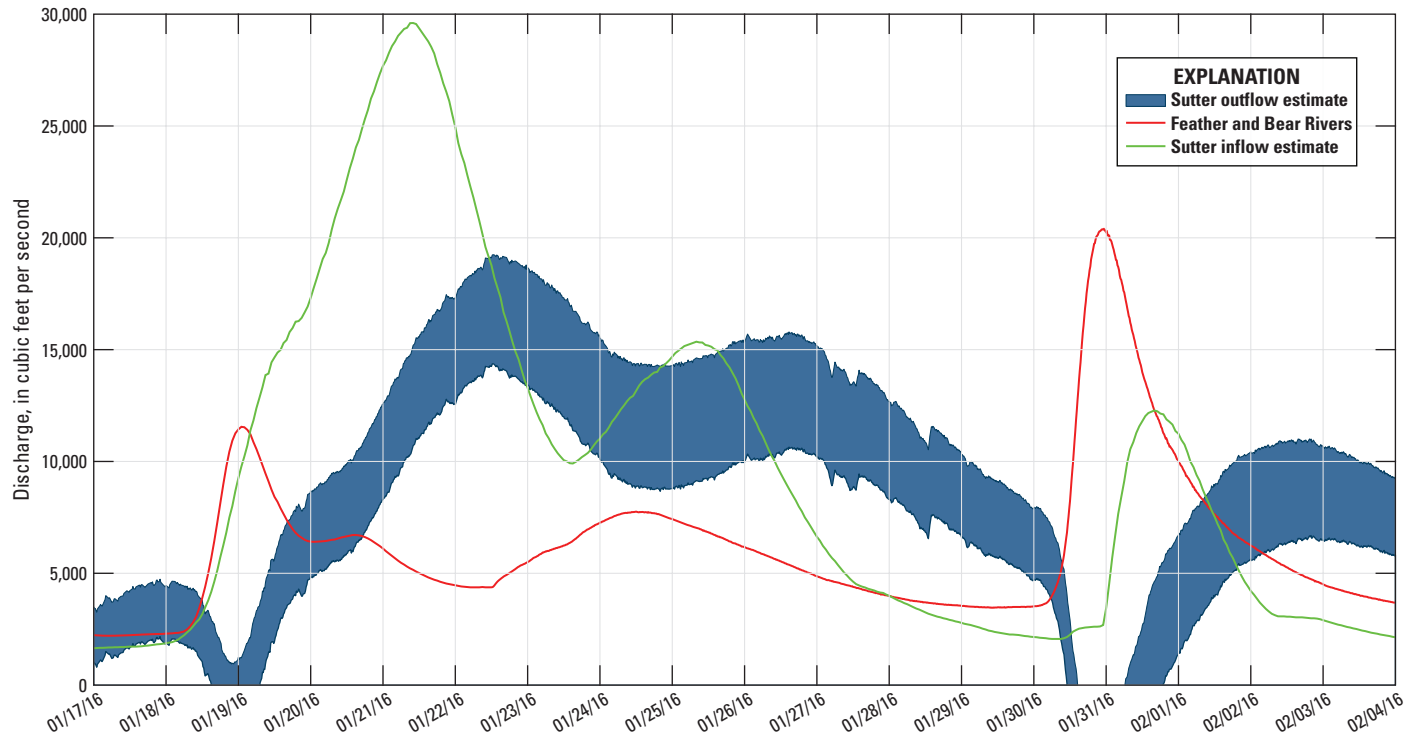

Figure 14. Time series of inflow and outflow estimates for the Sutter Bypass compared to the Feather and Bear Rivers, California, from January 17 to February 4, 2016.

Discharge events on the Feather River were flashy and short lived, compared to discharge events on the Sacramento River, which were generally longer in duration and steadier (fig. 13). The magnitude of variability in Sacramento River discharge, as observed at the FRE.temp station, caused by the Feather River was greater than that caused by the Sutter Bypass, but the Sutter Bypass outflow typically was longer duration so the integrated effect of outflow from the Sutter Bypass might have been greater overall. Furthermore, the area of discharge for the Sutter Bypass into the Sacramento River was likely spatially variable as a function of outflow magnitude. The width of the Sutter Bypass is about 4.5 mi along the Sacramento River. The eastern side of the Sutter Bypass near the Sacramento and Feather River junction exchanged water with the Sacramento River at lower magnitudes of Sutter Bypass outflow, but as the Sutter Bypass outflow magnitude increased, the outlet near the Fremont Weir became engaged. An estimate of the water level at which this occurred was not possible, and it is worthy of investigation because this exchange likely affected the local hydrodynamics in the Sacramento River at this location.

The magnitude and duration of flow on the Feather River and Sutter Bypass outflow shows that both of these boundary conditions are needed for two reasons: (1) to accurately characterize the hydrology of this region, whether this be with field data or hydrodynamic models, and (2) to understand the degree of variability in the stage-discharge relation for the Sacramento River in the vicinity of the Fremont Weir, which is needed to accurately make entrainment estimates.

Statistical Model to Predict Discharge on the Sacramento River Near the Fremont Weir

The range of conditions in 2016 did not include the full range of variability in backwater effects, and therefore, variability in the stage-discharge relation that exists at this location. A statistical model to predict discharge on the Sacramento River near the western end of the Fremont Weir was developed to assess the range of variability in the stage-discharge relation in the historical data. Historical data and data collected in 2016 were used to estimate discharge near the Fremont Weir for a 27-year period (April 1990 to April 2017). Hourly historical stage data on the Sacramento River near the Fremont Weir (FRE) are available back to 1984, stage and discharge data for Sacramento River below Wilkins Slough (WLK) are available back to 1987, and stage and discharge data for the Sacramento River at Verona (VON) are available back to April 1990 (table 1). Daily data existed for these gages before the dates mentioned earlier, but were not used for this analysis because river stages in this region can change greatly over a daily time step. For example, stage at FRE often increases at a rate of 0.4 foot per hour during flow pulses. Predicted discharge was output at hourly time steps for the 27-year period to match the sampling frequency of data collected at FRE. Stage data at WLK and VON were lag corrected to account for travel time. Discharge data at the temporary Fremont Weir gage (FRE.temp) for 2016 showed no lag compared to VON, so historical WLK discharge data were lag corrected to VON. The average lag correction from WLK to VON was about 12 hours for an approximate 37-mile stretch of river.

Five predictor variables (X) were used for the response variable (Y) in the development of the statistical model for discharge:

$X1$ = Stage at FRE
$X2$ = Discharge at WLK
$X3$ = Discharge at VON
$X4$ = Stage difference: WLK–FRE (water-surface slope)
$X5$ = Stage difference: FRE–VON (water-surface slope)
Y = Discharge at FRE.temp

The $X4$ and $X5$ variables were used in the regression because all surface-water flows are driven by barotropic pressure gradients (in this case the water-surface slope). A stepwise linear regression was used in the Matlab statistical toolbox to determine the best model from the predictor variables (MathWorks® Inc., 2017). The stepwise regression is a procedure to automatically choose the best predictor variable by systematically adding or removing terms based on their statistical significance to the response variable. The Matlab function—stepwiselm—used a forward and backward regression; at each step in the regression, terms were added or removed based on minimizing the sum of the squared error using the p value of an F-statistic to select the optimal model. The final model equation and Matlab output is provided in the appendix, and has 15 terms in 5 predictor variables, which include products of pairs from almost all distinct predictors, has an R^2 of 0.998, and a root mean square error of 361 ft^3/s.

The linear regression model developed from stepwise regression explains much of the variability ($R^2 = 0.998$) in the 2016 observed data at FRE.temp (fig. 15). Most of the variability in model residuals was likely due to the noise in the velocity data used in the measured discharge estimate. The range of measured discharge (6,900–28,400 ft^3/s) was narrower than the range of predicted discharge (3,800–32,600 ft^3/s), but the extrapolated discharge was likely outside the range of operable notch stages and discharge, given that the range of discharge measured in 2016 spanned Sacramento River stage values lower than 19 ft (minimum stage for the notch stage-discharge rating), to Sacramento River stage values higher than the crest of the Fremont Weir (32.5 ft). The discharge at FRE.temp was generally less than at WLK for higher stage/discharge conditions due to backwater effects. On the hydrograph recession, the discharge at FRE.temp increased above that at WLK as the backwater was released (fig. 16).

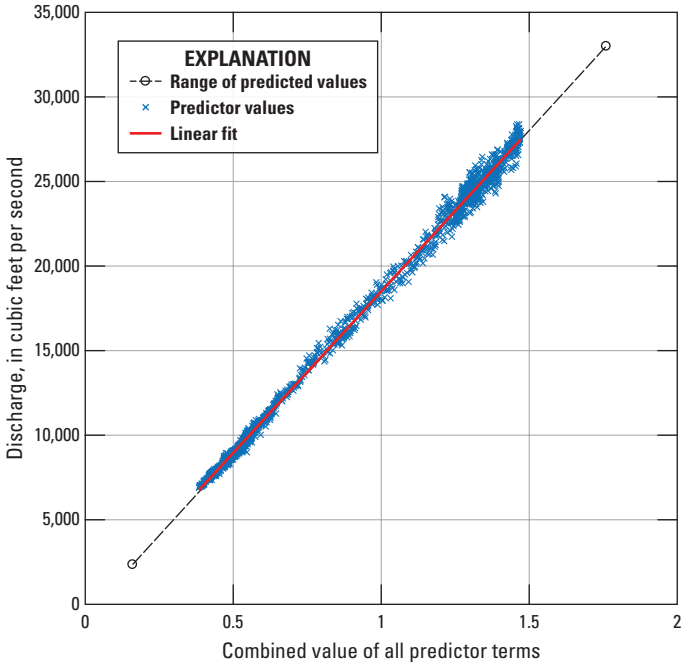

Figure 15. Fit of linear regression model used to predict discharge on the Sacramento River above Fremont Weir near Knights Landing, California.

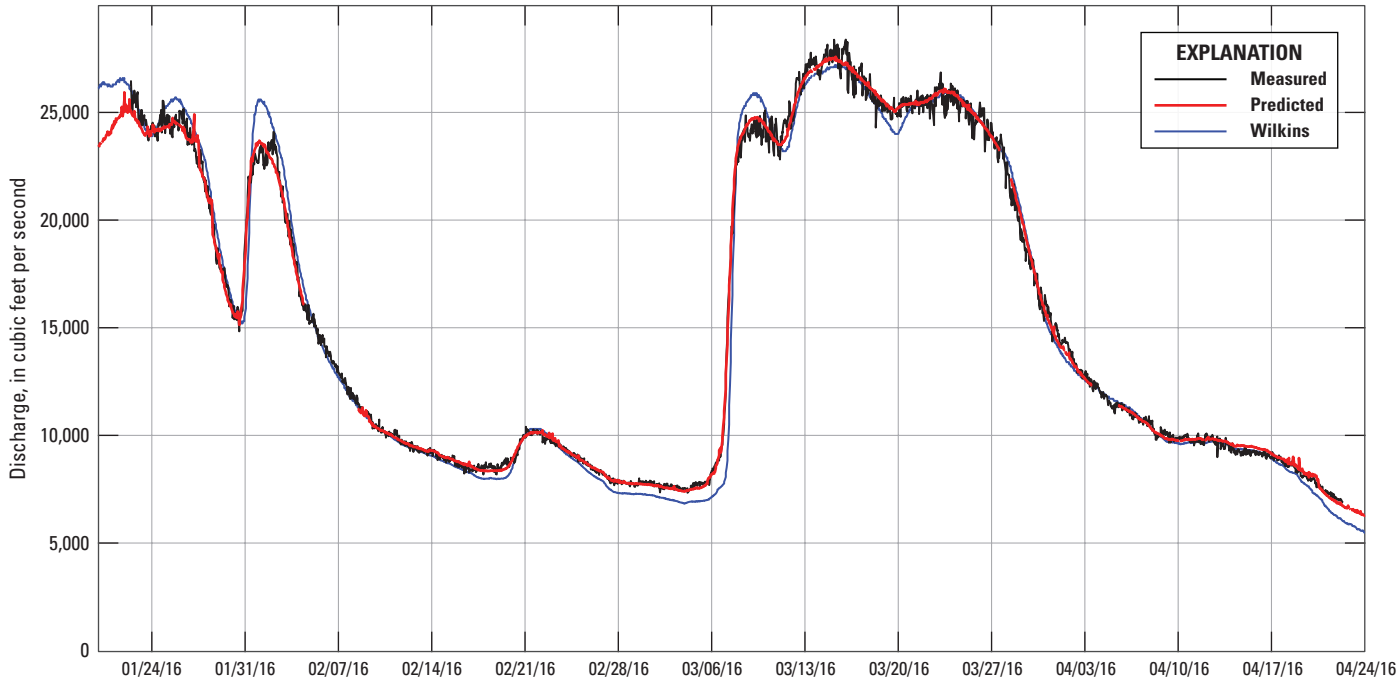

Figure 16. Discharge measured on the Sacramento River above Fremont Weir near Knights Landing, predicted discharge based on a linear regression model at the same location, and measured discharge of Sacramento River at Wilkins Slough, California, January 22–April 24, 2016.

Variability in the Stage-Discharge Relation

Variability in the stage-discharge relation near the western end of the Fremont Weir was due to backwater conditions caused by increased discharge from the Sutter Bypass and the Feather River. A first order approximation of the degree of backwater was made using the ratio (Qr) of the discharge at WLK (Q_{WLK}) to the discharge at VON (Q_{VON}):

$$Qr = \frac{Q_{WLK}}{Q_{VON}} \quad (2)$$

The discharge ratio was used to parameterize the variance in the critical streakline estimate (see "Variance Used in Hydraulic Entrainment Zone Calculation" section). The consequences of variability in the stage-discharge relation on the Sacramento River near the Fremont Weir are critical to notch design. River stage controls the notch flow, and the ratio of notch flow to the Sacramento River flow determines the fraction of Sacramento River discharge entrained into the notch, which in turn affects the juvenile salmon entrainment rate.

The degree of backwater near the Fremont Weir can be estimated if it is assumed that the discharge at WLK is upstream of backwater effects from the Sutter Bypass and Feather River. On the basis of the minimal scatter in the stage-discharge relation at WLK (not shown) this appears to be a reasonable assumption. The difference in discharge (Q_{VON}–Q_{WLK}) is equal to the combined discharge from the Feather River and Sutter Bypass. The Qr is therefore an estimate of the degree of backwater, where a ratio more than 0.5 signified more discharge from the Sacramento River, and a ratio less than 0.5 indicated more discharge from the Feather River and (or) Sutter Bypass and likely increased backwater effects on the Sacramento River near the Fremont Weir.

The probability of a given Qr for the 27-year historical record and for the 2016 data is shown on figure 17. The mean Qr of 0.58 for the historical record indicates that typically the Sacramento River has more discharge than the Feather River. The conditions measured in 2016 were closer to the mean (0.58), but there were some periods of backwater conditions (Qr less than 0.50), and some short periods where Qr was at or near the historical low value, indicating the highest degree of backwater. On the basis of the historical record, backwater conditions occurred less frequently than non-backwater conditions, but were still frequent enough that backwater had to be accounted for (Qr less than 0.5 occurred 24 percent of the time).

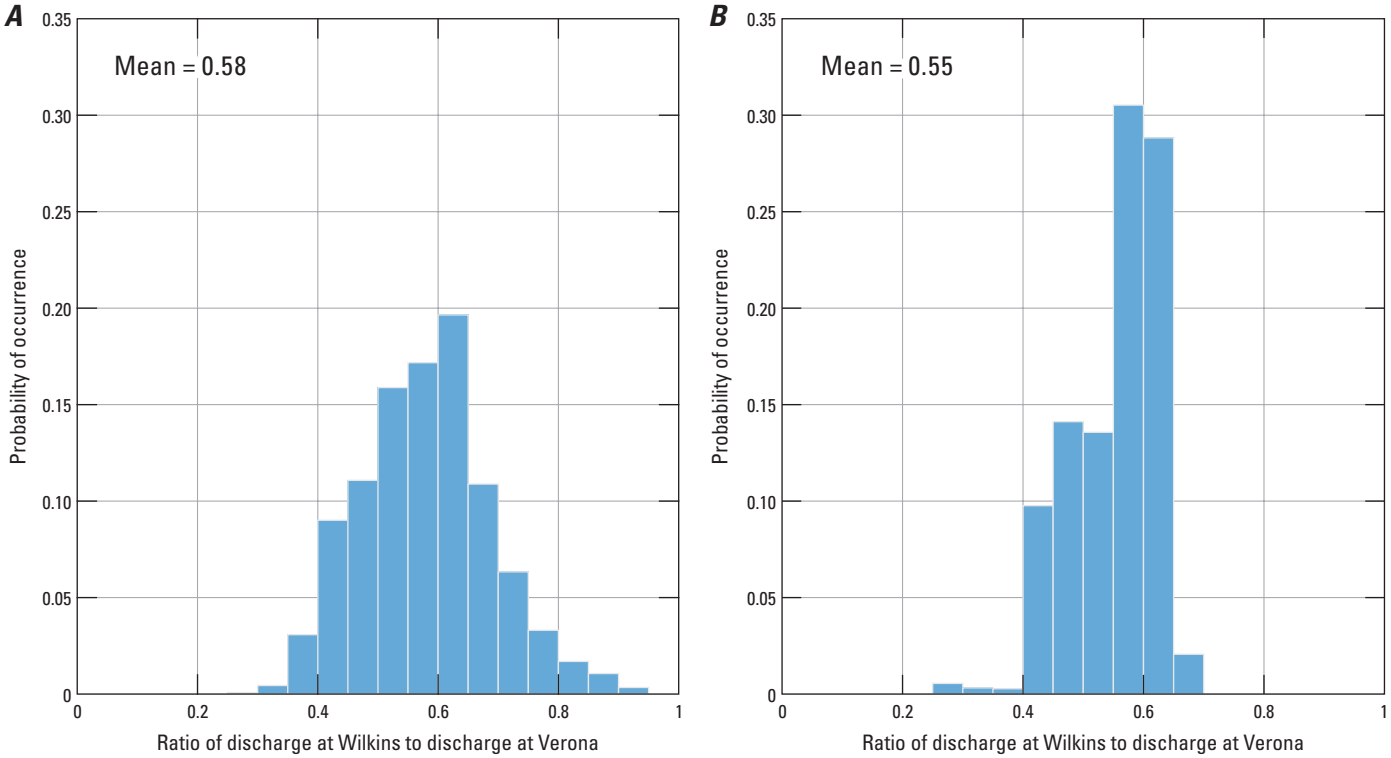

Figure 17. Probability of occurrence of the discharge ratio of Sacramento River at Wilkins Slough to the Sacramento River at Verona, California. The discharge ratio was used as an index for degree of backwater on the Sacramento River near the Fremont Weir: *A*, historical data from April 1990 to April 2017, for the period December 1–March 15, where western alternative notches will be operational; and *B*, data for the 2016 data-collection period (January 22–April 22, 2016).

Next, the variability in the stage-discharge relation and the frequency of occurrence based on the 27-year statistically modeled discharge and stage at the Fremont Weir were examined to determine the likely consequences of backwater conditions. For this analysis, a stage range of 19 to 32.5 ft and the period December 1–March 15 of an operable notch were used for the western alternatives (table 3). Figure 18 shows the statistically modeled discharge versus stage binned and colored to represent the number of occurrences, with the stage-discharge rating curve developed from 2016 data (see "Sacramento River Near Fremont Weir" section) overlain in black. This plot has several salient attributes. First, lower stages and correspondingly lower flow into the notch occurred more frequently. Second, at the lower and higher stages the frequency of discharge occurrence was in close agreement with what would be predicted by the stage-discharge curve, while at mid-range stage values the most frequent discharge was higher than what would be predicted by the stage-discharge curve. For the full range of stage, discharge was higher than what would be predicted by the 2016 stage-discharge curve. This indicates that backwater effects are less frequent, which is consistent with the bulk measure of backwater conditions. The stage-discharge rating curve developed from the 2016 data has a large range of discharge for higher stage values, so the rating curve could be more skewed toward measuring backwater effects. Likely, the true mean is not known because of the short duration of the 2016 deployment. Lastly, there was a considerable variability in the discharge for a given stage, on the order of 5,000 ft^3/s. Regardless of the true mean in the stage-discharge relation, the probability of not knowing the magnitude of flow for a given stage on the Sacramento River is fairly high if a stage-discharge rating curve is used to estimate discharge.

To quantify the influence that variability in the stage-discharge relation can have on entrainment, the variability in the ratio of river discharge to notch discharge was examined based on the notch stage-discharge ratings. Figures 19–21 are similar to figure 18, except the y-axis has the notch discharge ratio for each of the western alternatives colored by number of occurrences for a given stage and the discharge ratio predicted by the stage-discharge rating curve developed from the 2016 data. The notch stage-discharge rating curves show a constant flow at higher stage values (these values varying for alternatives 3, 4, and 6), which accounts for a decrease in flow ratio at the higher end of the curve. Similar to the stage-discharge plot, lower and higher stage values were in close agreement between the frequency of occurrence and what would be predicted by the 2016 stage-discharge rating curve. At mid-range stage values the central tendency of the estimated notch discharge ratio was generally lower than what the stage-discharge rating curve would predict for all alternatives. For alternatives 3 and 4, the variability in discharge ratio was on the order of 0.05 and for alternative 6, variability was on the order of 0.1, with a general increase in variability for higher discharge ratio values.

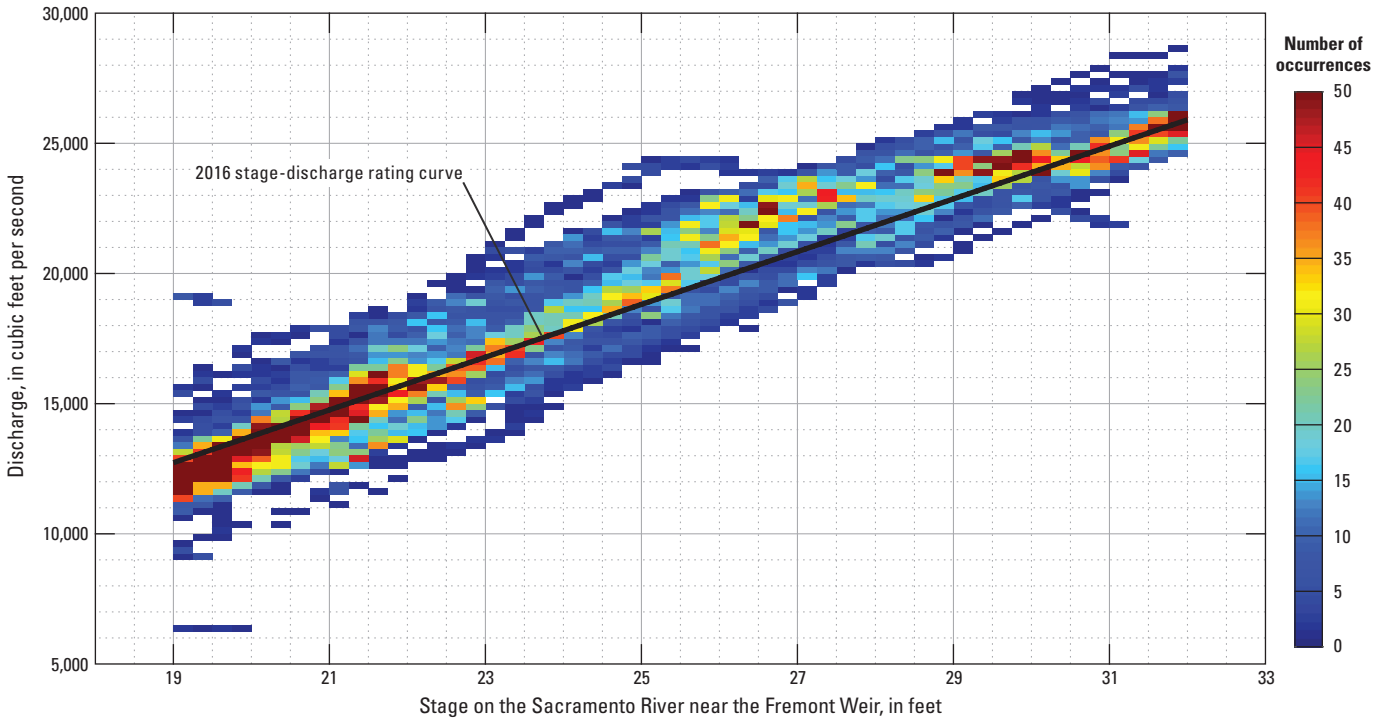

Figure 18. Discharge versus stage (19–32 feet) for the 27-year period (April 1990–April 2017) of modeled discharge on the Sacramento River near the Fremont Weir, California. Only data for the period December 1–March 15 of notch operation are included. Stage and discharge ratio are binned in 0.25-foot stage and 250 cubic foot per second discharge increments and colored by number of occurrences.

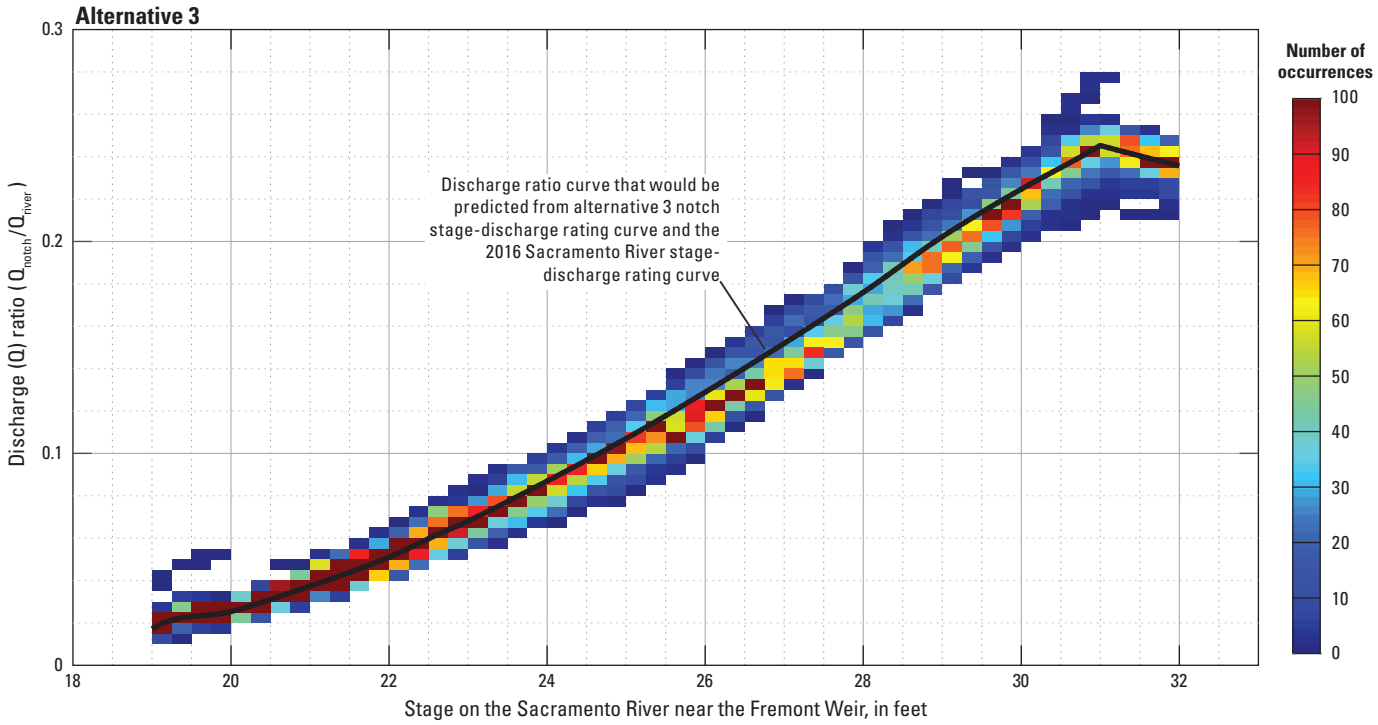

Figure 19. Discharge ratio (Q_{notch}/Q_{river}) versus stage (19–32 feet) for the 27-year period (April 1990–April 2017) of modeled discharge on the Sacramento River near the Fremont Weir, California, using the notch stage-discharge rating for alternative 3. Only data for the period December 1–March 15 of notch operation are included. Stage and discharge ratio are binned in 0.25-foot stage and 0.005 discharge ratio increments and colored by number of occurrences.

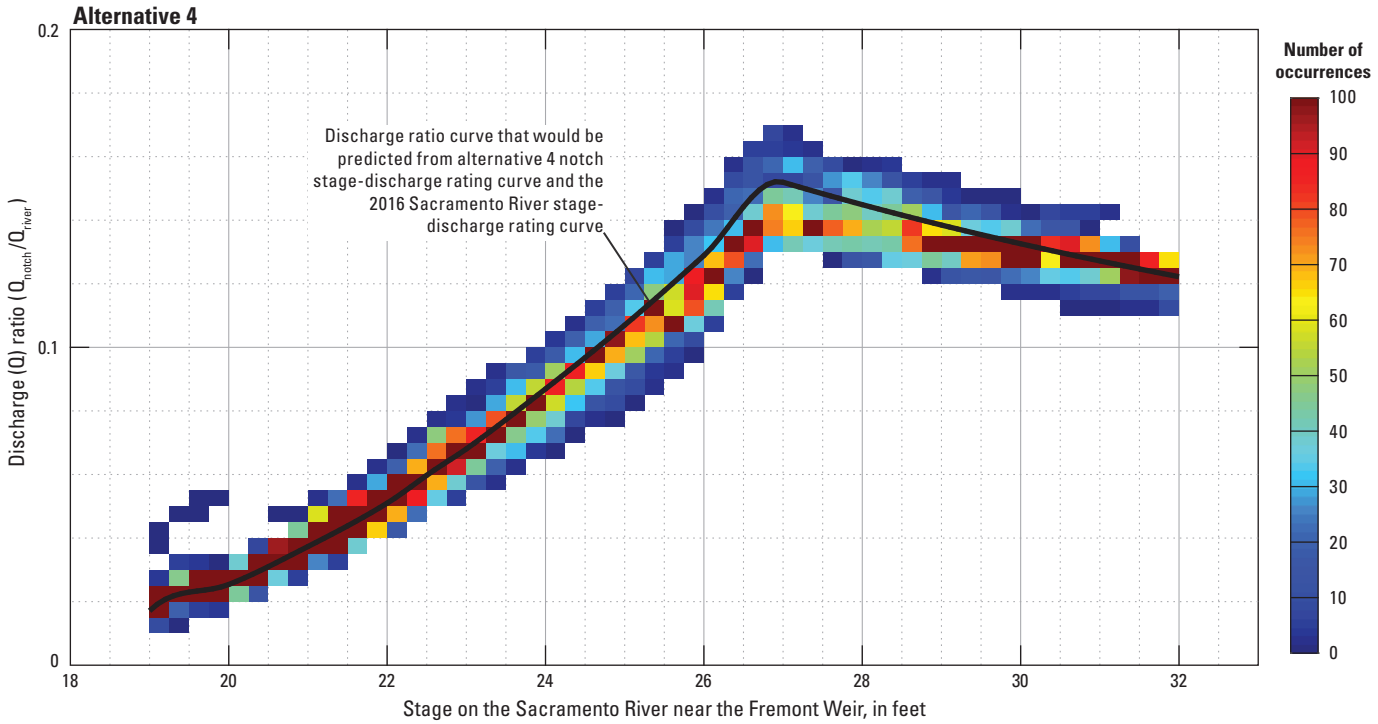

Figure 20. Discharge ratio (Q_{notch}/Q_{river}) versus stage (19–32 feet) for the 27-year period (April 1990–April 2017) of modeled discharge on the Sacramento River near the Fremont Weir, California, using the notch stage-discharge rating for alternative 4. Only data for the period December 1–March 15 of notch operation are included. Stage and discharge ratio are binned in 0.25-foot stage and 0.005 discharge ratio increments and colored by number of occurrences.

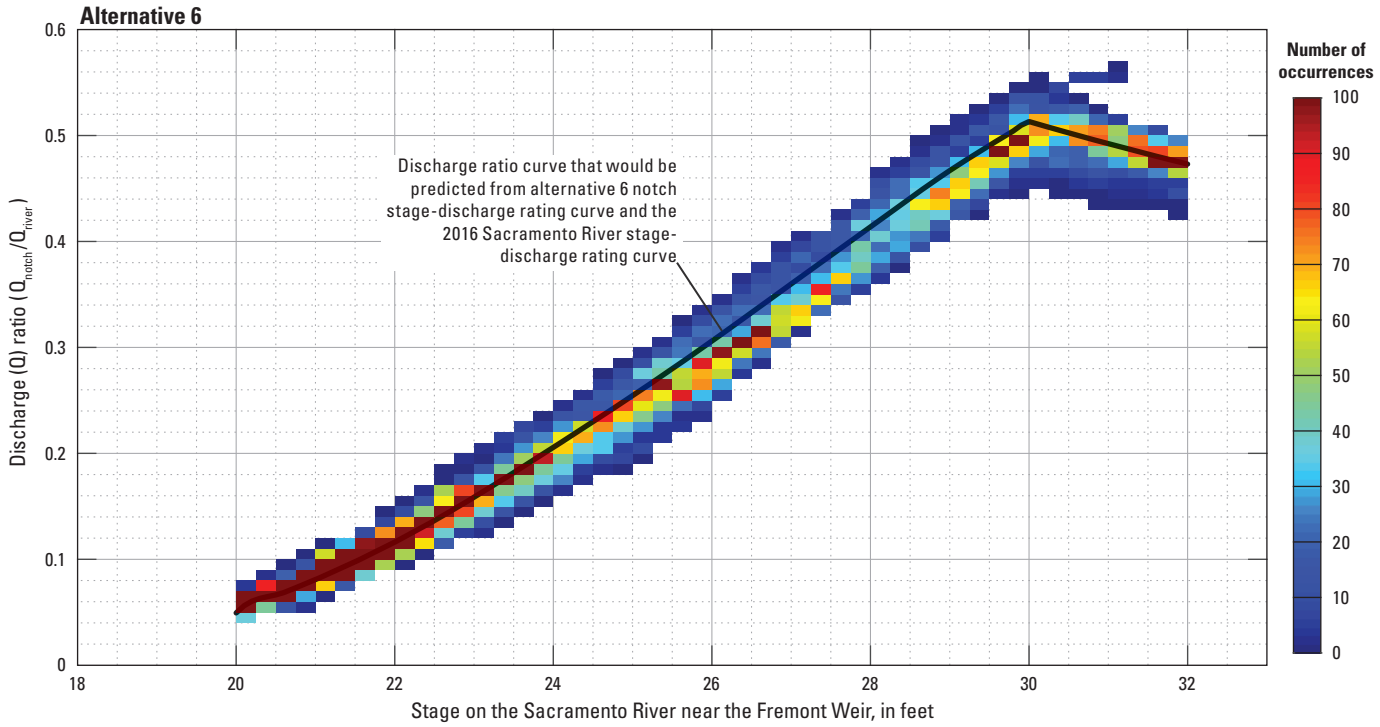

Figure 21. Discharge ratio (Q_{notch}/Q_{river}) versus stage (20–32 feet) for the 27-year period (April 1990–April 2017) of modeled discharge on the Sacramento River near the Fremont Weir, California, using the notch stage-discharge rating for alternative 6. Only data for the period December 1–March 15 of notch operation are included. Stage and discharge ratio are binned in 0.25-foot stage and 0.01 discharge ratio increments and colored by number of occurrences.

Integrating fish entrainment rates into a notch over time without knowing the variability or the true river discharge can seem unimportant because water entrainment into a notch will likely average out to the mean. However, in the context of maximizing population-level survival based on juvenile salmon entrainment into the notch that may happen over short periods (days to weeks), errors in water entrainment estimates may be magnified, fish entrainment may be grossly misestimated, and the direction of bias (either positively or negatively) will not be known.

In the "Hydraulic Entrainment Zone" section, the effect on entrainment estimates due to variability in the stage-discharge relation is discussed in greater detail. Generally, there are fairly sharp cross-stream gradients in fish distributions based on studies completed in the tidally affected Sacramento River and Georgiana Slough junction (California Department of Water Resources, 2012, 2015, 2016), so small changes in the discharge ratio could produce disproportionately larger changes in the number of fish entrained.

The authors postulate that the variability in the stage-discharge relation will have two effects. The first-order effect is that the magnitude of discharge at any particular stage will deviate significantly from the historical average discharge observed at that stage, as is shown on figure 18. The second-order effect is the velocity distribution at any particular stage will vary as a function of backwater conditions (see "Secondary Circulation at the Sacramento River Bend Near the Fremont Weir" section), and this effect can change the cross-channel distribution of discharge in a cross section. In the "Variance and Uncertainty in Hydraulic Entrainment Zone Estimate" section, it can be shown that the first-order effect on discharge can be reasonably accounted for, but the second-order effect on the velocity distribution and resulting cross-channel distribution of discharge in the river bend is more difficult to quantify.

Influence of Secondary Circulation on Velocity and Discharge Distributions

In the previous section the regional-scale hydrology using river-discharge data was examined and the conclusion was reached that there is a substantial amount of variability in the stage-discharge relation that can lead to errors in entrainment estimates if this variability is not taken into account. In this section the local-scale hydrodynamics at a river bend are examined, including multidimensional velocity and discharge distributions, and how these distributions vary as a function of river discharge, location along the river, and backwater conditions. Velocity transects taken along the river bend are used to (1) document the setup and relaxation of secondary circulation through the river bend, (2) investigate the variability and strength of secondary circulation over a range of discharge conditions, and (3) estimate the distribution of discharge at discrete cross sections. These results will be used to discuss the potential hydrodynamic influence on fish distributions along the 0.4-mile reach shown on figure 8.

Secondary Circulation at the Sacramento River Bend Near the Fremont Weir

The evolution of the velocity distribution and the strength of the secondary circulation for one stage and discharge condition is shown on figure 22. At the first cross section upstream from the bend, the channel was prismatic and the along-stream velocity distribution had a maximum (red values) near the center and a broad distribution of higher velocities. The secondary currents, indicated by the velocity arrows, are weak and there were no apparent coherent structures. Moving down river at cross-section 2, the velocity distribution was similar, and the secondary currents were a little stronger near the right bank. Moving farther into the river bend (cross-sections 3 and 4) the velocity distribution was more skewed toward the outside of the bend and the secondary currents were stronger (about 0.5 ft/s) with a significant down-welling zone and return flow along the bottom. In both of these cross sections the peak along-stream velocities were at a depth of about 18 ft, whereas the peak velocities at cross-sections 1 and 2 were near the surface. At cross-section 4 there was a narrow range of peak velocities compared to the preceding cross sections. At cross-section 5, the velocity distribution was still skewed toward the outside of the bend with a fairly strong and coherent secondary circulation cell, with the vortex in the center of the channel. The velocity distribution began to relax at cross-section 5, where strong velocities are apparent to the left of channel center. At cross-sections 6 and 7, the secondary currents were weaker and the higher velocities were more distributed through the cross section, but still slightly skewed toward the right bank. At cross-section 8, the channel was fairly prismatic, and the velocity distribution and secondary currents were similar to those in cross-sections 1 and 2, indicating relaxation of the secondary circulation and leftward shifting of the velocity distribution.

The strength of secondary circulation and velocity distribution also varied over the range of conditions that were measured (fig. 23). Data collected in 2016 at river stages of 15, 17, 22, 24, and 30 ft indicated there was little to no backwater influence, on the basis of the Wilkins to Verona discharge ratio (table 4). Data collected in 2017 at stages of 25, 28, and 31 ft evidenced significant backwater conditions. The banks of the river near the outside of the bend were overtopped at a stage of about 29 ft, and a large field between the river and the weir became inundated, so conditions measured at stages of 30 and 31 ft included effects of the overbank region. For conditions with neither backwater nor overbank flow (stages of 15, 17, 22, and 24 ft), the structure of the velocity profiles was qualitatively similar, with the peak along-stream velocity skewed toward the outside of the bend and the center of the circulation cell positioned close to mean depth at the center of the channel. However, the magnitude of along-stream and cross-stream velocity changed when either backwater or overbank flows were present.

For backwater present but no overbank-flow conditions, the velocity distribution and positioning of the circulation cell were similar at river stages of 25 and 28 ft, but the peak velocity was lower and the location of the down-welling zone was positioned closer to the center of the channel, as compared to river stages where no backwater was observed (river stages of 15, 17, 22, and 24 ft). For overbank conditions without and with backwater (river stages of 30 and 31 ft, respectively), the velocity profiles were different than for the previous conditions. Here, the peak velocity magnitude was close to the center of the channel, and there were two circulation cells to the left and right of the center of the channel (based on width) with the cell on the left located deeper due to the greater water depth. The salient feature for backwater and overbank conditions was a shift in peak velocity and down-welling zone toward the channel center. When the riverbank was overtopped, the transfer of momentum from the floodplain to the river (Morvan and others, 2002) increased the influence of the side-wall boundary layer, which caused a shift in the velocity distribution and location of secondary cells at river stages greater than 29 ft. For backwater conditions, both the along-stream and cross-stream velocity magnitudes were reduced compared to lower stage values; therefore, the strength of the secondary circulation cell did not have enough force to overcome the inertia of water mass near the riverbanks, which resulted in a shift in peak velocity and location of the down-welling zone. There were not enough data at discrete stage values to fully understand or quantify the range of variability in velocity distributions, but from the available data, it appears that backwater effects in the Sacramento River near the western end of the Fremont Weir resulted in significant observable first- and second-order effects on the cross-sectional velocity distributions at this river bend.

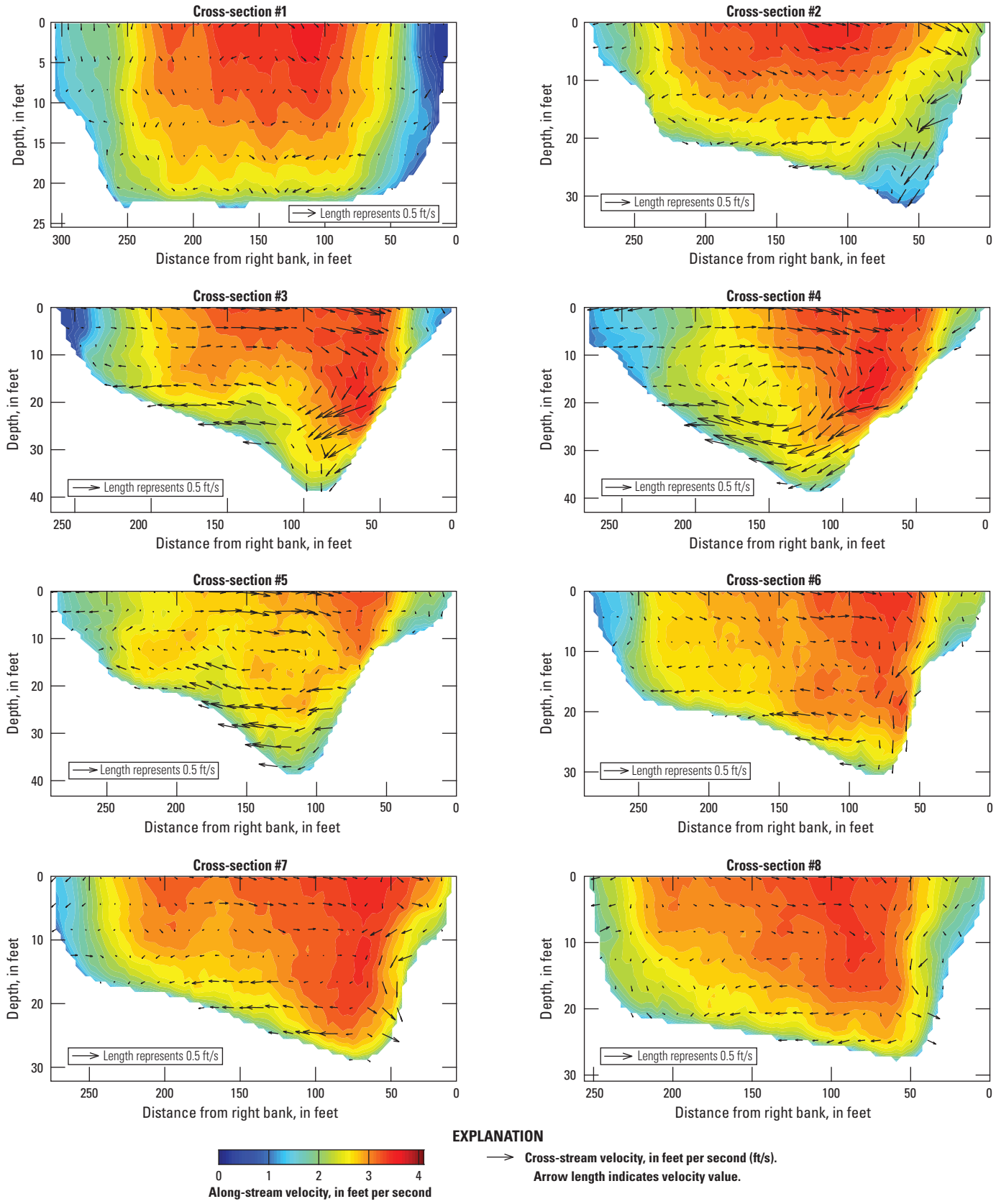

Figure 22. Velocity profiles along the Sacramento River near the river bend at the western end of the Fremont Weir, California, showing along-stream and cross-stream velocity in relation to depth and distance from the right bank. Profiles measured March 30, 2016, at a stage of 24.2 feet and discharge of 15,900 cubic feet per second.

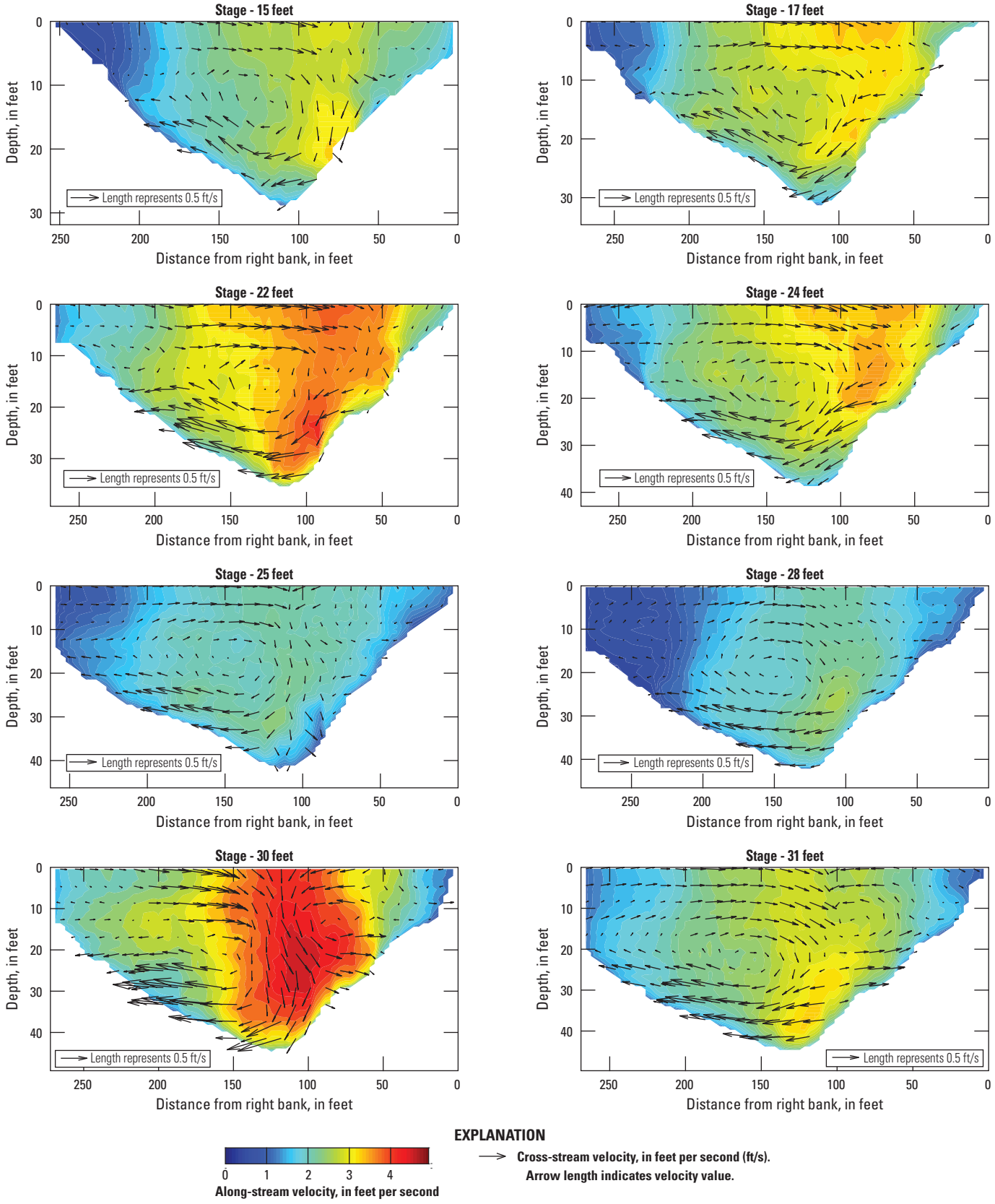

Figure 23. Velocity profiles for various stages at cross-section 4 along the Sacramento River at the western end of the Fremont Weir, California, showing along-stream and cross-stream velocity in relation to depth and distance from the right bank.

Discharge Distribution Along the River Bend

The conceptual model central to this analysis is that secondary currents will accumulate fish mass along the outside of the channel bend, such that notch locations can be optimized to maximize fish entrainment rates. The velocity distribution and magnitude of the secondary circulation were variable over the range of conditions measured, therefore, the rate of accumulation and the location of the peak in the fish spatial distribution varied as well (Blake and others, 2017).

As a first-order estimate, the ratio of the integrated cross-stream to along-stream velocity can be used to examine the concentration of discharge. The maximum surface layer velocity components at each cross section are presented on figure 24*A–C*. The along-stream velocities had a range of 2.3 to 4.6 ft/s, but did not increase monotonically with stage due to backwater conditions. There was minimal variability in the along-stream velocities for a given condition among the cross sections. The cross-stream velocities had more variability among the cross sections, but less variability across stage conditions. The cross-stream velocity increased and reached a maximum near the apex of the river bend (cross-sections 3–5) for all conditions, with a range of about 0.3 to 0.8 ft/s. The downward velocity showed a trend similar to the cross-stream velocity with a maximum near the apex of the river bend (cross-sections 3–5), but for some conditions there was a fairly uniform maximum along the river. The ratio of the mean cross-stream velocity to mean along-stream velocity is shown on figure 24*D*. For all conditions the discharge concentrated fastest at the river bend apex (cross-section 4) where secondary circulation was the strongest.

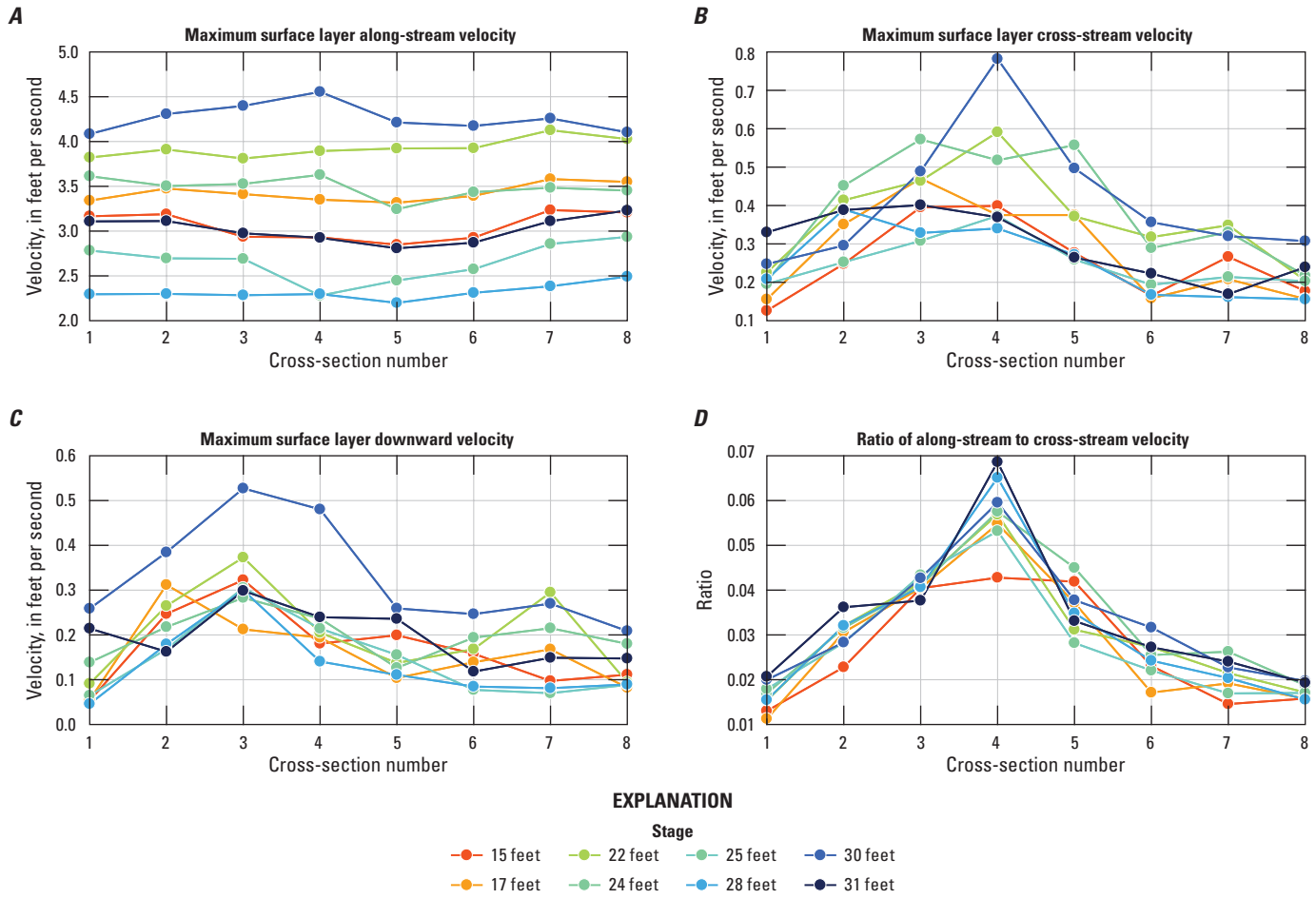

Figure 24. Surface layer velocity components in relation to stage at each cross section of the Sacramento River at the western end of the Fremont Weir, California: *A*, maximum along-stream velocity; *B*, maximum cross-stream velocity; *C*, maximum downward velocity; and *D*, ratio of mean cross-stream velocity to along-stream velocity.

The width of each cross section and the depth-integrated discharge along each cross section are normalized by using the maximum values of each per cross section to compare the cross sections and the range of conditions (fig. 25). The discharge profiles showed variability with respect to their shape and in the location of the peak flow over the range of conditions, but the following general pattern held: At cross-sections 1 and 2 the discharge profile was fairly normally distributed along the cross section, with total discharge divided about equally between the left and right halves of the river width. At the apex of the river bend (cross-sections 3–5) the discharge was skewed slightly toward the outside of the bend, and the shape of the discharge profile changed with a narrower zone of high discharge. Just downstream from the apex of the bend, at cross-sections 6 and 7, the discharge was skewed more toward the outside of the bend, but the cross-stream range of higher discharge was broader. By cross-section 8 the discharge was still skewed toward the outside of the bend, but the cross-stream range in higher discharge was closer to what was seen in cross-sections 1 and 2. At this river bend the secondary currents distributed the highest along-stream velocities toward the outside of the bend near the bend apex, but the maximum river depth was near channel center, resulting in discharge profiles that are only slightly outward-skewed near the apex. Downstream from the apex the maximum river depth was skewed toward the outside of the bend, and the resultant discharge profile was more skewed toward the outside of the bend, but the broader cross-stream range of higher discharge indicated that the velocity profile had become less outwardly skewed due to return flow along the bottom water layer.

Bed topography in a river bend is the integrated effect of strong secondary currents and down-welling that produces deeper scour holes toward the outside of the bend (Blanckaert, 2010). The overbank and backwater conditions that tended to shift the peak velocities and down-welling zone to nearly mid-channel at the apex of the bend could have been responsible for defining the bathymetry at the apex of the bend, resulting in a discharge distribution that was not skewed as much as one would expect near the apex of the river bend. At cross-sections 6 and 7, the along-stream velocity distribution was skewed toward the outside bank, but the magnitude of secondary and down-welling currents was reduced, and therefore, the deeper bathymetry was toward the outside of the bend. This resulted in a discharge distribution that was outwardly skewed equally or greater than at the apex of the bend.

To illustrate this effect, the ratio of discharge on river right (toward the outside of the bend), versus the discharge on river left, is shown on figure 26. All conditions show that at some point discharge was skewed toward the outside of the river bend, with two distinct peaks at cross-sections 3 and 7. There was considerable variability in how much discharge was distributed toward the outside of the bend, but there was a positive correlation between the discharge ratio of WLK to VON (or lack of backwater) and the percent discharge on river right averaged for all cross sections. Qualitatively, backwater and overbank conditions tended to centralize discharge for those particular conditions, which bears out in this example. An additional effect was deepening of the river bathymetry toward the center of the channel. As a result, during non-backwater conditions, the discharge did not become strongly skewed at cross-sections 4 and 5.

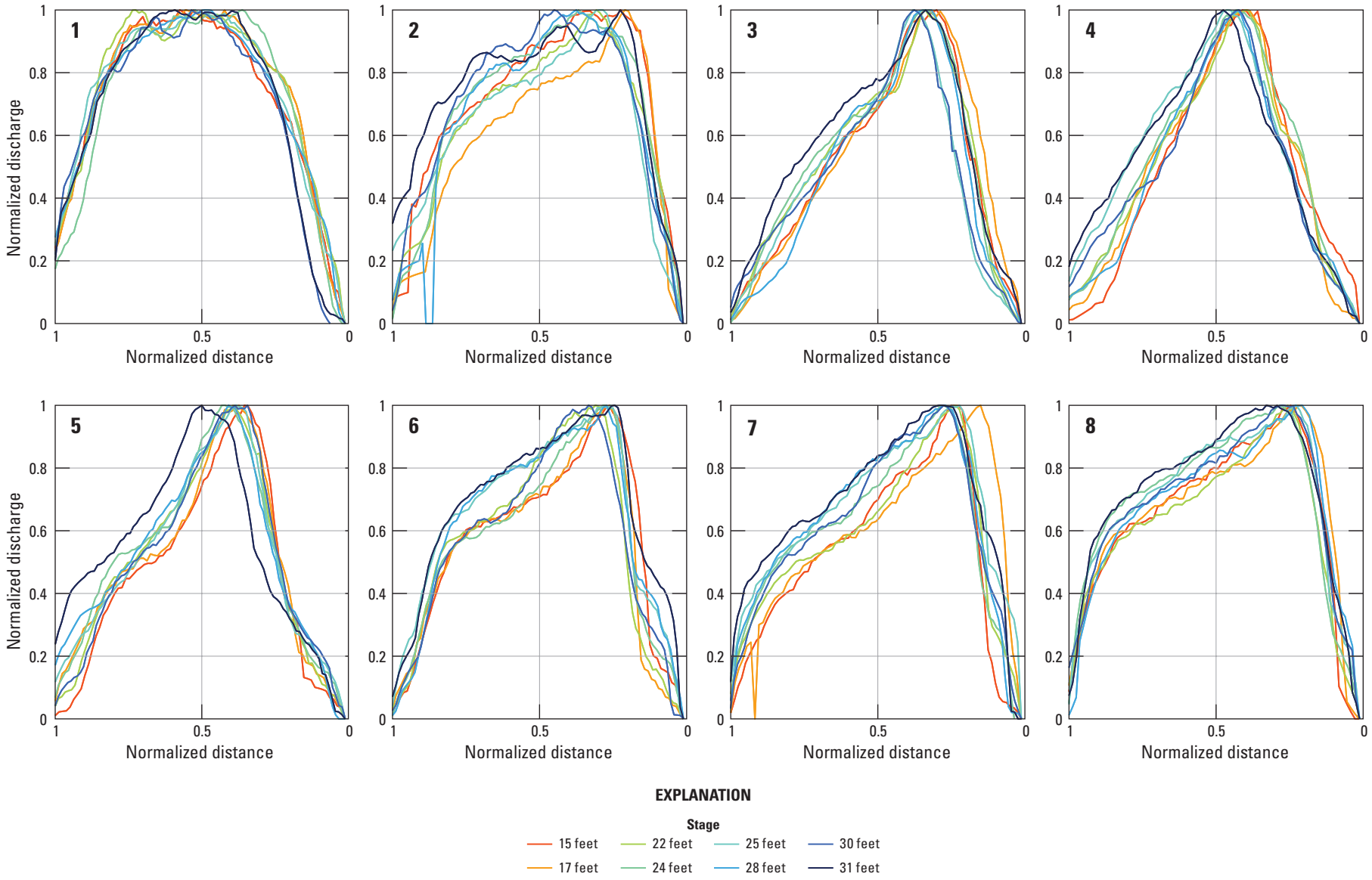

Figure 25. Normalized discharge profiles for cross-sections 1–8 in relation to stage of the Sacramento River at the western end of the Fremont Weir, California.

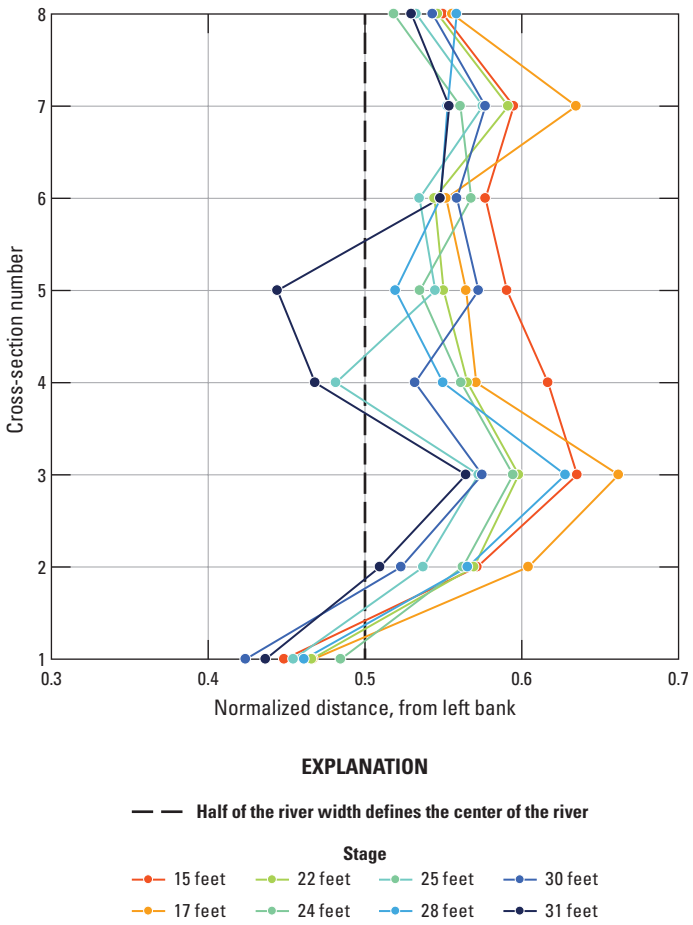

Figure 26. Position along a cross section where fraction of flow equals 0.5 to illustrate how discharge is skewed toward the outside of the bend in the channel as a function of stage of the Sacramento River, California.

Hydraulic Entrainment Zone

The critical streakline method is used to define the extent of the hydraulic entrainment zone. This is a two-dimensional approach to estimate a line extending upstream from a river junction, or engineered notch diversion, which separates the water that will be entrained down either side of the junction. The fish distribution data that were collected are in two dimensions in the horizontal plane. Detailed velocity measurements along the river bend were made, and the three-dimensional effects of secondary circulation on the redistribution of velocity and discharge along a cross section are accounted for. The velocity measurements were distilled into two dimensions to compare to the fish distributions for entrainment estimates.

The accuracy of fish entrainment estimates is reliant upon accurate estimates of the critical streakline location for proposed notch scenarios. The accuracy of critical streakline estimates is affected by (1) the variability in the stage-discharge relation, and (2) the influence of a specific notch design on the local small-scale (for example, velocity variability within several feet) hydrodynamics. Inaccuracies in critical streakline estimates could lead to relatively large errors in fish entrainment estimates, given that gradients in cross-channel fish mass near the riverbanks can be high relative to gradients in cross-channel flow distribution.

The method of hydraulic entrainment zone estimation is straightforward, and an estimate is provided to account for the variance in the critical streakline due to second-order effects of backwater conditions in the Sacramento River (first- and second-order effects are discussed in more detail in the "Variability in the Stage-Discharge Relation" section). The entrainment rate estimates based on the critical streakline approach are expected to be conservative (that is, underestimate fish entrainment) given the expectation that the momentum of secondary circulation toward the outside of the bend will improve the entrainment of surface-oriented fishes in surface-oriented notches.

Hydraulic Entrainment Zone Estimate

The width of the hydraulic entrainment zone, as defined by the cross-stream location of the critical streakline (X), was estimated from the right bank at eight locations where the velocity transects were made. The following process was used to calculate X.

1. The measured velocity was extrapolated to the surface, streambed, and riverbanks (fig. 27*A*) with the one-sixth power law using equation 3:

$$\frac{U}{U_A} = \left(\frac{y}{y_A}\right)^{\frac{1}{6}} \tag{3}$$

where

U is the last measured velocity at a point y, and

U_A is the unmeasured velocity to be extrapolated at a point y_A.

Extrapolation to the water surface and riverbed occur in the vertical plane, and then the velocities are extrapolated to the riverbanks in the horizontal plane. The vertical and horizontal planes are normalized (from 0 to 1) by the depth of water or the width of the cross section, respectively. An example of extrapolation to the surface is as follows: The last measured velocity $U = 1$ ft/s is at a point 7 ft above the riverbed for a depth of 10 ft, therefore $y = 0.7$; to extrapolate U at 7 ft to 8 ft above the riverbed then $y_A = 0.8$, and the extrapolated velocity is $U_A = 1 \times (0.8/0.7)^{1/6}$ or $U_A = 1.02$ ft/s.

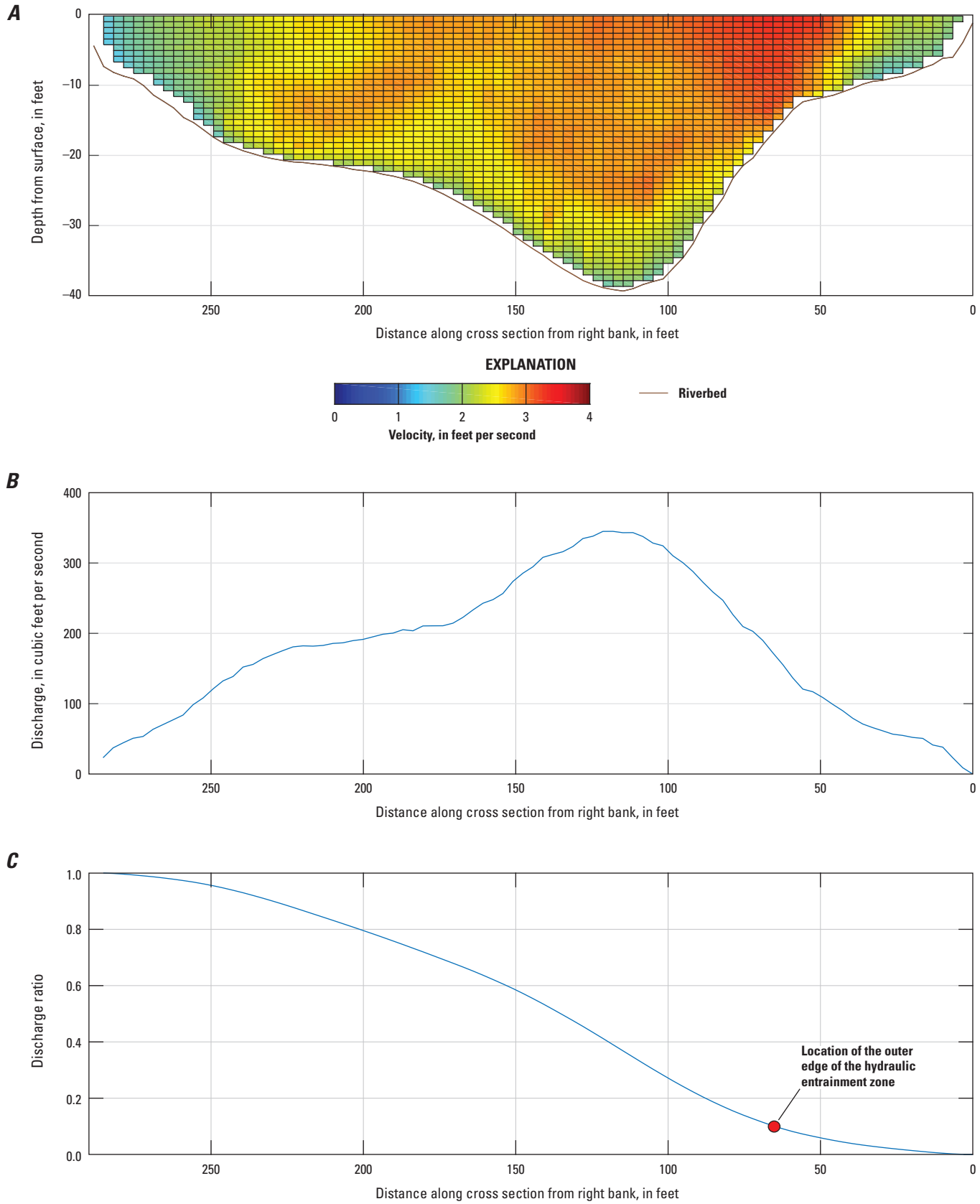

Figure 27. Critical streakline location at cross-section 4 along the Sacramento River near the Fremont Weir, California, at a stage of 24.2 feet, river discharge of 15,900 cubic feet per second, and a notch discharge of 1,550 cubic feet per second (alternative 4 notch stage-discharge rating): *A*, along-stream velocity distribution in relation to depth and distance from the right bank; *B*, discharge (velocity integrated to depth) in relation to distance from the right bank; and *C*, cumulative discharge distribution in relation to distance from the right bank.

2. The river discharge (Q_{river}) was calculated by numerically integrating velocity (V) with respect to the depth of the water (h) and distance along the river cross section (W) at each increment along the river (dy) (eq. 4; fig. 27*B*).

$$Q_{river} = \int_0^W V\ h\ dy \quad (4)$$

3. The cumulative sum of discharge along each cross section was calculated and normalized by the total discharge for that cross section to produce an empirical cumulative distribution function (CDF) of discharge along the river cross section from 0 to 1 (eq. 4; fig. 27*C*). The discharge CDFs were normalized so that they scaled equivalently to the discharge ratio. Additionally, normalizing the cross-section discharge CDFs by the total discharge in the cross section allows a correction for first-order effects to be made to account for variability in the stage-discharge relation as a result of backwater conditions. On the discharge CDF the value of the discharge ratio is found for a given Q_{river} and notch discharge (Q_{notch}).

4. The Q_{notch} from the notch stage-discharge rating for a given stage and alternative (see table 3) was divided by Q_{river} to determine the discharge ratio.

5. The point on the discharge CDF that equals the discharge ratio (red dot on fig. 27*C*) was used to determine the corresponding value of X (along the x-axis on fig. 27*C*). The position of X is the estimate of the outer edge of the hydraulic entrainment zone, shown by the red dot on figure 27*C*. For each cross section the location of X has an associated geo-referenced position. This allowed direct comparison of the hydraulic entrainment zone for an alternative (given stage, Q_{river}, and Q_{notch}) to fish spatial distribution.

6. From the discharge CDFs at each measured stage, a continuous three-dimensional interpolant was created to cover the range of conditions that were unmeasured. Only the CDFs collected at stages of 17, 22, 24, and 30 ft were used because these measurements were made during mean backwater conditions, whereas the measurements at other stages (25, 28, and 31 ft) were made during extreme backwater conditions; incorporating these measurements skewed the interpolation.

For the entrainment simulation, the location of the critical streakline was estimated from a continuous time series (27-year period) of statistically modeled discharge (see "Statistical Model to Predict Discharge on the Sacramento River Near the Fremont Weir" section) and measured stage at the Fremont Weir. Although limited data on the true range of variance associated with second-order effects of backwater conditions are available, an estimate of variance was generated by using a random effects model (Diggle, 2002).

Variance and Uncertainty in Hydraulic Entrainment Zone Estimate

One primary source for both the variance and uncertainty was identified in the procedure used to estimate the location of the critical streakline. The primary source of variance was due to variability in the stage-discharge relation at the western end of the Fremont Weir. Because the notch flow will be fixed for a given stage, this resulted in variability in the ratio of flow from the river into the notch (see "Variability in the Stage-Discharge Relation" section and fig. 19). The primary source of uncertainty was the estimate of the distance from the end of the velocity transect to the riverbank and the resultant velocity extrapolation to the riverbanks. The range of critical streaklines that resulted from changes to these computations were investigated to determine the best approximation on how to account for variance and uncertainty in the estimate of the critical streakline.

Effect of Variability in the Stage-Discharge Relation on Critical Streakline Location

The range of discharge for a given stage value was up to approximately 10,000 ft^3/s (fig. 18). The first-order effect was that at a given stage the discharge either increased or decreased. First-order effects were accounted for by normalizing the discharge CDF (from 0–1) to scale to the discharge ratio (notch flow to river flow) and looking up the value of X that corresponds to the discharge ratio. The second-order effect was a change in the velocity distribution, which resulted in a change to the shape of the discharge CDF. There is some evidence that this occurred when backwater effects increased. Two sets of velocity transects were made at similar stages (24.2 and 24.6 ft, and 30.2 and 31.2 ft) under varying degrees of backwater, and the velocity distribution and discharge CDFs differed for two transects collected at the same location and at similar river stages between each set of measurements.

An example of estimated values of critical streakline location X for stages 24.2 and 24.6 ft and notch alternatives 3, 4, and 6 is shown on figure 28. In this example, it was assumed that the two discharge CDFs represented first- and second-order effects of variability in discharge at similar stages. The vertical blue line in the figure shows an estimated value of X for a stage of 24.2 ft and a river flow of 15,900 ft^3/s. The dashed blue line shows the estimated value of X adjusted for the first-order effect at a stage of 24.2 ft and a river discharge of 12,500 ft^3/s, which was obtained by moving along the 24.2-foot CDF. The true estimate of X for a stage of 24.6 ft and discharge of 12,500 ft^3/s is shown by the dark blue line, which accounted for both first- and second-order effects of variability in discharge at similar stage values. Thus, if the 24.6-foot, 12,500 ft^3/s discharge CDF were not available, then the estimate of X would have been biased low by about 8 ft at this location for this condition.

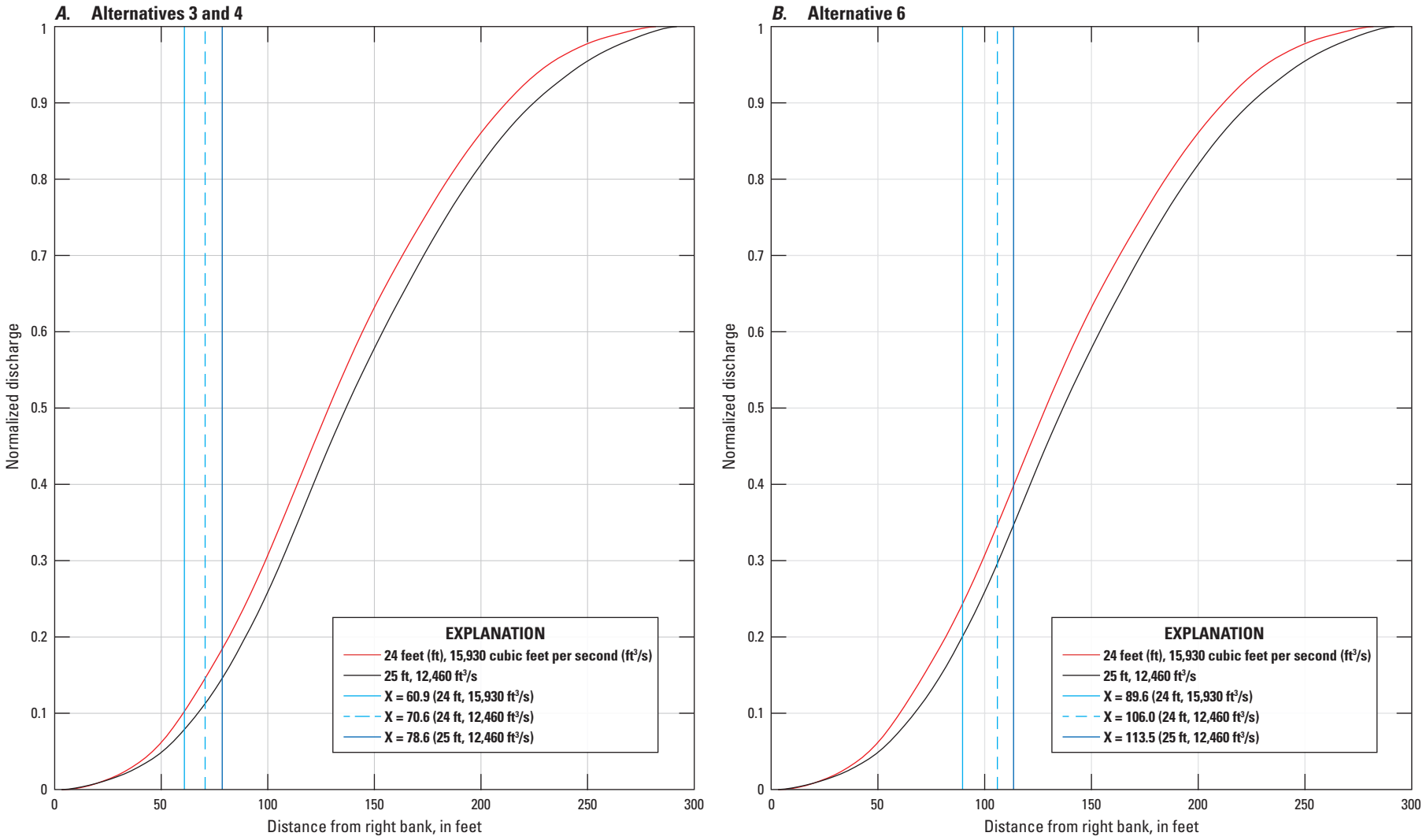

Figure 28. Critical streakline location at cross-section 4 along the Sacramento River, California, using different empirical cumulative discharge distributions for two similar stage conditions: *A*, estimates for alternatives 3 and 4; and *B*, estimates for alternative 6.

This analysis was extended for each cross section for the two sets of conditions at similar stages with varying degrees of backwater effects. The 24.2-foot and 30.2-foot stages are more representative of mean backwater conditions, given where they plotted on the stage-discharge relation calculated from the 2016 USGS gage data, and given their associated Wilkins to Verona discharge ratios (table 4). In contrast, the 24.6-foot and 31.2-foot stages were outliers in terms of where they plotted on both of these curves. The difference in *X* between using the 24.2-foot discharge CDF to correct for first-order effects compared with using the 24.6-foot discharge CDF to correct for both first- and second-order effects is shown on figure 29*A*. The mean difference in *X* for alternatives 3, 4, and 6 across all of the cross sections was −2 ft, and cross-section 3 had the greatest difference at 13 ft. The difference in *X* among alternatives 3, 4, and 6 is fairly small. The difference in *X* between using the 30.2- and 31.2-foot CDFs is shown on figure 29*B*. The mean difference for all alternatives across all of the cross sections was –0.01 ft, and cross-section 5 had the largest difference for alternative 6 of 18 ft. The discharge ratio for a given alternative was higher for the 30.2-foot and 31.2-foot stages; therefore, the true location of *X* moved farther toward the center of the river as backwater effects increased.

Effect Due to Uncertainty in Bank Estimates

The primary source of uncertainty in the location of *X* was due to uncertainty in the amount of discharge between the last measured point and the location of the riverbank at each cross section. The uncertainty in the true riverbank location is because of imperfect bathymetry data, the uncertainty of field estimates of the bank locations made during the velocity data collection, and the velocity extrapolation method, all of which changed the amount of unmeasured velocity and discharge near the riverbanks. As shown in table 4, the percentage of measured flow based on bank location and extrapolated velocity ranged from about 2 to 6 percent, which included both banks. To quantify the errors in both the location of the riverbanks and the velocity extrapolation method, a sensitivity analysis was done to determine how changes in the bank location and the discharge ratio affected the estimate of *X*.

The best estimates of the unmeasured distance to the riverbank for each velocity transect ranged from 3 to 50 ft with a mean of 25 ft. A sensitivity analysis of what the effects would be by changing the location of the riverbanks from 3 to 33 ft was done for all discharge CDFs used in the three-dimensional interpolant when the notch will be operational (stages of 22, 24, and 30 ft), and for notch alternatives 3, 4, and 6. Figure 30 shows the range in change of *X* in relation to the range of adjustment of riverbank location. There was a non-linear increase and more variation in the change of *X* for larger riverbank location errors. Likely, the error in the distance to the riverbanks was only 3–7 ft, so the uncertainty in *X* due to uncertainty in riverbank location was less than 3 ft. The change in *X* resulting from the change in bank location showed little dependency on downstream (cross-section) location (fig. 31), although cross-sections 1 and 7 showed the most variation at different stage or discharge conditions, but there was no consistent bias among conditions or location.

Changes in the discharge ratio were used to illustrate the effect that incorrect velocity extrapolation to the riverbanks will have on estimates of *X*. The average percentage of discharge extrapolated to the riverbanks was 4.5 percent with a range of 2–6 percent. A sensitivity analysis of what the effects would be by adjusting the discharge ratio from 0.5 to 5 percent was done for all alternatives but only for discharge CDFs corresponding to stages when the notch will be operational (fig. 32). If the velocity extrapolation method was 100 percent incorrect, then the discharge ratio would change, on average, by about 5 percent, which would amount to a change in *X* that is generally less than 13 ft. More likely, the velocity extrapolation method was not 100 percent incorrect, and the change in discharge ratio is on the order of 1 percent due to errors in the velocity extrapolation method, which would equate to a change in *X* of less than 3 ft. Therefore, the effects of errors in riverbank location and the velocity extrapolation method are estimated to amount to an uncertainty in the critical streakline that is 3 ft or less.

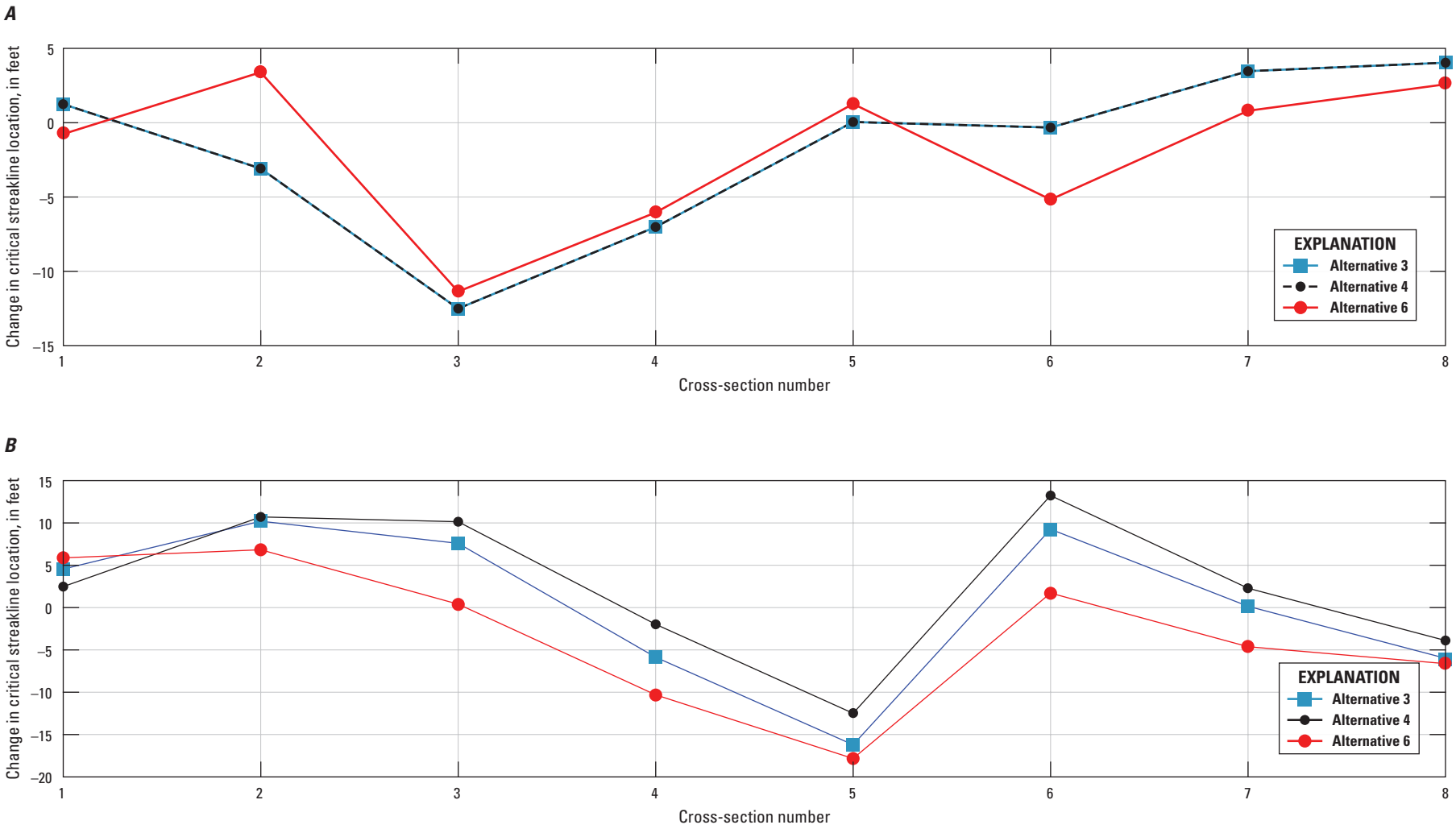

Figure 29. Difference in critical streakline location at each cross section along the Sacramento River, California, due to second-order effects of variability in the stage-discharge relation for alternatives 3, 4, and 6: *A*, comparison of 24- and 25-foot stage cumulative distribution functions (CDFs); and *B*, comparison of 30- and 31-foot stage CDFs.

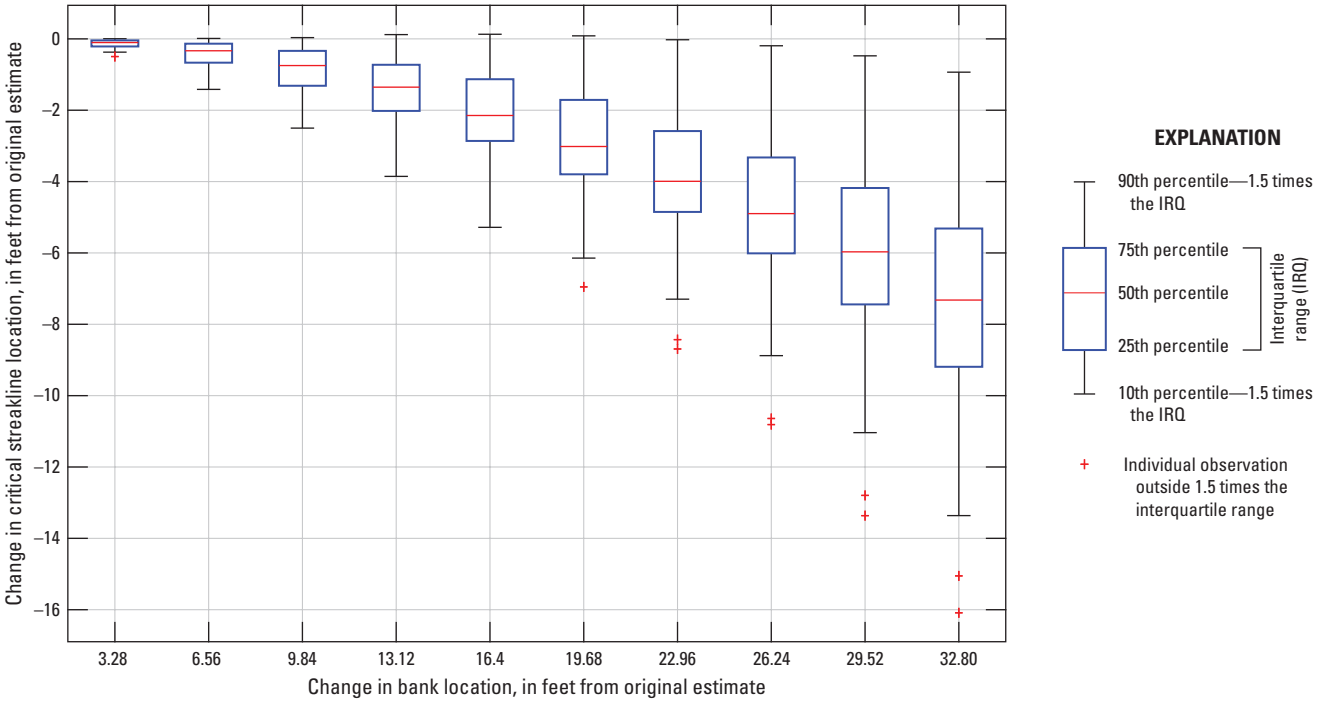

Figure 30. Range of change in critical streakline location as a function of change in bank location from original estimates. The fixed levels of change in bank location were based on a range of values chosen for the sensitivity analysis.

Variance Used in Hydraulic Entrainment Zone Calculation

Uncertainty in *X* due to uncertainty in riverbank locations and velocity extrapolation error was likely less than 3 ft. Because results were consistent over a range of a few conditions, and because techniques to estimate riverbank locations are consistent, this is a reasonable estimate of uncertainty in *X* due to uncertainty in bank estimates. It was more difficult to quantify the variance in *X* caused by second-order effects resulting from variability in the stage-discharge relation. Data to explicitly define the variability for a range of discharge at a given stage were insufficient; therefore, estimation of the variance using a random effects model served to represent stochastically the variance in *X*.

The random effects model included both the variance and uncertainty in *X*. Because estimates in the variance in *X* were larger than the estimates in the uncertainty of *X*, the random effects model was parameterized based solely on the estimated variance in *X*. There are two underlying assumptions used to parameterize the random effects model. First, the WLK/VON discharge ratio distribution can be used to approximate the degree of backwater at the Fremont Weir; therefore, the frequency of occurrence can be estimated for measured conditions. The second assumption was that the WLK/VON discharge ratio can be approximated as a normal distribution, which is a reasonable assumption (fig. 33). The two sets of conditions, discussed in the "Effect of Variability in the Stage-Discharge Relation on Critical Streakline Location" section, were examined by comparing mean backwater to extreme backwater conditions. The greatest uncertainty in *X* was estimated to be 18 ft, with a frequency of occurrence of less than 0.3 percent of the time based on where this condition plotted on the WLK/VON discharge ratio empirical CDF (fig. 33). Therefore, it was assumed that an error in the critical streakline of 18 ft was present less than 0.3 percent of the time due to backwater effects. The random effects model was represented as a normal distribution, with a mean of 0 ft (representing mean backwater conditions) and a standard deviation of 7 ft. This fit resulted in an error of 18 ft that occurred less than 0.3 percent of the time (representing extreme backwater conditions). The random effects model was used in the entrainment simulation to account for variance in the location of the critical streakline (Blake and others, 2017); as such, it accounted for uncertainty due to errors in bank location estimates, errors in velocity extrapolations, and variability in the cross-stream distribution of flow at a given stage because of backwater conditions on the Sacramento River near the western end of the Fremont Weir.

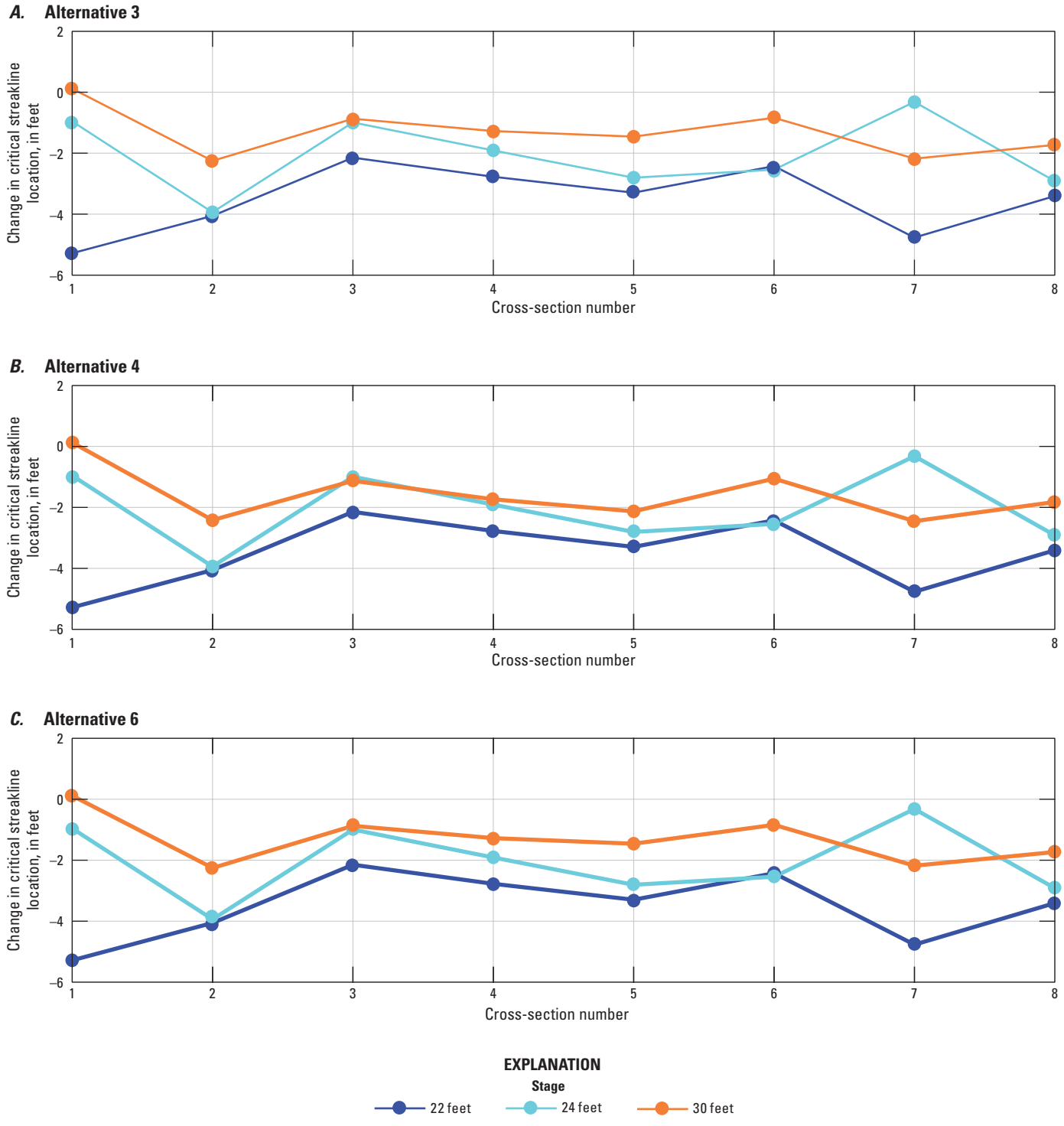

Figure 31. Differences in critical streakline location at each cross section along the Sacramento River, California, due to errors in bank distance estimates of 16.4 feet at each cross section for stage conditions of 22, 24, and 30 feet for *A*, alternative 3; *B*, alternative 4; and *C*, alternative 6.

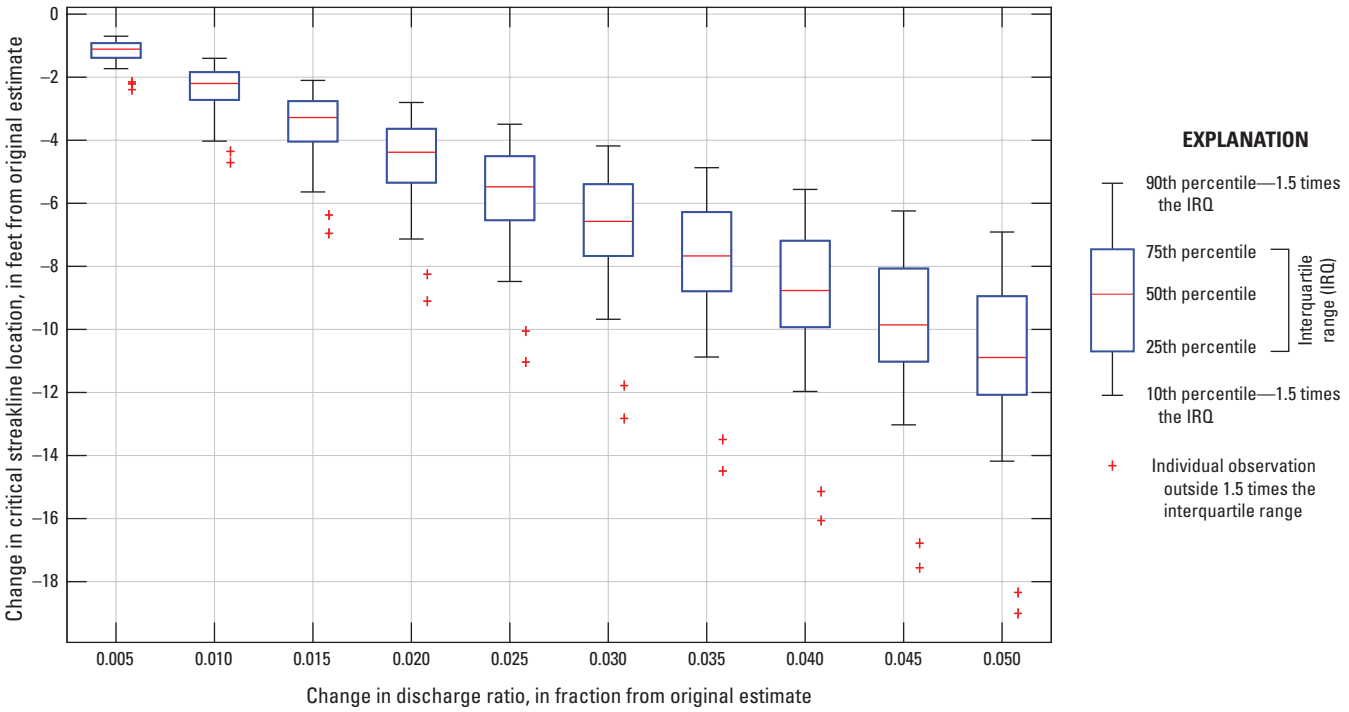

Figure 32. Range of change in critical streakline location as a function of change in discharge ratio from original estimates. The change in the discharge ratio was based on a range of values chosen for the sensitivity analysis.

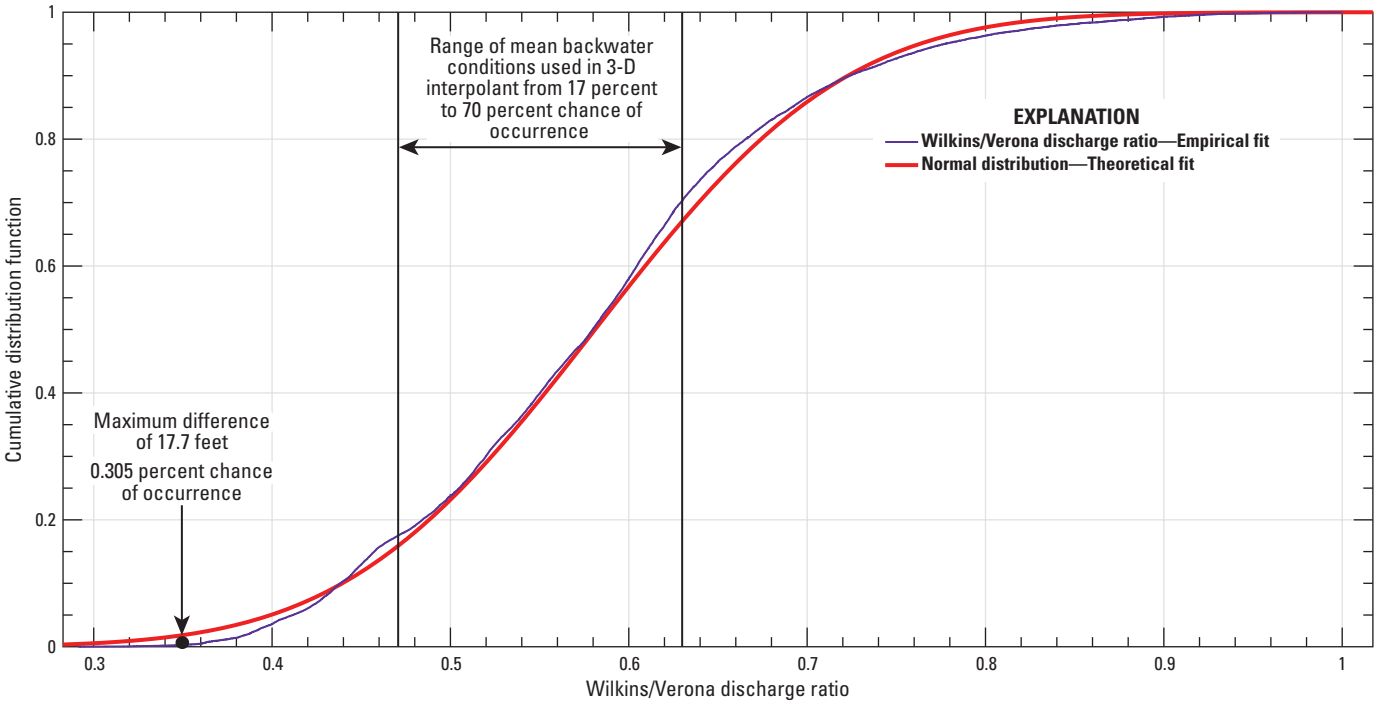

Figure 33. Empirical and theoretical cumulative distribution functions for the Wilkins/Verona discharge ratio for the 27-year period (April 1990–April 2017) of record. The theoretical distribution fit was used for the random effects model.

Conclusions and Recommendations

Detailed velocity measurements made near the western end of the Fremont Weir along the Sacramento River were used to estimate the width of the hydraulic entrainment zone and provide a framework to make predictions of fish entrainment into a proposed notch at the Fremont Weir. The variability in the stage-discharge relation that was observed will affect the ratio of notch discharge to river discharge, the location of the critical streakline, and eventually predictions of fish entrainment into the proposed notch. The degree of complex hydrologic conditions that exist in this region were not recognized when this study was initiated. Thus, estimates of the degree of variability in the stage-discharge relation are poorly understood and based on limited data. The key findings from this study are as follows:

1. The index-velocity method was better for estimating discharge near the western end of the Fremont Weir than the stage-discharge method because of backwater effects in the Sacramento River.

2. The Sutter Bypass was a significant inflow into the Sacramento River system prior to the Fremont Weir overtopping; therefore, this boundary condition needs to be accounted for in hydrodynamic numerical models. Because of the uncertainty of inputs into the mass-balance equation, additional measurements and analysis of Sutter Bypass flows are required.

3. There was a secondary circulation cell at the river bend for the conditions that were measured, and this acted as a mechanism to shift the distribution of water velocity and discharge toward the outside of the river bend.

4. The statistical model for predicting an hourly time series of discharge on the Sacramento River above Fremont Weir near Knights Landing, for the 27-year period from April 1990 to April 2017, based on a stepwise linear regression with 5 predictor variables and 15 terms, has an R^2 value of 0.998 and a root mean square error of 360 cubic feet per second. The discharge was predicted based on a range of measured discharge of approximately 7,000 to 28,000 cubic feet per second.

5. Because of the effects of backwater and overbank flow, the critical streakline moves toward the channel center when the Sacramento River overtops the right riverbank.

6. Uncertainty in the position of the critical streakline due to uncertainty in estimated bank locations and velocity extrapolation error was estimated to be less than 3 feet. The width of the river varies from about 250 to 300 feet, depending on river stage and cross-section location.

7. Uncertainty in the position of the critical streakline due to backwater effects was estimated to be greater than 3 feet, and the maximum observed was approximately 18 feet.

8. The cross-channel empirical cumulative distribution function for discharge at specific cross sections was a useful metric for comparing measurements taken at different conditions at a cross-section location, because it captures the spatial variability in the discharge at a cross section, which is a key factor in determining the critical streakline location.

9. Given the variability in the hydrodynamics along the Sacramento River near the Fremont Weir caused by backwater effects, numerical modeling of the hydrodynamics of this system should incorporate the variability in river conditions associated with backwater.

10. Our results show that three-dimensional aspects of the flow, such as secondary circulation, are important to consider; therefore, a three-dimensional numerical model should be used.

11. The critical streakline location estimates discussed in this report are appropriate for use in computing fish entrainment rates by superimposing the critical streakline estimates on the fish spatial distributions.

In order to refine estimates of the error in the critical streakline due to backwater effects and provide better entrainment estimates from a hydrodynamic standpoint, the following recommendations are made:

1. Estimates in the location of the critical streakline could be improved if a greater range of velocity transects were made to better define the variability in the velocity structure at a particular river cross section. The largest estimated uncertainty was 18 feet, and presumably would be greatly reduced if a more representative range of conditions were used. Velocity transects made over a range of discharge conditions for a particular stage would allow better quantification of the uncertainty in the critical streakline estimates.

2. Estimates of discharge immediately upstream from the western end of the Fremont Weir, based on a long-term record using the index-velocity method, are critical for correct entrainment estimates. The statistical model was a good first order estimation, but having a direct measurement of discharge that is unaffected by backwater conditions (index-velocity) would reduce uncertainty. As a result, an installation upstream from the western end of the Fremont Weir is recommended.

3. Because of frequent backwater effects caused by flow from the Sutter Bypass and Feather River, a stage gage should be installed immediately downstream from the Fremont Weir to monitor the water-surface slope in the Sacramento River in the vicinity of the weir. In the absence of these data there could be errors in the elevation of the water surface at the downstream notch locations.

4. An agreement amongst working groups and agencies is needed regarding the datum to use for stage measurements near the western end of the Fremont Weir. The survey completed during this study indicated that the river stage could be overestimated by 0.5 foot. Comparison of the stage data collected in 2016 and that collected at FRE showed that the FRE stage data could be biased high during higher river stages, but because the two data sets were collected from sites 1.24 miles apart, some differences may reflect actual changes in water slope due to backwater effects. A coordinated effort with agencies involved in this study (California Department of Water Resources, Bureau of Reclamation and the U.S. Geological Survey) to improve discharge and stage measurements at this location is necessary.

References

Bever, A.J., and MacWilliams, M.L., 2016, Factors influencing the calculation of periodic secondary circulation in a tidal river—Numerical modelling of the lower Sacramento River, USA: Hydrological Processes, v. 30, no. 7, p. 995–1016, https://doi.org/10.1002/hyp.10690.

Blake, A.R., Stumpner, P., and Burau, J.R., 2017, A simulation method for combining hydrodynamic data and acoustic tag tracks to predict the entrainment of juvenile salmonids onto the Yolo Bypass under future engineering scenarios: Delta Stewardship Council, 108 p., https://pubs.er.usgs.gov/publication/70197620.

Blanckaert, K., 2010, Topographic steering, flow recirculation, velocity redistribution, and bed topography in sharp meander bends: Water Resources Research, v. 46, no. 9, 23 p., https://doi.org/10.1029/2009WR008303.

Buchanan, T.J., and Somers, W.P., 1969, Discharge measurements at gaging stations: U.S. Geological Survey Techniques of Water-Resources Investigations, book 3, chap. A8, 65 p., https://pubs.usgs.gov/twri/twri3a8/.

Bureau of Reclamation and California Department of Water Resources, 2012, Yolo Bypass salmonid habitat restoration and fish passage implementation plan: Bureau of Reclamation and California Department of Water Resources, 140 p., https://www.water.ca.gov/LegacyFiles/environmentalservices/docs/yolo/yolo2.pdf.

California Department of Water Resources, 2003, Sacramento Valley flood control system: accessed July 28, 2017, at http://cdec.water.ca.gov/cgi-progs/products/sac_flow.pdf.

California Department of Water Resources, 2012, 2011 Georgiana Slough non-physical barrier performance evaluation project report: California Department of Water Resources, Sacramento, California, 228 p., http://baydeltaoffice.water.ca.gov/sdb/GS/docs/GSNPB_2011_Final_Report+Append_090512.pdf.

California Department of Water Resources, 2015, 2012 Georgiana Slough non-physical barrier performance evaluation project report: California Department of Water Resources, Sacramento, California, 298 p., http://baydeltaoffice.water.ca.gov/sdb/GS/docs/Final%20GSNPB%202012%20Report_Review%20Certified.pdf.

California Department of Water Resources, 2016, 2014 Georgiana Slough floating fish guidance structure performance evaluation project report: California Department of Water Resources, Sacramento, California, 486 p., http://baydeltaoffice.water.ca.gov/sdb/GS/docs/Final%20Report%20October%202016%20Edition%20103116-signed.pdf.

CBEC, 2012, Lower Feather River corridor management plan, Shanghai Rapids field data collection: West Sacramento, Calif., CBEC Eco Engineering, Technical Memorandum 11–1009, appendix J, 44 p., https://www.water.ca.gov/LegacyFiles/floodmgmt/fmo/docs/LFRCMP-AppJ-cbec2012-ShanghaiRapidsData-June2014.pdf.

Chen, C., 1991, Unified theory on power laws for flow resistance: Journal of Hydraulic Engineering, v. 117, no. 3, p. 371–389, https://doi.org/10.1061/(ASCE)0733-9429(1991)117:3(371).

Diggle, P., 2002, Analysis of longitudinal data, (2d ed.): Oxford, New York, Oxford University Press, 387 p.

Dinehart, R.L., and Burau, J.R., 2005, Averaged indicators of secondary flow in repeated acoustic Doppler current profiler crossings of bends: Water Resources Research, v. 41, no. 9, p. 1–18, https://doi.org/10.1029/2005WR004050.

Hoitink, A.J.F., Buschman, F.A., and Vermeulen, B., 2009, Continuous measurements of discharge from a horizontal acoustic Doppler current profiler in a tidal river: Water Resources Research, v. 45, no. 11, 13 p., https://doi.org/10.1029/2009WR007791.

Lane, S.N., Bradbrook, K.F., Richards, K.S., Biron, P.M., and Roy, A.G., 2000, Secondary circulation cells in river channel confluences—Measurement artefacts or coherent flow structures?: Hydrological Processes, v. 14, no. 11–12, p. 2047–2071, https://doi.org/10.1002/1099-1085(20000815/30)14:11/12<2047::AID-HYP54>3.0.CO;2-4.

Le Coz, J., Pierrefeu, G., and Paquier, A., 2008, Evaluation of river discharges monitored by a fixed side-looking Doppler profiler: Water Resources Research, v. 44, no. 4, p. 1–13, https://doi.org/10.1029/2008WR006967.

Levesque, V.A., and Oberg, K.A., 2012, Computing discharge using the index velocity method: U.S. Geological Survey Techniques and Methods 3–A23, 148 p., https://pubs.usgs.gov/tm/3a23/.

MathWorks® Inc., 2017, MATLAB Version 9.2 (R2017a): accessed July 28, 2017, at https://www.mathworks.com.

Morvan, H., Pender, G., Wright, N.G., and Ervine, D.A., 2002, Three-dimensional hydrodynamics of meandering compound channels: Journal of Hydraulic Engineering, v. 128, no. 7, p. 674–682, https://doi.org/10.1061/(ASCE)0733-9429(2002)128:7(674).

Mueller, D.S., 2013, *extrap*—Software to assist the selection of extrapolation methods for moving-boat ADCP streamflow measurements: Computers & Geosciences, v. 54, p. 211–218, https://doi.org/10.1016/j.cageo.2013.02.001.

Mueller, D.S., Wagner, C.R., Rehmel, M.S., Oberg, K.A., and Rainville, F., 2009, Measuring discharge with acoustic Doppler current profilers from a moving boat: U.S. Geological Survey Techniques and Methods 3–A22, ver. 1, 72 p., https://doi.org/10.3133/tm3A22.

National Geodetic Survey, 2017, VERTCON—North American Vertical Datum Conversion: accessed July 28, 2017, at https://www.ngs.noaa.gov/TOOLS/Vertcon/vertcon.html.

National Marine Fisheries Service, 1989, Endangered and threatened species; critical habitat; winter-run chinook salmon: Federal Register, v. 54, no. 149, August 4, 1989, 50 CFR Part 226 and 227, web page accessed September 10, 2018, at https://esadocs.cci-dev.org/ESAdocs/federal_register/fr1572.pdf.

National Marine Fisheries Service, 1999, Endangered and threatened species; threatened status for two chinook salmon Evolutionarily Significant Units (ESUs) in California: Federal Register, v. 64, no. 179, September 16, 1999, 50 CFR Part 223, web page accessed September 10, 2018, at http://www.westcoast.fisheries.noaa.gov/publications/frn/1999/64fr50394.pdf.

National Marine Fisheries Service, 2009, Biological opinion and conference opinion on the long-term operations of the Central Valley Project and State Water Project, Long Beach, California, National Marine Fisheries Service, 844 p., http://www.westcoast.fisheries.noaa.gov/publications/Central_Valley/Water%20Operations/Operations,%20Criteria%20and%20Plan/nmfs_biological_and_conference_opinion_on_the_long-term_operations_of_the_cvp_and_swp.pdf.

Nihei, Y., and Kimizu, A., 2008, A new monitoring system for river discharge with horizontal acoustic Doppler current profiler measurements and river flow simulation: Water Resources Research, v. 44, no. 4, p. 1–15, https://doi.org/10.1029/2008WR006970.

Parsons, D.R., Jackson, P.R., Czuba, J.A., Engel, F.L., Rhoads, B.L., Oberg, K.A., Best, J.L., Mueller, D.S., Johnson, K.K., and Riley, J.D., 2013, Velocity Mapping Toolbox (VMT)—A processing and visualization suite for moving-vessel ADCP measurements: Earth Surface Processes and Landforms, v. 38, no. 11, p. 1244–1260, https://doi.org/10.1002/esp.3367.

Perry, R.W., Buchanan, R.A., Brandes, P.L., Burau, J.R., and Israel, J.A., 2016, Anadromous salmonids in the Delta—New science 2006–2016: San Francisco Estuary and Watershed Science, v. 14, no. 2, 28 p., https://escholarship.org/uc/item/27f0s5kh.

Perry, R.W., Romine, J.G., Adams, N.S., Blake, A.R., Burau, J.R., Johnston, S.V., and Liedtke, T.L., 2014, Using a non-physical behavioural barrier to alter migration routing of juvenile Chinook salmon in the Sacramento–San Joaquin River Delta: River Research and Applications, v. 30, no. 2, p. 192–203, https://doi.org/10.1002/rra.2628.

Pope, A.C., Perry, R.W., Hance, D.J., and Hansel, H.C., 2018, Survival, travel time, and utilization of Yolo Bypass, California, by outmigrating acoustic-tagged late-fall Chinook salmon: U.S. Geological Survey Open-File Report 2018–1118, 33 p., https://doi.org/10.3133/ofr20181118.

Romine, J.G., Perry, R.W., Pope, A.C., Stumpner, P., Liedtke, T.L., Kumagai, K.K., and Reeves, R.L., 2017, Evaluation of a floating fish guidance structure at a hydrodynamically complex river junction in the Sacramento–San Joaquin River Delta, California, USA: Marine and Freshwater Research, v. 68, no. 5, p. 878–888, https://doi.org/10.1071/MF15285.

Rozovskiĭ, I.L., 1957, Flow of water in bends of open channels: Academy of Sciences of the Ukrainian SSR, 233 p.

Ruhl, C.A., and Simpson, M.R., 2005, Computation of discharge using the index-velocity method in tidally affected areas: U.S. Geological Survey Scientific Investigations Report 2005–5004, 41 p., https://doi.org/10.3133/sir20055004.

Sassi, M.G., Hoitink, A.J.F., Vermeulen, B., and Hidayat, 2011, Discharge estimation from H-ADCP measurements in a tidal river subject to sidewall effects and a mobile bed: Water Resources Research, v. 47, no. 6, https://doi.org/10.1029/2010wr009972.

Simpson, M.R., 2001, Discharge measurements using a broad-band acoustic Doppler current profiler: U.S. Geological Survey Open-File Report 2001–1, 123 p., https://doi.org/10.3133/ofr011.

Stumpner, P., 2018, Velocity mapping using moving boat acoustic Doppler current profiler on the Sacramento River near the western end of the Fremont Weir in February and March 2016, and May 2017: U.S. Geological Survey data release, https://doi.org/10.5066/F7QZ296Z.

Appendix. Linear Regression Model to Predict Discharge at the Fremont Weir

The final form of the modeled equation from the stepwise regression was

$$Y = \text{Intercept} + aX1 + bX2 + cX3 + dX4 + eX5 + fX1X2 + gX1X4 + hX1X5 + iX2X3 + jX3X4 + kX2X5 + lX3X4 + mX3X5 + nX4X5 \quad (1–1)$$

where the independent and dependent variables used in the linear model are

- Y = Discharge (cubic feet per second [ft³/s]) on the Sacramento River above Fremont Weir near Knights Landing (FRE.temp),
- $X1$ = Stage (feet [ft]) on the Sacramento River near the Fremont Weir (FRE),
- $X2$ = Discharge (ft³/s) on the Sacramento River below Wilkins Slough (WLK),
- $X3$ = Discharge (ft³/s) on the Sacramento River at Verona (VON),
- $X4$ = Stage difference (head loss in ft) between the Sacramento River below Wilkins Slough (WLK) and Sacramento River near Fremont Weir (FRE), and
- $X5$ = Stage difference (head loss in ft) between the Sacramento near the Fremont Weir and Sacramento River at Verona (VON).

Parameter Estimations for Linear Regression Model

Intercept = –579.19 ft³/s

a = 479.66

b = –0.69017

c = 0.0006358

d = 900.21

e = –19,018

f = 0.098745

g = –107.31

h = 896.64

i = –0.000034491

j = 0.013777

k = –0.77084

l = 0.037772

m = –0.047459

n = 801.59

Final Regression Model Output and Summary Statistics

Output from Matlab stepwise regression tool (Matlab function—stepwiselm):

1. Adding x1, FStat = 215432.8601, pValue = 0
2. Adding x2, FStat = 4703.7847, pValue = 0
3. Adding x1:x2, FStat = 34.656, pValue = 4.57467e-09
4. Adding x5, FStat = 16.553, pValue = 4.9075e-05
5. Adding x1:x5, FStat = 55.321, pValue = 1.48865e-13
6. Adding x3, FStat = 104.3061, pValue = 6.300758e-24
7. Adding x2:x3, FStat = 21.7334, pValue = 3.33176e-06
8. Adding x4, FStat = 37.3692, pValue = 1.16437e-09
9. Adding x3:x5, FStat = 18.0732, pValue = 2.21989e-05
10. Adding x2:x5, FStat = 48.0542, pValue = 5.51509e-12
11. Adding x4:x5, FStat = 44.6301, pValue = 3.04771e-11
12. Adding x2:x4, FStat = 13.6676, pValue = 0.00022385
13. Adding x1:x4, FStat = 4.2823, pValue = 0.038634
14. Adding x3:x4, FStat = 9.0694, pValue = 0.0026307

Linear regression model output:

y ~ [Linear formula with 15 terms in 5 predictors]

Estimated coefficients:

Model term	Coefficient estimate	Standard error	*t*-stat	*p*-value (significance)
Intercept	–579.19	8,177.5	–0.070827	0.94354
x1	479.66	590.8	0.81189	0.41695
x2	–0.69017	0.32931	–2.0958	0.036218
x3	0.0006358	0.2161	0.0029422	0.99765
x4	900.21	422.25	2.1319	0.033129
x5	–19,018	2,821.2	–6.741	2.0328e-11
x1:x2	0.098745	0.0094089	10.495	3.8501e-25
x1:x4	–107.31	31.143	–3.4457	0.00058095
x1:x5	896.64	109.98	8.1526	6.0967e-16
x2:x3	–3.4491e-05	3.1341e-06	–11.005	2.0469e-27
x2:x4	0.013777	0.0062975	2.1877	0.028804
x2:x5	–0.77084	0.11417	–6.7516	1.8932e-11
x3:x4	0.037772	0.012542	3.0115	0.0026307
x3:x5	–0.047459	0.013065	–3.6325	0.00028754
x4:x5	801.59	131.32	6.104	1.2316e-09

Number of observations: 2,086.

Error degrees of freedom: 2,071.

Root mean squared error: 361 ft^3/s.

R-squared: 0.998; Adjusted R-squared: 0.998.

F-statistic vs. constant model: 6.09e+04, p-value < 0.0001.

Publishing support provided by the U.S. Geological Survey
Science Publishing Network, Sacramento Publishing Service Center

For more information concerning the research in this report, contact the
Director, California Water Science Center
U.S. Geological Survey
6000 J Street, Placer Hall
Sacramento, California 95819
https://ca.water.usgs.gov

ISSN 2328-0328 (online)
https://doi.org/10.3133/sir20185115

USGS

Stumpner and others—**Hydrology and Hydrodynamics on the Sacramento River Near the Fremont Weir, California—Implications for Juvenile Salmon Entrainment Estimates**—Scientific Investigations Report 2018–5115